TECHNICAL REPORT STANDARD PAGE

1. Report No.	2. Government Accession No.	3. Recipient's Catalog No.
FHWA/LA.11/499		

4. Title and Subtitle	5. Report Date
Characterization of Louisiana Asphalt Mixtures Using Simple Performance Tests and MEPDG	April 2014
	6. Performing Organization Code

7. Author(s)	8. Performing Organization Report No.
Louay N. Mohammad, Ph.D., Minkyum Kim, Ph.D., Amar Raghavendra, P.E., Sandeep Obulareddy	

9. Performing Organization Name and Address	10. Work Unit No.
Louisiana Transportation Research Center Baton Rouge, LA 70808	
	11. Contract or Grant No. State Project Number: 736-99-1104 LTRC Project Number: 04-6B

12. Sponsoring Agency Name and Address	13. Type of Report and Period Covered
Louisiana Department of Transportation and Development P.O. Box 94245 Baton Rouge, LA 70804-9245	**Final Report** **January 2008 - June 2011**
	14. Sponsoring Agency Code

15. Supplementary Notes

Conducted in Cooperation with the U.S. Department of Transportation, Federal Highway Administration

16. Abstract

The National Cooperative Highway Research Program (NCHRP) Project 9-19, Superpave Support and Performance Models Management, recommended three Simple Performance Tests (SPTs) to complement the Superpave volumetric mixture design method. These are the dynamic modulus, flow time, and flow number tests. In addition, the Mechanistic Empirical Pavement Design Guide (MEPDG) developed under NCHRP project 1-37A uses dynamic modulus to characterize Hot Mix Asphalt mixtures for pavement structural design. The objectives of this study were to (1) characterize common Louisiana asphalt mixtures using SPT protocols, (2) develop a catalog of dynamic modulus values for input into the MEPDG software, (3) evaluate the sensitivity of rut prediction of the MEPDG program, (4) assess the prediction of dynamic modulus values using Witczak and Hirsch models, and (5) compare dynamic modulus data obtained from axial and Indirect Tensile (IDT) modes of testing. Fourteen rehabilitation projects across Louisiana were selected to provide a total of 28 asphalt mixtures for this study. Laboratory mechanistic tests were performed to characterize the asphalt mixtures including the dynamic modulus in axial and IDT modes, flow time, flow number, and Hamburg type loaded wheel tracking tests. A catalog of dynamic modulus values was developed and grouped by design traffic level. Test results indicated that dynamic modulus was sensitive to the design traffic level, nominal maximum aggregate size, and the high temperature performance grade of the binder. Mixtures designed for higher traffic levels, with larger aggregate, and higher grade binder tended to have higher dynamic modulus values at high temperature. The MEPDG simulations carried out using the "nationally calibrated" default calibration factors overestimated the rut predictions by a significant amount. To address this problem, a local calibration of the MEPDG rut prediction model was performed and preliminary ranges of local calibration factors were developed. Both the Witczak and Hirsch models predicted dynamic modulus with reasonable accuracy. Dynamic modulus test results obtained from axial and IDT modes showed no statistical differences for the majority of the mixtures tested.

17. Key Words	18. Distribution Statement
MEPDG, DARWIN-ME, asphalt mixtures, performance tests, dynamic modulus, flow number, loaded wheel tester,	**Unrestricted. This document is available through the National Technical Information Service, Springfield, VA 21161.**

19. Security Classif. (of this report)	20. Security Classif. (of this page)	21. No. of Pages	22. Price

Project Review Committee

Each research project will have an advisory committee appointed by the LTRC Director. The Project Review Committee is responsible for assisting the LTRC Administrator or Manager in the development of acceptable research problem statements, requests for proposals, review of research proposals, oversight of approved research projects, and the implementation of findings. LTRC appreciates the dedication of the following Project Review Committee Members in guiding this research study to fruition.

LTRC Administrator

Bill King
Materials Research Administrator

Members

Luanna Cambas, LADOTD
Phil Arena, FHWA
Danny Smith, LADOTD
Ronnie Robinson, LADOTD
Don Weathers, LAPA
Gary Fitts, Asphalt Institute

Directorate Implementation Sponsor

Richard Savoie, P.E.
DOTD Chief Engineer

Characterization of Louisiana Asphalt Mixtures Using Simple Performance Tests and MEPDG

by
Louay Mohammad, Ph.D.
Minkyum Kim, Ph.D.
Amar Raghavendra, P.E.
Sandeep Obulareddy

Louisiana Transportation Research Center
Baton Rouge, LA 70808

LTRC Project No. 04-6B
State Project No. 736-99-1104

conducted for

Louisiana Department of Transportation and Development
Louisiana Transportation Research Center

The contents of this report reflect the views of the author/principal investigator who is responsible for the facts and the accuracy of the data presented herein. The contents of do not necessarily reflect the views or policies of the Louisiana Department of Transportation and Development [if the project is federally funded as well, add the Federal Highway Administration, or delete this portion] or the Louisiana Transportation Research Center. This report does not constitute a standard, specification, or regulation.

April 2014

ABSTRACT

The National Cooperative Highway Research Program (NCHRP) project 9-19, Superpave Support and Performance Models Management, recommended three Simple Performance Tests (SPTs) to complement the Superpave volumetric mixture design method. These are the dynamic modulus (E*), flow time (Ft), and flow number (F_N) tests. In addition, the Mechanistic Empirical Pavement Design Guide (MEPDG) developed under NCHRP project 1-37A uses dynamic modulus to characterize hot mix asphalt (HMA) mixtures for pavement structural design.

The objectives of this study were to (1) characterize common Louisiana asphalt mixtures using SPT protocols, (2) develop a catalog of dynamic modulus values for input into the MEPDG software, (3) evaluate the sensitivity of rut prediction of the MEPDG program, (4) assess the prediction of dynamic modulus values using Witczak and Hirsch models, and (5) compare dynamic modulus data obtained from axial and Indirect Tensile (IDT) modes of testing. Fourteen rehabilitation projects across Louisiana were selected to provide a total of 28 asphalt mixtures for this study. Laboratory mechanistic tests were performed to characterize the asphalt mixtures including the dynamic modulus in axial and IDT modes, flow time, flow number, and Hamburg type loaded wheel tracking tests. A catalog of dynamic modulus values was developed and grouped by design traffic level. Test results indicated that dynamic modulus was sensitive to the design traffic level, nominal maximum aggregate size, and the high temperature performance grade of the binder. Mixtures designed for higher traffic levels, with larger aggregate, and higher grade binder tended to have higher dynamic modulus values at high temperature. The MEPDG simulations carried out using the "nationally calibrated" default calibration factors overestimated the rut predictions by a significant amount. To address this problem a local calibration of the MEPDG rut prediction model was performed and preliminary ranges of local calibration factors were developed. Both the Witczak and Hirsch models predicted dynamic modulus with reasonable accuracy. Dynamic modulus test results obtained from axial and IDT modes showed no statistical differences for the majority of the mixtures tested.

ACKNOWLEDGMENTS

The research work reported in this paper was sponsored by the Louisiana Department of Transportation and Development (LADOTD) through the Louisiana Transportation Research Center (LTRC). The authors would like to express thanks to all whom have provided valuable help in this study, especially the staff of the Asphalt Research Laboratory and the Engineering Materials Characterization Research Facility.

IMPLEMENTATION STATEMENT

Based on the findings and the results of this project, a catalog of dynamic modulus was developed; the catalog had values of various asphalt mixtures designed for Level 1 and Level 2 traffic categories at multiple temperatures and loading frequencies, and it is provided as one of the project deliverables. The catalog, together with the findings of this research study, should be a practical source of information, which will assist LADOTD design engineers in determining reasonable ranges of dynamic modulus values under various design conditions they are subjected to while using the new MEPDG software. The catalog was also created as a user-friendly spreadsheet and Microsoft Access based database, which is submitted as a separate CD.

In order for the provided catalog to be fully implemented, further research effort to include a wider range of asphalt mixtures, typically used in pavements across all major regions in Louisiana, is needed. In addition, it is recommended that the calibrated rutting model be confirmed through long term field performance monitoring.

TABLE OF CONTENTS

LIST OF TABLES

LIST OF FIGURES

INTRODUCTION

Background

The Federal Highway Administration's 1995-1997 National Pavement Design Review found that nearly 80 percent of the States use the 1972, 1986, or 1993 AASHTO Design Guides *[1]*. All these versions of design guides are relying on empirical relationships between paving material properties and structural performance of pavement layers developed mainly based on the 1950's AASHO Road Test data. In recognition of the limitations of these older AASHTO Design Guides, the Joint Task Force on Pavements (JTFP) initiated an effort to develop an improved design guide based as fully as possible on mechanistic principles *[1]*. The FHWA's Mechanistic-Empirical Pavement Design Guide (MEPDG) is the recently released result of such an effort.

An integrated hierarchical approach was elected as the main framework of the new design guide, in such a way that the input items are broadly categorized into four main aspects: general, traffic, climatic, and structural information. Details of these categories can be provided depending upon the importance of a project in concern; they are classified as Level 1, Level 2, and Level 3 from the most to least important *[1]*. These input items and their relative requirements are summarized in Table 1.

Table 1
Input items in the MEPDG software

Material	Input Level 1	Input Level 2	Input Level 3
Asphalt Concrete	Measured |E*| (mixture-specific lab testing)	Estimated |E*| (Predicted models & lab measured binder data)	Default |E*| (Assumed |E*|& assumed binder data)
Stabilized Materials	Measured M_R	Estimated M_R	Default M_R
Granular Materials	Measured M_R	Estimated M_R	Default M_R
Subgrade	Measured M_R	Estimated M_R	Default M_R

Level 1 input items are provided for highly trafficked pavements to provide the highest level of accuracy and the least level of uncertainty. Inputs for Level 1 require laboratory or field testing, such as the dynamic modulus testing of hot-mix asphalt and complex shear modulus

of the binder. Acquiring inputs for Level 1 requires more time and resources than other levels. Level 2 inputs provide an intermediate level of accuracy and could be used when resources or testing equipment are not available for required tests. Level 2 inputs could be generally acquired from limited testing, selected from an agency database, or derived through correlations. Level 3 inputs provide the lowest level of accuracy and are generally default values or typical average values for the region. The dynamic modulus (|E*|) is used as input for the hot mix asphalt layers in the MEPDG. The |E*| test is a part of the Asphalt Mixture Performance Tests (AMPTs), which includes flow number (F_N), and flow time (F_T) tests, that were developed during NCHRP Project 9-19 *[2]*. These tests were recommended to complement the Superpave volumetric mixture design method, since the Superpave volumetric mixture design method alone was not sufficient to ensure reliable mixture performance over a wide range of traffic and climatic conditions *[3]*.

Problem Statement

The Superpave volumetric mix design procedure developed during the Strategic Highway Research Program (SHRP) did not include a mechanical "proof" test similar to the ones commonly used in the Marshall mix design or Hveem mix design. These tests include the Marshall stability and flow tests or the Hveem stabilometer method, respectively. The Superpave mix design method, however, did use stricter requirements to material specifications and volumetric mix criteria to ensure satisfactory performance of mix designs that were intended for low volume traffic. In addition, the original Superpave mix design protocol required mix verification for intermediate and high volume traffic through advanced material characterizations tests utilizing the Superpave Shear Tester protocols. The complexity of those test protocols for routine mix design application was quickly recognized and it was also acknowledged that a simple performance test is needed to complement the Superpave volumetric mix design procedure. In response to this need, NCHRP Project 9-19, Superpave Support and Performance Models Management, recently recommended three candidate Simple Performance Tests (SPTs) to complement the Superpave volumetric mixture design method. These are flow time (F_T), flow number (F_N), and dynamic modulus (|E*|) tests. In addition, the dynamic modulus test was selected for the HMA materials characterization input utilized in the Mechanistic Empirical Pavement Design Guide (MEPDG) developed under NCHRP Project 1-37A *[1]*.

The primary objective of this research is to characterize common Louisiana hot mix asphalt mixtures as defined by the SPTs protocols for quality assurance (QA) and to create a catalog for dynamic modulus value inputs in the MEPDG software. The secondary objective is to

evaluate the sensitivity of rut prediction models from MEPDG software using the dynamic modulus (|E*|) test results. In addition, the Witczak and Hirch models will be evaluated, for the prediction of dynamic modulus (|E*|) values for the asphalt mixtures.

OBJECTIVE

The objective of this research is to characterize common Louisiana hot mix asphalt mixtures and to develop a catalog for dynamic modulus value inputs in the MEPDG software. The specific objectives included are:

- Determine the dynamic modulus, |E*|, and phase angle, δ, at various temperatures and frequencies, in axial and indirect tension (IDT) modes;
- Compare the dynamic modulus test results from the axial and IDT mode;
- Determine the flow time (F_T) values;
- Determine the flow number (F_N) values;
- Evaluate the performance of mixtures from master curves of |E*|;
- Validate the Witczak and Hirsch models in |E*| prediction for local mixtures;
- Investigate the sensitivity of rutting, as computed by the MEPDG software due to variation in |E*| values; and
- Calibrate the rutting prediction model in the MEPDG.

SCOPE

Commonly used Louisiana asphalt mixtures designed for different traffic volumes, as per the Louisiana Standard Specifications for Roads and Bridges (2000 Edition), were selected in this study *[4]*. The total of 28 mixtures included in the study have the following properties:

Materials included:

- Hot-mix asphalt (HMA) and warm-mix asphalt (WMA) mixtures designed as Superpave, Marshall, and Stone Mastic Asphalt (SMA)
- Nominal maximum aggregate size (NMAS): three levels of NMAS are included in this study. These are 1.0 (25.0), 0.75 (19.0), and 0.50-in. (12.5-mm);
- Asphalt Cement: three asphalt binders, PG76-22, PG70-22, and PG 64-22, as specified in the LADOTD Standard Specification;
- Compaction Level (N_{des}): Asphalt mixtures were compacted at three N_{des} levels, which are 75, 100, and 125 for Level 1, Level 2, and Level 3 traffic in the Superpave system, respectively.

Laboratory tests to characterize the selected materials include a series of asphalt binder characterization tests and a suite of asphalt concrete characterization tests as listed below.

Binder tests:

- Dynamic Shear Rheometer (DSR) test: Complex shear modulus (G*) and phase angle (δ) test on Original, Rolling Thin Film Oven (RTFO), and Pressure Aging Vessel (PAV) aged binders at a frequency of 10 rad/sec per AASHTO T315 specification
- Rotational Viscometer (RV) test: Viscosity tests at three temperatures (60, 135, 165ºC)

Mixture tests:

- Dynamic modulus (|E*|) in the axial mode at various temperature and frequencies
- Flow number (F_N) test
- Flow time (F_T) test
- Loaded Wheel Tracking (LWT) device test
- Indirect Tension (IDT) Dynamic modulus test

Three replicate samples were tested for all laboratory tests except the LWT test, where two replicate samples were tested.

LITERATURE REVIEW

Evolution of the MEPDG

The historical development of pavement design dates back to the 1920s. Several significant road tests have been conducted since the early 1920s, but the American Association of State Highway Officials (AASHO) Road Test was the most comprehensive of all the tests. The AASHO Road Test was conceived and sponsored by AASHO to study the performance of pavement structures of known thickness under moving loads of known magnitude and frequency *[5]*. This test was conducted in Ottawa, Illinois, in the late 1950s and early 1960s. It revolutionized pavement design with the introduction of Pavement Serviceability, Equivalent Single Axle Load (ESAL) and Structural Number (SN) concepts and developed equations relating these concepts which form the basis of the design procedures recommended by AASHO Design procedure *[6]*. The AASHO Road Test data provided empirical relationships between asphalt concrete slab thickness, load magnitude, axle type, number of load applications, and serviceability loss of the pavement for road test conditions.

The AASHO Committee on Design first published an interim design guide in 1961 based on the results obtained from the AASHO Road Test. Interim versions of the AASHO Design Guide were published in 1972 and 1981, although no changes were made to the flexible pavement design procedure in the latter interim guide *[7], [8]*. In 1984-85, the subcommittee on pavement design and a team of consultants revised and expanded the guide under National Cooperative Highway Research Program (NCHRP) Project 20-7/24 and issued the AASHTO Design Guide in 1986. The 1986 AASHTO Design Guide for flexible pavement model represented a major extension of the original pavement performance model developed from the results of the AASHO Road Test *[9]*. Several extensions and enhancements of the 1986 model were made in an attempt to expand the applicability of the model to different climates, designs, materials, and soils that exist across the United States. In 1993, a revised version of the AASHTO Design Guide was published *[10]*.

The various versions of the AASHTO Design Guide were based on the results obtained from the AASHO Road Test that included the influence of environment, roadbed soil and paving materials of only northern Illinois. Some other limitations of the AASHO Road Test are:

- Design levels of heavy truck traffic volume have increased significantly (i.e., about 10 to 20 times) since the first design of the Interstate highway system in the 1960s *[1]*. The original Interstate pavements were designed for 5 to 15 million trucks,

whereas today these same pavements must be designed for 50 to 200 million trucks. The existing AASHO Design Guide cannot be used reliably to design for this level of traffic *[1]*.

- Pavement rehabilitation design procedures were not considered at the AASHO Road Test. Procedures in the 1993 AASHTO Guide are completely empirical and very limited, especially in consideration of heavy traffic.
- Because the AASHO Road Test was conducted at one specific geographic location, it is impossible to address the effects of different climatic conditions on pavement performance.
- One type of subgrade was used in all of the test sections at the AASHO Road Test, but many types exist nationally that result in different performance of highway pavements.
- Vehicle suspensions, axle configurations, tire types, and tire pressures were representative of the traffic load characteristics used in the late 1950s. Many of these characteristics have been changed considerably (e.g., tire pressure of 80 (0.6) psi (MPa) versus 120 (0.8) psi (MPa) today), resulting in deficient pavement designs to carry these loadings.

The principal disadvantage of the empirical approach is that the validity of the relationships is limited to the conditions in the underlying data from which they were inferred. These relationships generally do not have a firm scientific basis, but are often used as an expedient when it is too difficult to define the precise cause-and-effect relationships of a phenomenon theoretically. The various versions of the AASHO Design Guide have served well for several decades. However, low design traffic volumes, out-of-date traffic load characteristics, short test duration, limited material types and climate conditions, and other deficiencies of the original AASHO Road Test raised questions and concerns regarding the continuous reliance on the AASHO Design Guide as the nation's primary pavement design procedure.

In recent years, pavement design has been experiencing a shift from the traditional empirical approach to the mechanistic-based approach. Mechanistic pavement design procedures are based on relationships between pavement loading conditions and the corresponding pavement's responses to these loads (such as stresses, strains, or deformations). In practice, however, it is extremely difficult to thoroughly characterize the loads or the material responses. The result is that most mechanistic design procedures are actually a combination of mechanistic theory and empirical observations, so are more accurately referred to as mechanistic-empirical design methods. Mechanistic-empirical design approaches use empirical equations to relate observed field performance to pavement responses, thus

combining the theory and physical testing of a mechanistic method with observed performance.

The perceived deficiencies of the empirical design approach were the motivation for the development of the mechanistic-empirical pavement design methodology in NCHRP 1-37A, "Development of the 2002 Guide for the Design of New and Rehabilitated Pavement Structures." Numerous efforts have been made in this regard; however, the most comprehensive and recent effort was carried out through NCHRP Research Project 1-37A *[1]*.

The Mechanistic-Empirical Pavement Design Guide (MEPDG) is a new product resulting from the efforts initiated by the AASHTO Joint Task Force on Pavements and NCHRP to enhance and improve existing design procedures *[1]*. The models were calibrated using data from the long term pavement performance (LTPP) database for conditions representative of the entire U.S. The MEPDG requires the dynamic modulus in the asphalt concrete layer as shown in Table 1. The dynamic modulus test, which is a part of the AMPTs, is obtained from laboratory testing of asphalt mixtures or prediction equations. The following sections present the literature review of the usage of the MEPDG and evaluation of AMPT parameters conducted by several researchers.

Research Studies on the Evaluation of the MEPDG

The MEPDG was investigated in many studies to verify its performance and prediction of pavement distresses. This section documents some of the studies that were performed to evaluate the MEPDG.

Rodenzo et al. conducted a study to assess the distresses predicted using the new MEPDG for conventional HMA reconstruction on the Interstate 40 highway *[11]*. Actual data measurements that summarize the pavement performance were compared to calculated values obtained using the MEPDG. Three pavement performance parameters were evaluated based on the available data: rutting, cracking, and International Roughness Index (IRI) ride smoothness. The findings in this study indicated that the rutting in conventional HMA was one of the distresses that the MEPDG predicted more accurately. The predicted fatigue cracking from the MEPDG was not as accurate as expected. The predicted IRI results for the conventional HMA varied significantly from the measured field performance. This could be a consequence of inaccurate results for the predicted distress.

Yang et al. performed a preliminary sensitivity analysis of the MEPDG for new flexible pavements *[12]*. The study was divided into two parts: the first was a sensitivity analysis of the overall software; and the second a comparative study between measured data at the AASHO Road Test and predicted by the MEPDG software. Three pavement structures that matched the AASHO Road Test pavement sections were used for the comparative study: AASHO test sections 258, 418, and 602. The findings from the study indicated that, for most cases, computer output trends appeared to follow the predictive algorithms given in the MEPDG. Rutting measured after 500,000 passes was twice the predicted rutting and measured cracking was quite lower than the predicted cracking obtained from the MEPDG. It was reported at the time of this study that the MEPDG software did not have the functionality for allowing the user to specify exactly the desired material properties and environmental conditions as those thought to exist at the AASHO test site.

The MEPDG requires the Dynamic modulus (|E*|) as its input in the asphalt concrete layer as shown in Table 1.1. The dynamic modulus used in Level-1 is obtained by laboratory testing of asphalt mixtures and prediction models are used to obtain the dynamic modulus in Level-2. This section presents the theoretical background of the dynamic modulus, development of dynamic modulus master curves, and prediction equations. In addition, also documented are studies performed by several researchers to evaluate the dynamic modulus.

Background of Dynamic Modulus (|E*|)

Complex Modulus, E*, is a complex number that defines the relationship between stress and strain under sinusoidal loading for linear viscoelastic materials like asphalt mixtures *[2]*. The real part of the complex number represents the elastic stiffness and the imaginary part represents the viscous part of the materials *[6]*. The real and imaginary portions of E* can be divided as shown in equation (1).

$$E^* = E' + iE'' \quad (1)$$

and,

$E^* = |E^*| \cos\delta + i|E^*| \sin\delta$

E′ is generally referred to as the storage modulus or elastic modulus component of the complex modulus, and E″ is referred to as the loss or viscous modulus. The absolute value of the complex modulus, i.e., |E*|, is defined as the dynamic modulus. The dynamic modulus is mathematically defined as the maximum (i.e., peak) dynamic stress (σ_o) amplitude divided by the peak recoverable strain (ε_o) amplitude, as shown in equation (2).

$$|E^*| = \frac{\sigma_o}{\varepsilon_o} \tag{2}$$

The phase angle, δ, is the angle by which ε_o lags behind σ_o as shown in Figure 1. It is an indicator of the viscous property of the material being evaluated and it is expressed as shown in equation (3). For a pure elastic material, δ=0, and for pure viscous materials, δ=90°. It is computed as follows:

$$\delta = \frac{T_i}{T_p} \times 360^\circ \tag{3}$$

where,

T_i = time lag between stress and strain

T_p = period of applied stress

Research Studies on the Evaluation of Dynamic Modulus (|E*|)

The dynamic modulus test is one of the oldest mechanistic tests used to measure the fundamental properties of hot mix asphalt mixtures *[2]*. Several studies have been conducted in evaluating the dynamic modulus as an indicator for pavement rutting and cracking.

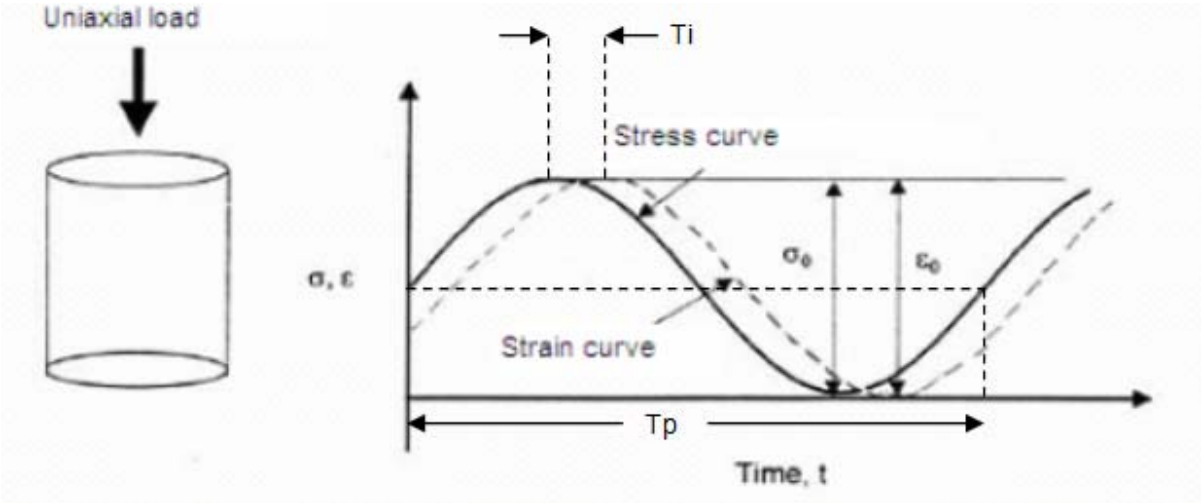

Figure 1
Mixture stress-strain response under sinusoidal load

Pellinen evaluated several mixtures from different test sites to demonstrate that dynamic modulus (stiffness) could be used as a performance indicator to compliment the Superpave volumetric mix design system *[13]*. A total of thirty mixtures were tested from MnRoad

(Minnesota), ALF (Virginia), and WesTrack (Nevada) test sites. The mixtures evaluated from the MnRoad test site were 1.0-in. (12.5-mm) nominal maximum aggregate size (NMAS) dense graded mixtures and the binders used in these mixtures were two unmodified binders (AC-20 and 120/150 PEN). The mixtures evaluated from the ALF test site were 0.75-in. (19.0-mm) and 1.5-in. (37.5-mm) dense graded and the binders used in these mixtures were, three conventional binders (AC-5, AC-10, AC-20) and two modified binders (Styrelf and Novophalt). The third test site, WesTrack, evaluated 19-mm fine and coarse dense graded mixtures and an unmodified binder (PG 64-22) was used. The following findings were reported *[13], [14]*:

- Dynamic modulus correlated well with the in-situ permanent deformation of the evaluated field test sections.
- Dynamic modulus correlated well with fatigue cracking and moderately with thermal cracking.
- Dynamic modulus reached its peak value at minimum VMA.

Zhou et al. conducted a study on premature rutted sections on Route US 281 in Texas *[15]*. The main objective of this study was to validate the AMPTs for permanent deformation. The testing site consisted of twenty sections. AC-20 binder without any modification was used in all the test sections and all the sections were subjected to identical traffic loadings. It was concluded from this case study that the dynamic modulus and E*/Sinδ clearly distinguished the good mixtures from the bad ones.

Kim et al. developed a database of forty-two mixtures commonly used in North Carolina, which consisted of various aggregate sources, aggregate gradations, asphalt sources, asphalt grades, and asphalt contents *[16]*. This database was used to investigate the effects of different mixture variables on the dynamic modulus. The following conclusions were determined:

- Aggregate sources and gradation, within the NCDOT Superpave classification, did not seem to have a significant effect on dynamic modulus.
- The binder source, binder PG, and asphalt content seemed to affect the dynamic modulus of asphalt mixtures.

Amit et al. conducted dynamic modulus, flow time, flow number, and asphalt pavement analyzer tests on twelve field mixtures and three laboratory mixtures to evaluate rutting *[17]*. Two of the laboratory mixtures were prepared using a modified binder with two types of

aggregate, crushed rhyolite and crushed river gravel. A third laboratory mixture contained uncrushed river gravel as well as conventional asphalt and was intentionally designed to be rut susceptible. The findings indicated that caution must be exercised in interpreting rut susceptibility of mixtures based on dynamic modulus test parameters, especially when evaluating mixtures containing polymer-modified asphalts.

Mohammad et al. conducted a laboratory study in order to characterize the permanent deformation characteristics of hot mix asphalt mixtures based on four laboratory tests, namely, the dynamic modulus (|E*|), flow number, frequency sweep at constant height (FSCH), and Hamburg-type loaded wheel tracking tests *[18]***.** In addition, sensitivity of the dynamic modulus (|E*|) test results in pavement rutting performance prediction using the MEPDG was also evaluated. Three nominal maximum aggregate size mixtures— 0.5(12.5), 0.75 (19) and 1.0-in. (25-mm)—were used in this study. The binder used in the study was PG76-22M for all the mixtures. The following were some of the observations made from this study:

- The dynamic modulus (|E*|) test was sensitive to the nominal maximum aggregate size (NMAS) in a mixture. Larger aggregates tend to have high |E*| values at high temperatures.
- The |E*| test results at high temperatures could not differentiate the permanent deformation characteristics for the six asphalt mixtures evaluated in this study.

Mohammad et al. performed a collaborative study between the Louisiana Transportation Research Center (LTRC) and the Federal Highway Administration's (FHWA) Mobile Asphalt Mixture Laboratory *[19]***.** The main objective of the study was to compare test results of two SPTs—dynamic modulus and flow number tests—measured from the two laboratories. In addition, empirical dynamic modulus prediction models, namely the Hirsch and Witczak's models, were evaluated by comparing the predicted dynamic modulus values to the measured dynamic modulus values. Two asphalt mixtures, a 1.0-in. (25-mm) Superpave binder mixture containing PG76-22M binder and a 1.0-in. (25-mm) Superpave base mixture containing PG 64-22 binder, were considered in this study. The following conclusions were determined from this study:

- The dynamic modulus test results were sensitive to the PG grade of the binder.
- Both the dynamic modulus and flow number tests provided consistent results for plant-produced mixtures.

- Both the dynamic modulus and flow number values seemed to be sensitive to binder contents in the mixture.
- Both the Witczak's and the Hirsch models predicted the dynamic modulus values within a reasonable reliability.

Nam et al. evaluated the effects of strain levels on the recorded dynamic modulus values and predicted pavement performance *[20]*. A 0.5-in. (12.5-mm) surface mixture using a PG70-22 binder was used in this study. The findings in this study indicated that:

- The difference in the dynamic modulus values for different strain levels was more significant at higher temperatures.
- The predicted rutting values from the MEPDG were higher for mixtures tested at higher strain levels than similar mixtures tested at lower strain levels.

Development of Master Curves

In the MEPDG, asphalt mixtures are characterized by a master curve incorporating time and temperature effects directly into the solution methodology *[1]*. The rheological properties of hot mix asphalt mixtures depend on both temperature and loading frequency. At short loading times or low temperatures, the elastic response dominates; at long loading times or high temperatures, the viscous response dominates; and at intermediate loading times and temperatures, the delayed elastic response dominates. Therefore, to understand the mechanical properties of asphalt concrete, it has to be characterized under combinations of wide ranges of temperatures and loading frequencies. At each temperature, the |E*| vs. frequency data are obtained from the testing and these data are combined into a single "master curve" by shifting the individual curves along the frequency axis at an arbitrarily selected reference temperature, as shown in Figure 2. The master curve of the dynamic modulus formed in this manner describes the loading rate dependency of the material.

For each curve determined at a particular test temperature, a horizontal shift factor a(T) is computed and these shift factors are a function of temperature. The amount of shifting at each temperature required to form the master curve describes the temperature dependency of the material. Thus, both the master curve and the shift factors are needed for a complete description of the rate and temperature effects. The dynamic modulus master curve can be represented by a sigmoid function shown in equation (4).

$$\log(|E^*|) = \delta + \frac{\alpha}{1 + e^{\beta + \lambda(\log t_r)}} \quad (4)$$

where,

|E*| = dynamic modulus

t_r = time of loading at reference temperature

δ = minimum value of |E*|

$\alpha + \delta$ = maximum value of |E*|

β, γ = parameters describing the shape of the sigmoidal function.

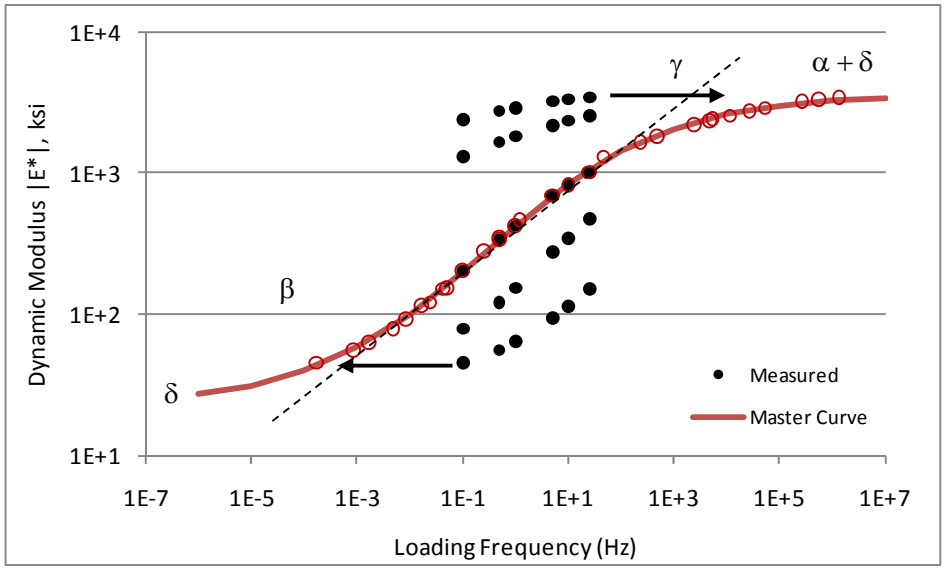

Figure 2

Construction of |E*| master curve and master curve parameters

The parameters as shown in equation (4) and Figure 2, δ and α, depend on aggregate gradation, binder content, and air void content, whereas β and γ depend on the characteristics of the asphalt binder and the magnitude of δ and α *[21]*. Parameter β determines the horizontal location of the transition zone and parameter γ determines the slope (23). The shift factors describe the temperature dependency of the modulus. equation (5) provides the general form of the shift factors *[21]*:

$$t_r = \frac{t}{a(T)} \qquad (5a)$$

and

$$\text{Log}(t_r) = \log(t) - \log[a(T)] \qquad (5b)$$

where,

t_r = time of loading at the reference temperature

t = time of loading

a(T) = shift factor as a function of temperature (T).

The dynamic modulus master curve constructed from values obtained from the laboratory testing or from predictive equations is utilized in the MEPDG to account for temperature and rate of loading effects of asphalt mixtures at all analysis levels.

Prediction Equations for the Dynamic Modulus (|E*|)

Several regression models have been developed to predict the asphalt concrete modulus over a number of years. Among them, the models developed by Witczak and Christensen have been reported to be reasonably accurate *[22], [23].* These models relate | E*| to loading rate, temperature-dependant binder viscosity, and mixture volumetric and gradation parameters.

Witczak Predictive Equation. The Witczak's model could provide sufficiently accurate and robust estimates of | E*| for use in mechanistic-empirical pavement performance prediction and design *[24].* Witczak's prediction model uses a symmetrical sigmoidal function as shown in equation (6).

$$Log|E^*| = 3.750063 + 0.029232p_{200} - 0.001767(p_{200})^2 - 0.002841p_4 - 0.058097V_a - 0.802208\left(\frac{V_{beff}}{V_{beff}+V_a}\right) + \frac{3.87197 - 0.0021p_4 + 0.003958p_{38} - 0.000017(p_{38})^2 + 0.00547p_{34}}{1+e^{(-0.603313-0.31335log(f)-0.393532log(\eta))}} \quad (6)$$

where,

E = Asphalt Mix Dynamic Modulus, in 10^5 psi

η = Binder viscosity in 10^6 poise

f = Load frequency in Hz

Va = % air voids in the mix, by volume

Vb_{eff} = % effective binder content, by volume

p_{34} = % retained on the ¾ in. sieve, by total aggregate weight (cumulative)

p_{38} = % retained on the 3/8-in. sieve, by total aggregate weight (cumulative)

p_4 = % retained on the No. 4 sieve, by total aggregate weight (cumulative)

p_{200} = % passing the No. 200 sieve, by total aggregate weight.

The Witczak's prediction model is a purely empirical regression model developed from a large database of over 2700 laboratory test measurements of | E*| compiled over nearly 30 years *[24].*

Hirsch Prediction Model. The Hirsch model developed by Christensen is both simpler and rational and requires only binder modulus, VMA, VFA for predicting asphalt concrete modulus *[23]*. The Hirsch model is given by equation (7).

$$|E^*| = P_c\left[4{,}200{,}000\left(1-\frac{VMA}{100}\right)+3|G^*|_{binder}\left(\frac{VFA\times VMA}{10{,}000}\right)\right]+(1-P_c)\left[\frac{1-VMA/100}{4{,}200{,}000}+\frac{VMA}{3VFA|G^*|_{binder}}\right]^{-1}$$

$$P_c = \frac{\left(20+\frac{VFA\times 3|G^*|_{binder}}{VMA}\right)^{0.58}}{650+\left(\frac{VFA\times 3|G^*|_{binder}}{VMA}\right)^{0.58}} \qquad (7)$$

where,

$|E^*|$ = Dynamic Modulus of the asphalt mixture, in psi
$|G^*|_{\text{binder}}$ = Complex Shear Modulus of the binder, in psi
P_c = Contact Factor
VMA = Voids in the mineral aggregate, percent
VFA = Voids filled with asphalt, percent.

It is observed from equation (7) that the dynamic modulus obtained from the Hirsch model is a function of binder and volumetric properties.

Asphalt Mixture Performance Tests (AMPTs)

Flow time (F_T) and Flow number (F_N) tests are part of the AMPTs that were recommended by the NCHRP Project 9-19 to complement the Superpave volumetric mixture design method *[2]*. The theoretical background of these tests, as well as the studies conducted to evaluate the flow time and flow number as indicators of pavement rutting, has been documented in the following sections.

Theoretical Background of Static Creep Test (Flow Time)

The modulus of a material is an important property, as it relates stress to strain. For visco-elastic materials, however, it is more advantageous to use the term compliance D(t). Compliance is the reciprocal of modulus and is expressed by equation (8) *[25]*.

$$D(t) = E(t)^{-1} = \frac{\varepsilon(t)}{\sigma_d} \quad (8)$$

The advantage of using the compliance for viscoelastic materials is that it allows for the separation of the strain components (e.g., ε_e, ε_p, ε_{ve}, and ε_{vp}) at a constant stress level as shown in equation (9) *[25]*.

$$\varepsilon(t) = \sigma_d * D(t) = \sigma_d (D_e + D_p + D_{ve}(t) + D_{vp}(t)) \quad (9)$$

where,

D_e = instantaneous recoverable elastic compliance

D_p = instantaneous non-recoverable plastic compliance

$D_{ve}(t)$ = time dependant viscoelastic (recoverable) compliance

$D_{vp}(t)$ = time dependant viscoplastic (non-recoverable) compliance.

This test aims at measuring the viscoelastic response of hot mix asphalt mixtures under a static load. In this test, a total strain-time relationship for a mixture is measured under unconfined or confined conditions. In a typical plot of log compliances versus log time, three basic zones have been identified, i.e., primary, secondary, and tertiary *[26]*. In the primary zone, the strain rate decreases sharply with loading time and tends to stabilize reaching the secondary zone. In the secondary zone, the strain rate is constant and starts increasing in the tertiary zone with loading time. These three zones are shown in Figure 3.

The large increase in compliance occurs at a constant volume within the tertiary zone. The starting point of the tertiary zone is referred to as the flow time *[26]*. It is viewed as the time when the rate of change of compliance is the lowest. Therefore, the flow time, F_T, is defined as the time at which the shear deformation under constant volume begins *[7]*. The flow time has been found to be a significant parameter in evaluating hot mix asphalt mixture's rutting resistance *[2]*.

The total compliance D(t) in the secondary zone at any given time can be expressed as a power function represented by equation (10).

$$D(t) = at^m \quad (10)$$

where,

t = time

a, m = regression constants

The regression constants are obtained by plotting compliance versus time on a log-log scale in the secondary zone, as shown in Figure 4. The expression can then be rewritten as:

$$\text{Log } D(t) = m \log (t) + \log (a) \qquad (11)$$

where,

m = slope of the curve on a log-log scale

a = intercept.

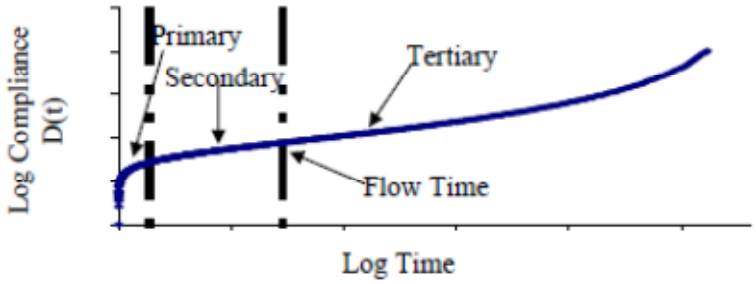

Figure 3
Compliance versus Time on log-log scale

The regression constants "a" and "m" are generally referred to as the compliance parameters. These parameters are generally good indicators of permanent deformation behavior of the asphalt mixtures *[2]*. The larger the value of a, the larger the compliance value, D(t), the lower the modulus, and the larger the permanent deformation. For a constant a-value, an increase in the slope parameter m, means higher permanent deformation. For tests at a given temperature, axial stress, and confining stress, the rutting resistance of the mixtures increases as the flow time increases.

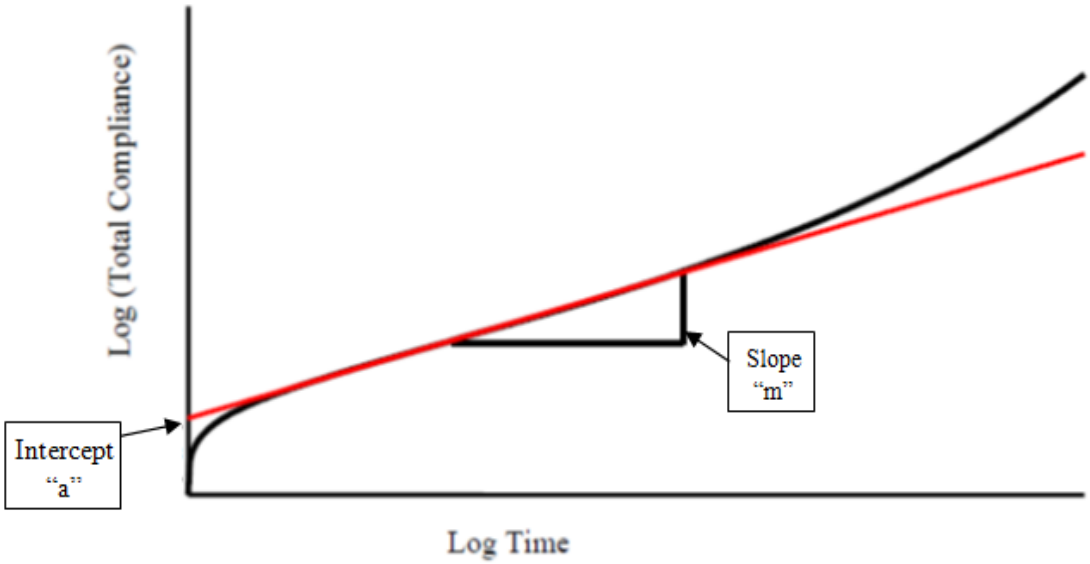

Figure 4
Regression constants a and m when plotted on a log-log scale

Theoretical Background of Repeated Load Test (Flow Number)

The repeated load test is one more test to identify the permanent deformation characteristics of hot mix asphalt mixtures, by applying several thousand repetitions of a repeated load and recording the cumulative deformation as a function of the number of load cycles. A number of parameters describing the accumulated permanent deformation response are obtained from this test. The cumulative permanent strain curve is generally defined by three zones: primary, secondary, and tertiary, like the static creep test. The permanent deformation accumulates rapidly in the primary zone, and in the secondary zone the incremental deformations decrease reaching a constant value, as shown in Figure 5. In the tertiary zone, the permanent deformations again increase and accumulate rapidly. The starting point, or cycle number, at which tertiary flow occurs, was referred to as the flow number *[2]*. The permanent strain is also expressed a power function in terms of the number of cycles represented by equation (12).

$$\varepsilon_p = aN^b \qquad (12)$$

where,

a, b = regression constants

N = number of load cycles.

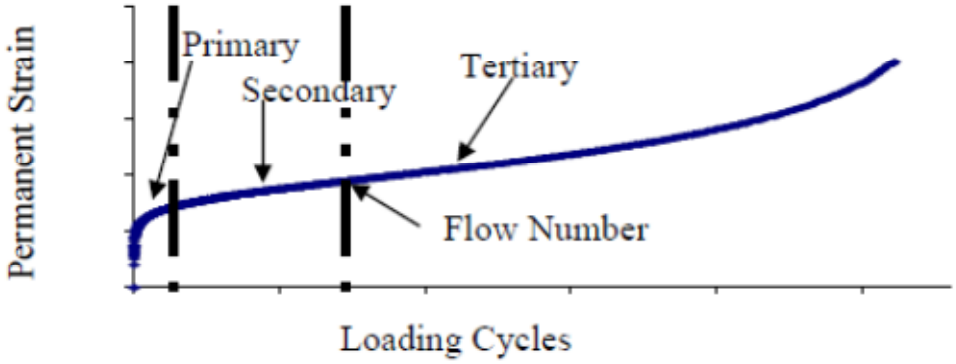

Figure 5
Permanent strain versus loading cycles on a log-log scale

The regression constants are obtained by plotting permanent strain versus number of cycles on a log-log scale in the secondary zone, as shown in Figure 6. The above expression can then be rewritten as shown in equation (13).

$$\text{Log } \varepsilon_p = b \log (N) + \log (a) \qquad (13)$$

where,

b = slope of the curve on a log-log scale

a = intercept.

Several parameters were obtained and analyzed from the repeated load permanent deformation test. However, the regression constants “a” and “b” were found to have good correlations with field rutting *[2]*.

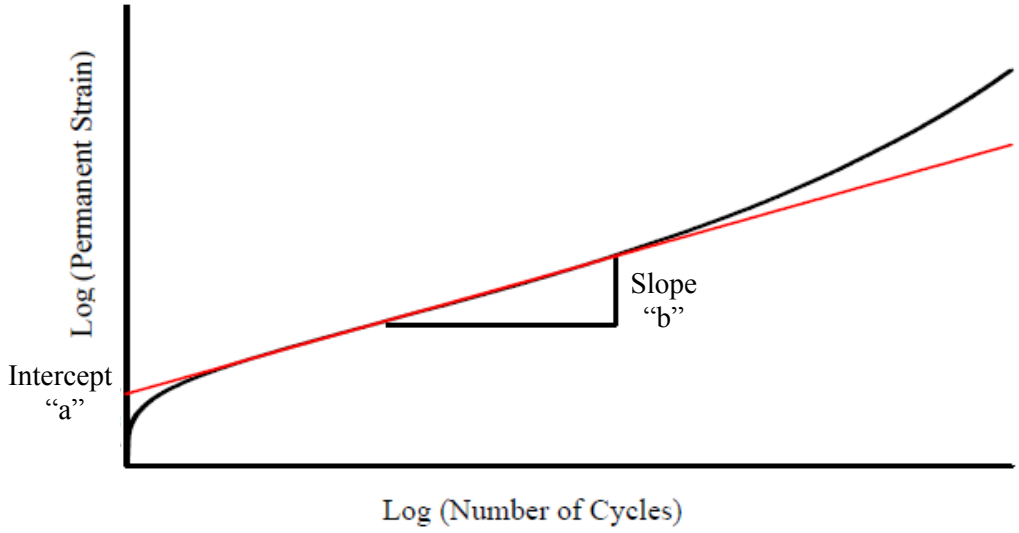

Figure 6
Regression constants a and b when plotted on a log-log scale

Research Studies on the Evaluation of Flow Time and Flow Number

The repeated load test (Flow Number) and the static load test (Flow Time) are part of the AMPTs that were developed to compliment the Superpave volumetric design procedure. The flow number and flow time tests are two different tests to identify the permanent deformation characteristics of hot mix asphalt mixtures. Many studies have been conducted for evaluating the flow number and flow time test results as rut indicators. Some of the studies conducted by several researchers to evaluate the flow number and flow time test results have been documented.

Kaloush et al. evaluated the AMPTs for permanent deformation to be used with the Superpave volumetric mixture design procedure *[27]*. The flow number and flow time tests were evaluated using mixtures and performance data from three experimental sites: the Minnesota Road Project (MnRoad), the Federal Highway Administration (FHWA) Accelerated Loading Facility Study (ALF), and the FHWA Performance-Related Specifications Study (WesTrack). The findings in this study indicated that the flow number and the flow time values test stood out to have excellent correlation with field rut depth data. These two parameters were found to be repeatable and reliable in distinguishing among a wide range of asphalt mixtures. The research team ranked the tests/parameters based on the comprehensive evaluation conducted. The top three tests for permanent deformation were: 1) the dynamic modulus, (E^*, $E^*/\sin\delta$), 2) the flow time, and 3) the flow number *[28]*.

Amit et al. conducted a critical evaluation of the dynamic modulus, flow number, and flow time tests along with the Superpave shear test - frequency sweep at constant height (SST-FSCH) with the Asphalt Pavement Analyzer (APA) as the torture test to identify mixes susceptible to permanent deformation *[29]*. Nine hot mix asphalt mixtures were obtained from state DOTs in the South Central Region of the U.S. including Arkansas, Arizona, Louisiana, New Mexico, Oklahoma, and Texas, with varied degrees of reported field performance. Three nominal maximum aggregate size mixtures—0.375 (9.5), 0.5 (12.5) and 0.75-in. (19-mm)—were used in this study. The binders used in the study were PG 64-22, PG70-22, PG70-22M, PG 82-16, PG76-22M and PG 64-40. Results indicated that flow number value and flow time slope correlated better with laboratory rutting (APA and LWT) than dynamic modulus.

METHODOLOGY

Field Projects and Materials

Field Projects

A total of 14 field projects were identified and selected to provide a total of 28 asphalt concrete mixtures for the proposed characterization testing suite. Locations of these field projects are shown in Figure 7. Details of locations, mixture designations, NMAS, traffic levels, and design methods are also summarized in Table 2. The selection of projects was coordinated with the Louisiana Department of Transportation and Development (LADOTD) construction and research personnel.

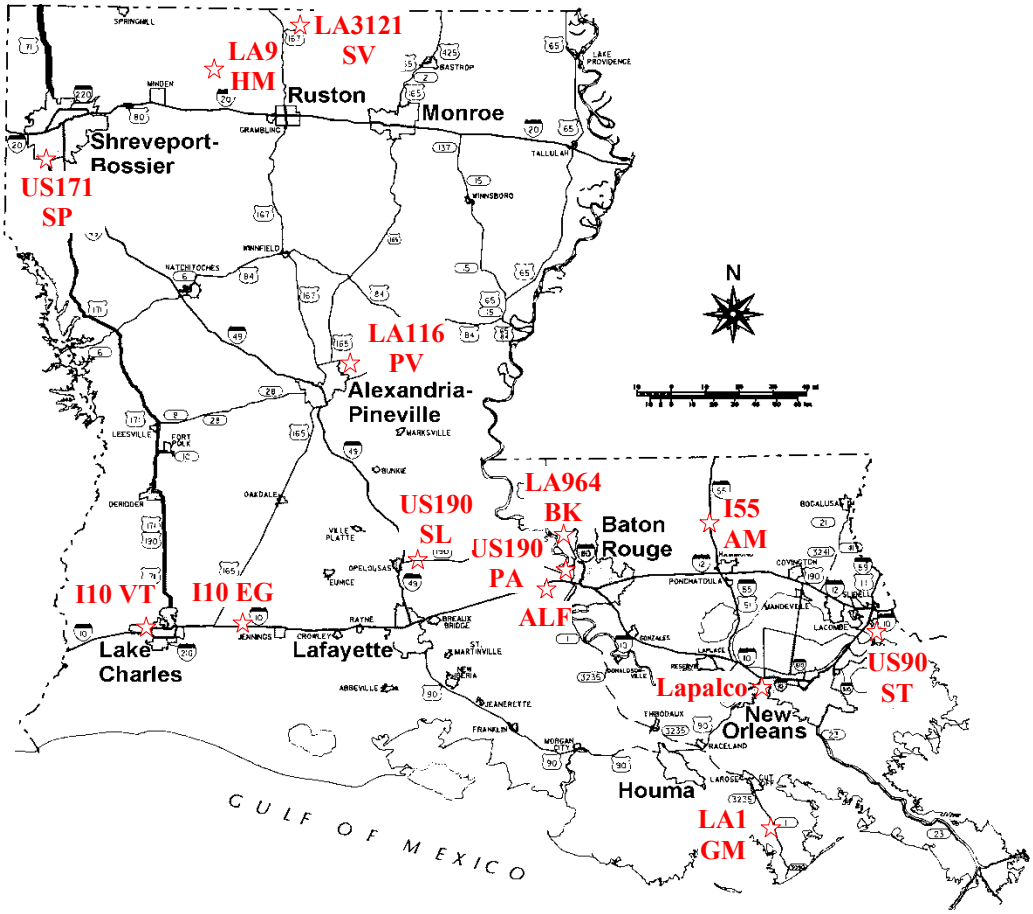

Figure 7
Field projects evaluated in the study

Table 2
Field projects and mixtures

Traffic Level	Mix Type	Project Location	Mix Code	Mix Type	Asphalt Grade	NMAS (mm)	Remarks
Level 1	Superpave	LA9 HM (Homer)	LA9-1	HMA[4]-Wearing	PG70-22M	12.5	
		Lapalco (New Orleans)	LPC-1	HMA-Binder	PG70-22M	25	
		US90 ST (St. Tammany)	US90-1	HMA-Binder	PG70-22M	25	
		LA3121 SV (Spearsville)	3121-1	HMA	PG70-22M	12.5	15% RAP
			3121-2	WMA[5]	PG70-22M	12.5	15% RAP
			3121-3	WMA	PG70-22M	12.5	30% RAP
		US171 SP (Shreveport)	171-1	HMA	PG70-22M	12.5	15% RAP
			171-2	WMA	PG70-22M	12.5	15% RAP
			171-3	WMA	PG70-22M	12.5	30% RAP
			171-4	WMA	PG70-22M	12.5	Rediset
		LA116 PV (Pineville)	116-1	HMA	PG70-22M	12.5	15% RAP
			116-2	HMA	PG70-22M	19	20% RAP
			116-3	WMA	PG70-22M	12.5	15% RAP
			116-4	WMA	PG70-22M	19	20% RAP
Level 2	Superpave	US190 PA (Port Allen)	190-1	HMA-Binder	PG76-22M	25	
			190-2	HMA-Binder	PG76-22M	25	
			190-3	HMA-Base	PG64-22	25	
		US190 SL (St. Landry)	190-4	HMA-Binder	PG76-22M	25	
		ALF (Baton Rouge)	ALF-1	HMA-Wearing	PG76-22M	19	
		LA1 GM (Golden Meadow)	LA1-1	HMA-Binder	PG76-22M	25	
			LA1-2	WMA-Binder	PG76-22M1	25	Sasobit®
Level 3	Superpave	I10 EG (Egan)	I10-1	HMA-Binder	PG76-22M	25	
			I10-2	HMA-Wearing	PG76-22M	12.5	
		I55 AM (Amite)	I55-1	HMA-Binder	PG82-22rm[3]	12.5	PF[1]
			I55-2	HMA-Wearing	PG82-22rm[3]	12.5	PL[2]
	SMA	I10 VT (Vinton)	I10-3	HMA-Wearing	PG76-22M	12.5	
	Marshall	LA964 BK (Baker)	964-1	HMA-Wearing	PG76-22M	19	
			964-2	HMA-Binder	PG76-22M	25	

[1] PF: Plant produced and field compacted asphalt mixture

2) PL: Plant produced and laboratory compacted asphalt mixture
3) PG82-22rm: Crumb Rubber modified asphalt binder
4) HMA: Hot-Mix Asphalt
5) WMA: Warm-Mix Asphalt

Materials

Three asphalt binders, PG76-22M, PG70-22M and PG64-22, meeting LADOTD specifications (Table 3) were used in this study. In addition to these initially specified asphalt binders, a Crumb Rubber Modified (CRM) asphalt binder graded as PG82-22rm was added to the experimental factorial at a later stage of the study as a newly emerged asphalt binder type that has received an increasing amount of attention in Louisiana. The letter "m" after the asphalt binder's PG stands for polymer modification. The Styrene-Butadiene-Styrene (SBS) block copolymers are typically used as the modifier. Mixtures were designed by the contractors. Tables 4 through 6 present the job mix formula for the asphalt mixtures at the design traffic levels of 1, 2, and 3, respectively, according to the earlier version of the Louisiana Standard Specifications for Roads and Bridges (2000 Edition) *[4]*.

Seven mixtures designed for the traffic Level 3 (Table 4) include four Superpave mixtures, which include three 0.5-in. (12.5-mm) and one 1.0-in. (25-mm) NMAS; one 0.5-in. (12.5-mm) NMAS SMA mixture; and two Marshall mixtures, which are 0.75-in. (19-mm) and 1.0-in. (25-mm) NMAS, respectively. Note that one mixture from I-55 was sampled and tested as field cores (PF: Plant mixed Field compacted), while the other 27 mixtures included in the study were sampled and tested as Plant mixed and Lab compacted (PL). It should be also noted that the asphalt binder used for the two I-55 mixtures was Crumb Rubber Modified, PG82-22rm.

Job mix formulas of seven mixtures designed for the Level 2 mixtures are shown in Table 5. Level 2 mixtures include six conventional Superpave mixtures and one Superpave designed WMA mixture. All mixtures in the Level 2 traffic category were produced using PG76-22M asphalt binder except the 190-3 mixture, which used PG64-22 unmodified asphalt binder. The asphalt binder used in LA 1-2 mixture was Sasobit®, a type of modifier used for warm-mix asphalt production, to produce the PG76-22M1 asphalt binder, which slightly differs from the regular PG76-22M asphalt binder. The ALF-1 mixture from an ALF (Accelerated Loading Facility of LTRC located in Baton Rouge) project was a wearing course mixture taken from the 4th experimental section of the ALF *[30]*.

Fourteen Level 1 mixtures designed for low volume traffic are shown in Table 6. In this group, seven conventional Superpave HMA mixtures and seven Superpave WMA mixtures

are included. Three NMAS of 0.5 (12.5), 0.75 (19), and 1.0-in. (25-mm) are included. All 14 mixtures were produced using PG70-22M asphalt binders.

Table 3
Louisiana specification requirements and sample test result for the binders

Test Property	PG 64-22		PG70-22M		PG76-22M		PG76-22M1	
	Spec	Result	Spec	Result	Spec	Result	Spec	Result
Original Binder								
Rotational Viscosity @135°C Pa-s	3.0-	0.5	3.0-	0.9	3.0-	1.34	3.0-	1.6
G*/ Sin δ (kPa) (Dynamic Shear@10rad/sec)	1.30+	1.59	1.00+	1.25	1.00+	1.22	1.00+	2.57
Flash Point (°C)	232+	290	232+	295	232 +	279		
Solubility (%)	99.0+	99.9	99.0+	99.7	99.0+	99.9		
Force Ductility Ratio (F2/ F1, 4°C, 5cm/min, F2 @30cm Elongation)			0.30+	0.31	0.30+	0.42	.30+	broken*
Rolling Thin Film oven (RTFO) Residue								
Mass Loss %	1.00-	0.297	1.00-	0.03	1.00-	0.31		
G*/Sin δ (kPa) (Dynamic Shear@10 rad/sec)	2.20+	3.14	2.20+	2.5	2.20+	2.46		
Elastic Recovery (25°C, 10 cm Elongation %)			40+	65	60+	75	60+	70
Pressure Aging Vessel (PAV) Residue								
G* Sin δ, (kPa) (25°C Dynamic Shear@10 rad/sec)	5000-	2210	5000-	4615	5000-	3212	5000-	3503
BBR Creep Stiffness, Smax (MPa) (–12°C)	300-	204	300-	193	300-	240	300-	169
BBR m Value (Min at -12°C)	0.300+	0.342	0.300+	0.315	0.300+	0.362	0.300+	0.32

Table 4

Job mix formula of asphalt mixtures designed for Level 3 traffic

Mixture Code		I10-1	I10-2	I10-3	964-1	964-2	I55-1	I55-2
Mix type		25-mm HMA	12.5-mm HMA	12.5-mm HMA (SMA)	19mm HMA	25-mm HMA	12.5-mm HMA	12.5-mm HMA
Aggregate blend		32% #5 LS 20% #67 LS 22% #8 LS 18% #11 LS 8% Sand	13% ¾ SS 32% ½ SS 10% #7 LS 5% #8 LS 40% #11 LS	50% #78 SS 25% #78 LS 13% #11 LS 12% LS	44.2% #67Granite 24.7% #11 LS 10.1% C.Sand 6%CR.Grv 15% Rap	33.3% #5 LS 6.4% #67LS 13.4% #11 LS 12% C.Sand 14.3%CR.Grv 20.6% Rap	30%#78 Granite 43%Cr.Grc 13%C.Sand 14%Rap	30%#78 Granite 43%Cr.Grc 13%C.Sand 14%Rap
Binder type		PG76-22M	PG76-22M	PG76-22M	PG76-22M	PG76-22M	PG82-22rm	PG82-22rm
Design volumetric properties	% G_{mm} at N_I	85.4	84.1	N/A	N/A	N/A	N/A	N/A
	% G_{mm} at N_D	96.1	95.9	N/A	N/A	N/A	96.5	96.5
	% G_{mm} at N_M	97.1	97	N/A	N/A	N/A	97.5	97.5
	Design AC, %	4.0	5.0	6.0	4.2	4.0	4.7	4.7
	Design AV, %	4.0	4.0	4.0	4.0	4.0	3.5	3.5
	VMA, %	12.8	14.5	16.6	13.8	12.7	13.5	13.5
	VFA, %	69.5	72	76	71	69	74	74
Gradation, % passing Sieve sizes in mm (US unit)	37.5 (1½ in)	100	100	100	100	100	100	100
	25 (1 in)	96	100	100	100	97	100	100
	19 (¾ in)	87	100	100	96	86	98	100
	12.5 (½ in)	68	98	93	82	68	87	97
	9.5 (⅜ in)	59	89	71	72	62	83	85
	4.75 (No.4)	35	50	30	50	48	65	56
	2.36 (No.8)	23	29	20	34	36	46	40
	1.18 (No.16)	17	19	-	25	27	34	29
	0.6 (No.30)	13	13	15	19	21	26	23
	0.3 (No.50)	7	10	12	11	12	15	13
	0.15 (No.100)	4	-	-	7	6.6	9	6
	0.075 ((No.200)	3.6	6.5	8	5.3	5	6.3	5

Table 5

Job mix formula of asphalt mixtures designed for Level 2 traffic

Mixture Code		190-1	190-2	190-3	190-4	ALF-1	LA1-1	LA1-2
Mix type		25-mm HMA	25-mm HMA	25-mm HMA	25-mm HMA	19-mm HMA	25-mm HMA	25-mm WMA
Aggregate blend		31.6% #5 LS 13.8% #67LS 19.4% #78LS 8% C.Sand 8.1% CR.Grv 19.1% Rap	31.6% #5 LS 8.1% #67LS 19.4%#78 LS 8.1% C.Sand 8.1% CR.Grv 5.7 #11 LS 19% Rap	33.9% #5 LS 6.3% #67LS 12.1%#78 LS 8.1%#11LS 10.5% C.Sand 9.7% CR.Grv 19.4% Rap	25% #5 LS 30%#78LS 30% #11 LS 10% C.Sand 5%F.Sand	45.4%Granite 10.3%csand 17.1%stone 12.9%Cr.Grv 14.3% RAP	34.8% #5 LS 9.0% #7LS 17.4% #78LS 13.6% #11LS 6.2% C.Sand 19% Rap	34.8% #5 LS 9.0% #7LS 17.4% #78LS 13.6% #11LS 6.2% C.Sand 19% Rap
Binder type		PG76-22M	PG76-22M	PG64-22	PG76-22M	PG76-22M	PG76-22M	PG76-22M1
Design volumetric properties	% G_{mm} at N_I	87.9	88.2	89.0	89.4	88.4	87.1	87.1
	% G_{mm} at N_D	96.0	96.4	96.4	96.5	96.1	96.5	96.5
	% G_{mm} at N_M	97.1	97.1	97.0	97.0	96.8	96.7	96.7
	Design AC, %	3.6	3.8	3.3	3.8	4.4	3.8	3.8
	Design AV, %	4.0	3.6	3.6	3.5	3.9	3.5	3.5
	VMA, %	11.8	11.5	11.1	11.8	13.8	12	12
	VFA, %	67	69	67	70	71.0	71	71
Gradation, % passing Sieve sizes in mm (US unit)	37.5 (1½ in)	100	100	100	100	100	100	100
	25 (1 in)	97	95	98	98	100	95	95
	19 (¾ in)	84	86	88	87	97	89	89
	12.5 (½ in)	65	67	65	72	83	76	76
	9.5 (⅜ in)	52	53	53	62	73	67	67
	4.75 (No.4)	32	35	37	49	49	47	47
	2.36 (No.8)	24	27	27	42	33	31	31
	1.18 (No.16)	20	21	22	28	24	23	23
	0.6 (No.30)	15	16	17	22	18	18	18
	0.3 (No.50)	8	9	9	13	10	12	12
	0.15 (No.100)	4.9	6	5	5	5.7	9	9
	0.075 ((No.200)	3.6	4.5	4.2	4.0	4.6	6.8	6.8

Table 6

Job mix formula of asphalt mixtures designed for Level 1 traffic

Mixture Code		LA9-1	US90-1	LPC-1	3121-1	3121-2	3121-3
Mix type		12.5-mm HMA	25-mm HMA	25-mm HMA	12.5-mm HMA	12.5-mm WMA	12.5-mm WMA
Aggregate blend		18%Rhyolite 37% Gravel 15%screens Rhyolite 8% C.Sand 7% F.Sand 15% Rap	23.8% #5 LS 18.2%#7LS 15.5% #911 LS 14.6#11LS 7.1% C.Sand 20.8% Rap	24.2% #5 LS 18.6% #7LS 7.3% C.Sand 14.9%#11LS 15.8%#911LS 19.2% Rap	25.7% #78 25.7% #11 SP 21.4% KY 11 12.9% C.Sand 14.3% RAP	25.7% #78 25.7% #11 SP 21.4% KY 11 12.9% C.Sand 14.3% RAP	21.4% #78 21.4% #11 SP 17.9% KY 11 10.7% C.Sand 28.6% RAP
Binder type		PG70-22M	PG70-22M	PG70-22M	PG70-22M	PG70-22M	PG70-22M
Design volumetric properties	% G_{mm} at N_I	89.5	86.2	87.3	84.2	84.2	84.2
	% G_{mm} at N_D	96.5	95.7	96.4	N/A	N/A	N/A
	% G_{mm} at N_M	97.3	--	95.2	97.3	97.3	97.3
	Design AC, %	4.9	4.0	4.2	4.8	4.8	4.8
	Design AV, %	3.5	4.3	3.6	4.1	4.1	4.1
	VMA, %	13.2	13.1	13	15	15	15
	VFA, %	73.5	67.4	72	73	73	73
Gradation, % passing Sieve sizes in mm (US unit)	37.5 (1½ in)	100	100	100	100	100	100
	25 (1 in)	100	95.3	94	100	100	100
	19 (¾ in)	100	89.8	87	100	100	100
	12.5 (½ in)	92	80.6	75	96	96	96
	9.5 (⅜ in)	82	69.1	67	87	87	87
	4.75 (No.4)	53	46.9	44	53	53	53
	2.36 (No.8)	37	30	26	34	34	34
	1.18 (No.16)	27	21.7	19	23	23	23
	0.6 (No.30)	24	16.8	15	18	18	18
	0.3 (No.50)	17	10.9	10	11	11	11
	0.15 (No.100)	9	7.5	7	6	6	6
	0.075 ((No.200)	5.2	5.6	5.5	3.8	3.8	3.8

Table 6

Job mix formula of asphalt mixtures designed for Level 1 traffic (continued)

Mixture Code		171-1	171-2	171-3	171-4	116-1	116-2	116-3	116-4
Mix type		12.5-mm HMA	12.5-mm WMA	12.5-mm WMA	12.5-mm WMA	12.5-mm HMA	19-mm HMA	12.5-mm WMA	19-mm WMA
Aggregate blend		10% 5/8" Stone 52% 1/2" Stone 15% RAP 10% Screens 7% C.Sand 6% F.Sand	11% 5/8" Stone 46% 1/2" Stone 15% RAP 15% Screens 13% C.Sand	10% 5/8" Stone 38% 1/2" Stone 30% RAP 15% Screens 7% C.Sand	11% 5/8" Stone 46% 1/2" Stone 15% RAP 15% Screens 13% C.Sand	21.5% #78 LS 14.6% # 89 LS 14.1% RAP 36.9% 11 LS 12.9% C Sand	#78 LS 24.3% RAP 18.9% 11 LS 26.8% C Sand 12.2% #67 LS 17.8%	21.5% #78 LS 14.6% # 89 LS 14.1% RAP 36.9% 11 LS 12.9% C Sand	#78 LS 24.3% RAP 18.9% 11 LS 26.8% C Sand 12.2% #67 LS 17.8%
Binder type		PG70-22M	PG70-22M	PG70-22M	PG70-22M	PG70-22M	PG70-22M	PG70-22M	PG70-22M
Design volumetric properties	% G_{mm} at N_I	88.7	88.7	88.2	88.2	88.1	88.4	88.1	88.4
	% G_{mm} at N_D	N/A	N/A	N/A	N/A	N/A	N/A	N/A	N/A
	% G_{mm} at N_M	98	98	97.4	97.5	97.4	97.3	97.4	97.3
	Design AC, %	5	5	5.4	5	4.6	4.1	4.6	4.1
	Design AV, %	3.4	3.3	3.6	3.4	3.7	3.5	3.7	3.5
	VMA, %	14.5	14.5	14	14	14	13	14	13
	VFA, %	78	78	75	76	74	73	74	73
Gradation, % passing Sieve sizes in mm (US unit)	37.5 (1½ in)	100	100	100	100	100	100	100	100
	25 (1 in)	100	100	100	100	100	100	100	100
	19 (¾ in)	100	100	100	100	100	96	100	96
	12.5 (½ in)	93	94	93	94	99	86	99	86
	9.5 (⅜ in)	82	81	82	82	88	73	88	73
	4.75 (No.4)	50	55	53	54	63	50	63	50
	2.36 (No.8)	34	40	38	40	44	37	44	37
	1.18 (No.16)	27	30	28	29	33	29	33	29
	0.6 (No.30)	23	25	22	24	26	23	26	23
	0.3 (No.50)	18	20	17	18	15	13	15	13
	0.15 (No.100)	8	10	10	9	8	8	8	8
	0.075 ((No.200)	5	5	6	5	6	6	6	6

Figure 8, Figure 9, and Figure 10 graphically illustrate the aggregate gradations of 1.0 (25), 0.75 (19) and 0.5-in. (12.5-mm) NMAS mixtures, respectively. Ten 1.0-in. (25-mm), four 0.75-in. (19-mm), and fourteen 0.5-in. (12.5-mm) mixtures are shown in the figures.

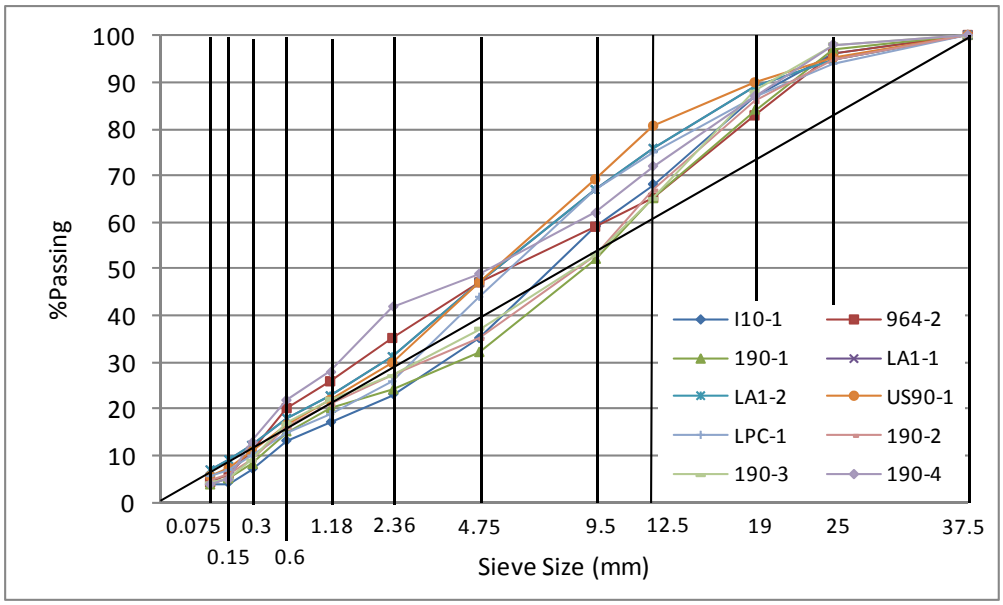

Figure 8
Gradation chart for 1.0-in. (25-mm) mixtures

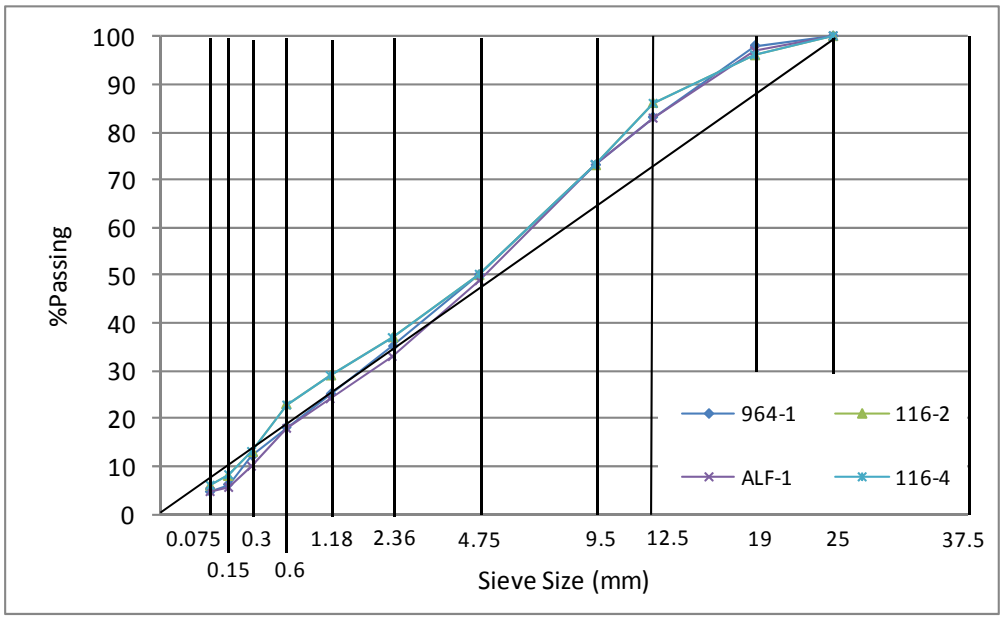

Figure 9
Gradation chart for 0.75-in. (19-mm) mixtures

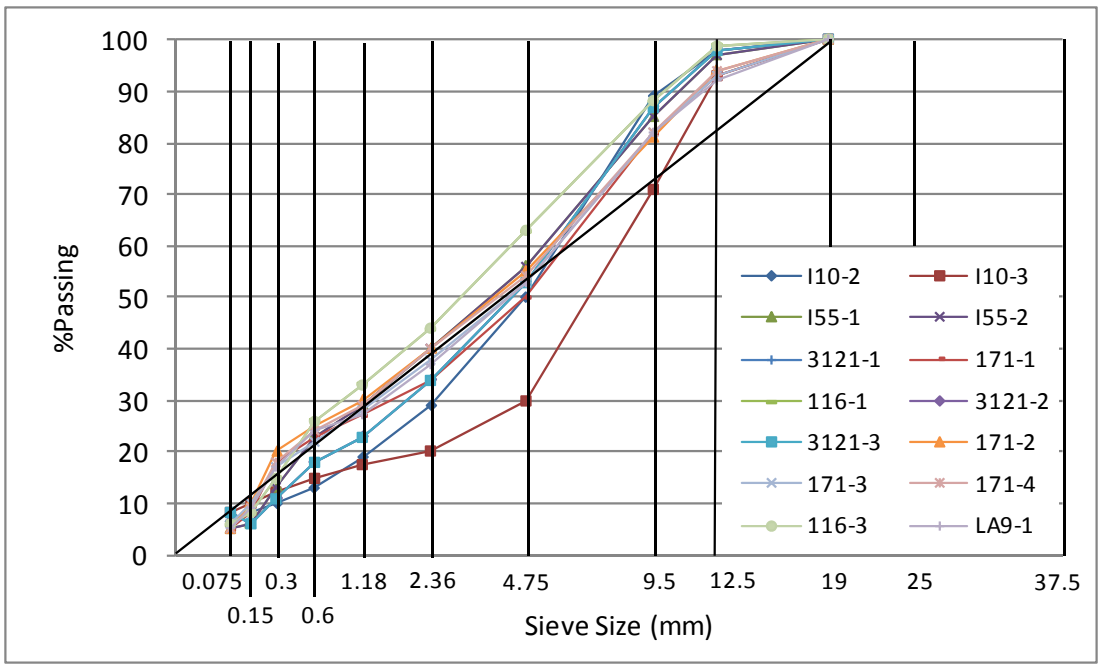

Figure 10
Gradation chart for 0.5-in. (12.5-mm) mixtures

Specimen Preparation and Test Methods

Specific details regarding the specimen preparation procedures are discussed in the Appendix section. Laboratory tests outlined in the previous sections were conducted in accordance with relevant standard test methods, as described in the Appendix section.

DISCUSSION OF RESULTS

Laboratory tests performed in this study included dynamic modulus tests in axial and indirect tension (IDT) modes, flow time (F_T), flow number (F_N), and Hamburg type loaded wheel tracking (LWT) tests. Results of these tests were analyzed by comparing the effects of different design traffic levels, nominal maximum aggregate sizes, and asphalt binder PG grades on the test parameters. Statistical analysis was performed using SAS software. An analysis of variance procedure was used to test for significant differences for the effects listed above. The level of confidence used in the tests was 95%. Also, the mixtures' rankings in terms of four test parameters ($|E^*|_{54C, 5Hz}$, $|E^*|/\sin(\delta)_{54C, 5Hz}$, F_N, and LWT) were compared to evaluate the potential rutting resistance.

Dynamic Modulus (|E*|) Test Results

The axial dynamic modulus (|E*|) test was conducted on three replicate samples for each mixture. The test was performed at five temperatures (i.e., -10, 4.4, 25, 37.8 and 54.4ºC) and six frequencies (i.e., 25, 10, 5, 1, 0.5 and 0.1 Hz). Two properties, |E*| and phase angle (δ), were obtained from this test. The |E*| test results with summary statistics are presented in Appendix A.

The parameter, $|E^*|_{54C, 5Hz}$, was used to evaluate the high temperature performance of mixtures included in this study. Higher $|E^*|_{54C, 5Hz}$ values indicate better rutting resistance.

Figure 11 presents the mean $|E^*|_{54C, 5Hz}$ values of mixtures grouped by the design traffic level. The green and blue bars denote WMA and HMA mixtures, respectively. The average $|E^*|_{54C, 5Hz}$ values for Level 1, Level 2, and Level 3 mixtures were approximately 63 (434), 106 (731), and 112 (772) ksi (MPa), respectively. The Level 1, Level 2, and Level 3 $|E^*|_{54C, 5Hz}$ ranges were 38 (262) to 90 (621) ksi (MPa), 72 (496) to 140 (965) ksi (MPa), and 89 (614) to 182 (1,255) ksi (MPa), respectively. It is worth noting that the WMA mixtures exhibited similar $|E^*|_{54C, 5Hz}$ values as compared to their companion HMA mixtures. The results of the statistical analysis indicated that the mean $|E^*|_{54C, 5Hz}$ value for the Level 1 group was significantly lower than the means for Levels 2 and 3. Furthermore, there was no significant difference between the mean values of $|E^*|_{54C, 5Hz}$ for Levels 2 and 3. This is consistent with the LADOTD 2006 specification change that merged Levels 2 and 3.

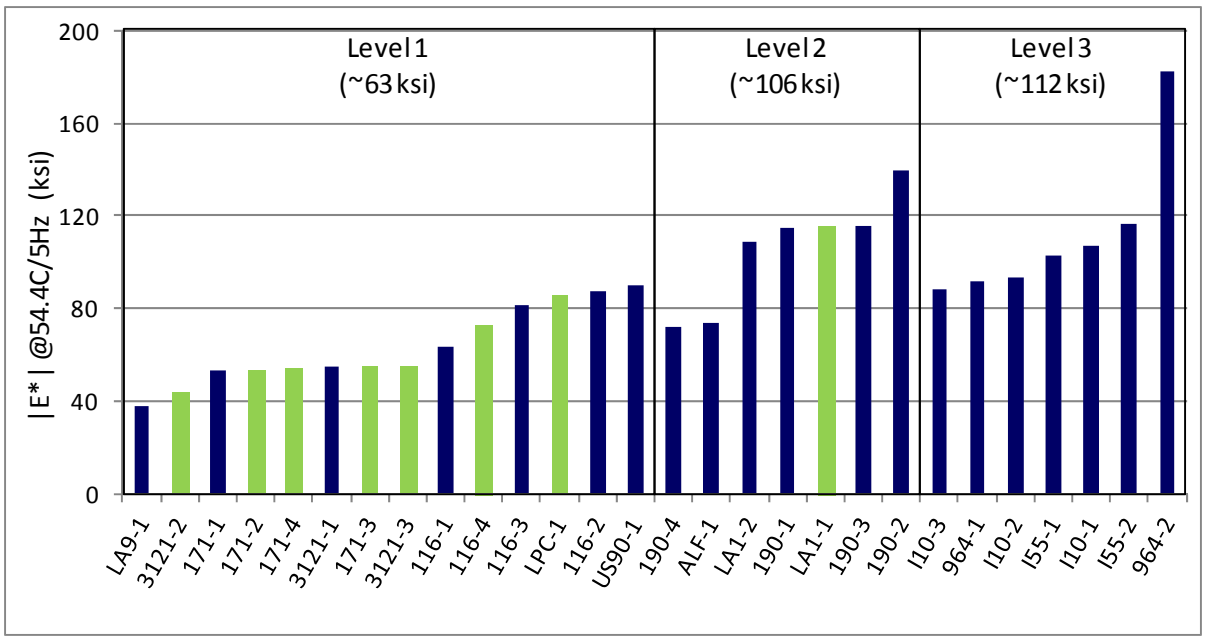

Figure 11
$|E^*|_{54C,\ 5Hz}$ grouped by traffic levels

Figure 12 presents the mean $|E^*|_{54C,\ 5Hz}$ values grouped by the NMAS. The average $|E^*|_{54C,\ 5Hz}$ values of 0.5 (12.5), 0.75 (19.0), and 1.0-in. (25.0-mm) NMAS mixtures were 68 (469), 81 (558), and 113 (779) ksi (MPa), respectively. The range of the $|E^*|_{54C,\ 5Hz}$ values for 0.5 (12.5), 0.75 (19.0), and 1.0-in. (25.0-mm) mixtures were 38 (262) to 117 (807) ksi (MPa), 73 (503) to 91 (627) ksi (MPa), and 72 (496) to 182 (1,255) ksi (MPa), respectively. It is worth noting that the mean $|E^*|_{54C,\ 5Hz}$ values increased with an increase in NMAS. However, there was a statistical difference between only the mean levels of 0.5 (12.5) and 1.0-in. (25-mm) mixtures. The 0.75-in. (19-mm) mixtures were not significantly different from either 0.5 (12.5) or 1.0-in. (25-mm) mixtures. There were a limited number of 19-mm mixtures (four) as compared to the 0.5-in. (12.5-mm) (fourteen) and 1.0-in. (25-mm) (ten) mixtures. This small number of 0.75-in. (19-mm) samples may have contributed to these findings.

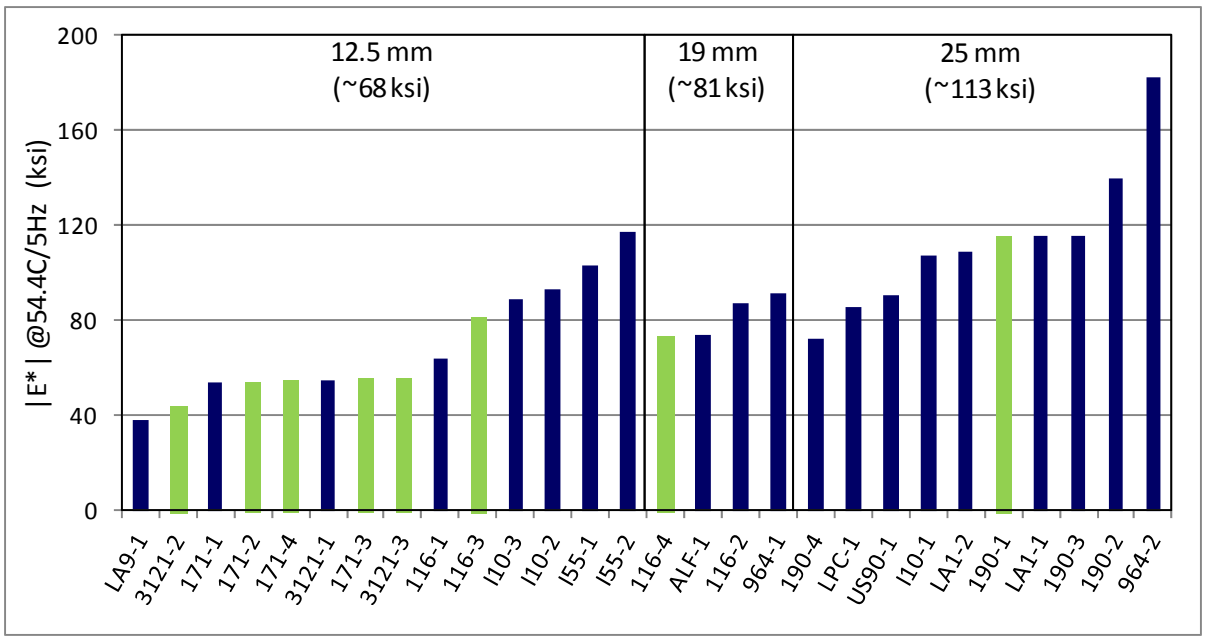

Figure 12
$|E^*|_{54C,\ 5Hz}$ values of mixtures grouped by NMAS

Figure 13 presents the mean $|E^*|_{54C,\ 5Hz}$ values grouped by asphalt binder types, namely PG64-22, PG70-22M, PG76-22M, and PG82-22rm. The $|E^*|_{54C,\ 5Hz}$ averages of the PG70-22M, PG76-22M, and PG82-22rm mixtures are 63 (434) ksi (MPa), 108 (745) ksi (MPa), and 110 (758) ksi (MPa), respectively. In general, mixtures with higher temperature grade binders had higher $|E^*|_{54C,\ 5Hz}$ values compared to those with lower temperature grades, except for mixture 190-3 that contained PG64-22 binder. Statistical analysis indicated that the mean $|E^*|_{54C,\ 5Hz}$ value of the PG70-22M mixtures was significantly lower than the means for the PG76-22M and PG82-22rm mixtures. Although the mean of the PG82-22rm group was algebraically higher than the mean of the PG76-22M group, the difference was not statistically significant. It is noted that there were a limited number of PG82-22rm mixtures (two) as compared to the PG70-22M (fourteen) and PG76-22M (eleven) mixtures, which could have contributed to these findings. It should be noted that the PG64-22 group was not included in the analysis due to lack of replicates.

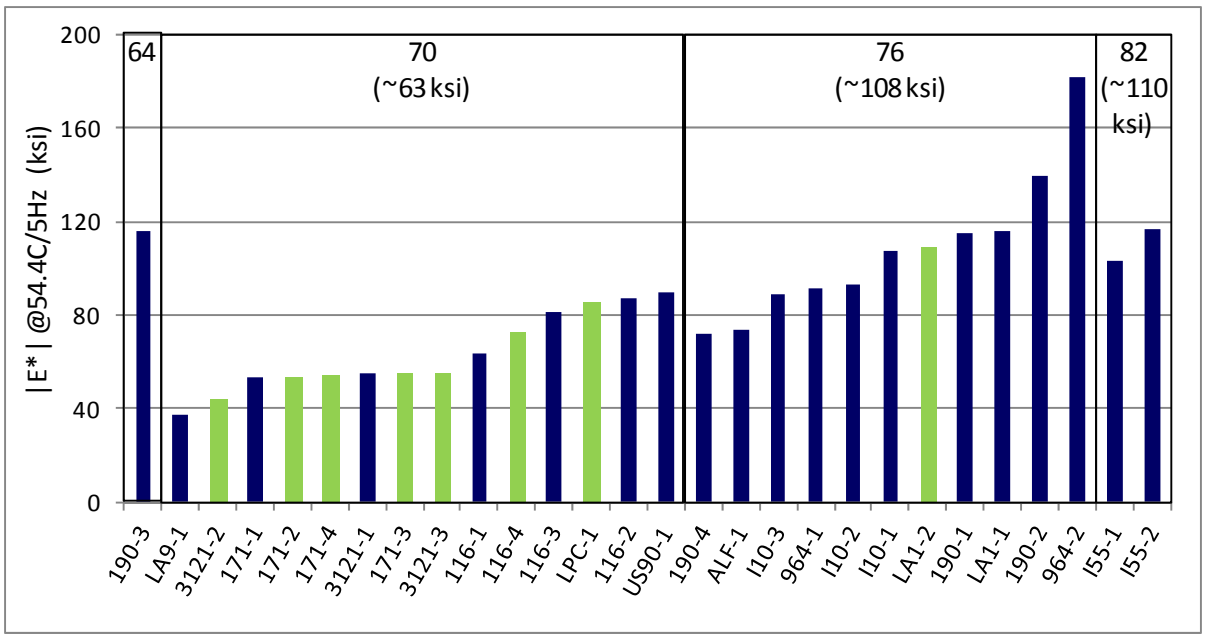

Figure 13
$|E^*|_{54C,\ 5Hz}$ values of mixtures grouped by PG high grade

Rutting Parameter: $|E^*|_{54C,\ 5Hz}/\sin(\delta)$. The dynamic modulus test results were further evaluated using the mixture rut factor as defined by $|E^*|_{54C,\ 5Hz}/\sin(\delta)$ *[31]* to include the effects of phase angle. A higher |E*| and a lower phase angle yields a higher rut parameter |E*|/sin(δ), which is desirable for rut-resistant mixtures.

Figure 14 presents the mean mixture rut factor values grouped by design traffic level. The average rut factor values for Level 1, Level 2, and Level 3 mixtures were approximately 129 (889), 232 (1,600), and 241 (1,662) ksi (MPa), respectively. The Level 1, Level 2, and Level 3 mixture rut factor ranges were approximately 80 (552) to 182 (1,255) ksi (MPa), 161 (1,110) to 293 (2,020) ksi, and 188 (1,296) to 388 (2,675) ksi, respectively. The mean mixture rut factor value for the Level 1 group was statistically lower than the means for Levels 2 and 3. Furthermore, there were no significant differences between the mean mixture rut factor values for Levels 2 and 3. This finding was similar to the one observed in the analysis of the $|E^*|_{54C,\ 5Hz}$ parameter.

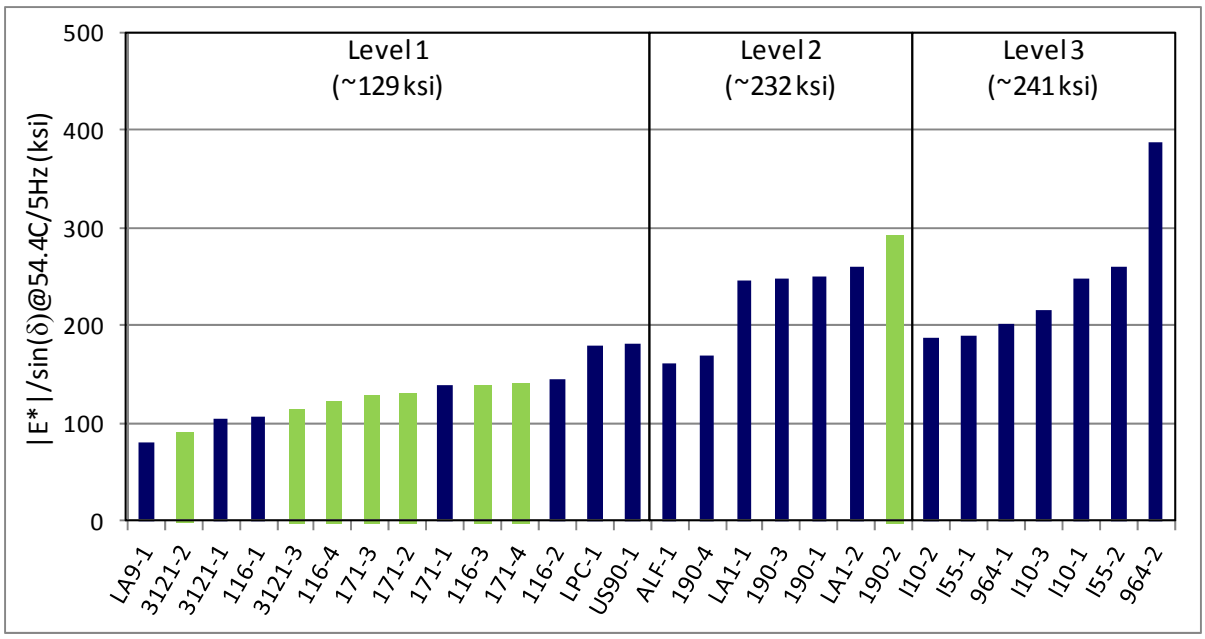

Figure 14
Mixture rut factor grouped by traffic levels

Figure 15 presents the mean mixture rut factor values grouped by the NMAS. The mean mixture rut factor values for 0.5 (12.5), 0.75 (19), and 1.0-in. (25-mm) NMAS mixtures were approximately 145 (1,000), 157 (1,082), and 246 (1696) ksi (MPa), respectively. The rut factor ranges for the 0.5 (12.5), 0.75 (19), and 1.0-in. (25-mm) NMAS mixtures were 80 (552) to 260 (1,793) ksi, 123 (848) to 201 (1,386) ksi, and 169 (1,165) to 388 (2675) ksi (MPa), respectively. It is worth noting that the mean mixture rut factor values increased with an increase in NMAS. Statistical analysis indicated that the mean of the 1.0-in. (25-mm) mixtures was significantly higher than the means for the 0.5 (12.5) and 0.75-in. (19-mm) mixtures. However, there was no significant difference between the means of the 0.5 (12.5) and 0.75-in. (19-mm) mixtures. It is worth mentioning that incorporating the phase angle in the analysis yielded a distinct separation in the rut factor between the 0.75 (19) and 1.0-in. (25-mm) NMAS mixture groups. In this analysis, a decrease in mixture NMAS may yield a lower resistance to rutting. This observation is consistent with the one reported by Bhasin, et.al *[32]*.

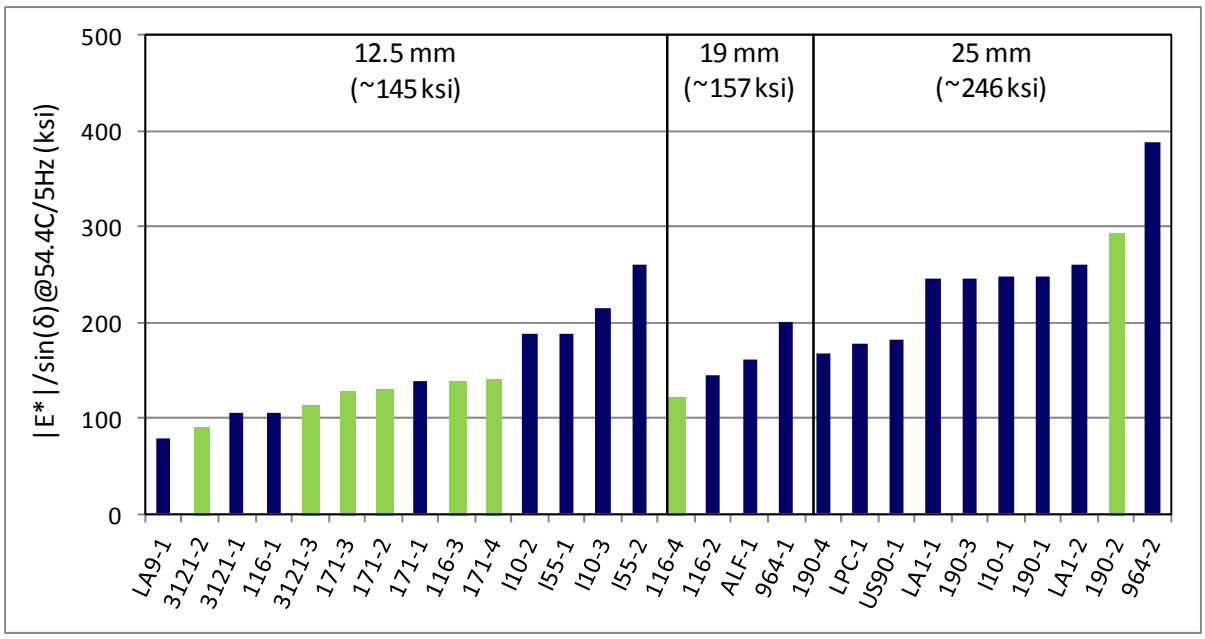

Figure 15
Mixture rut factor grouped by NMAS

Figure 16 presents the mean mixture rut factor values grouped by the PG high temperature grade. The average rut factor values for the PG70-22M, PG76-22M, and PG82-22rm mixtures were approximately 129 (889), 238 (1641), and 224 (1,544) ksi (MPa), respectively. The rut factor ranges for the PG70-22M, PG76-22M, and PG82-22rm mixtures were 80 (552) to 182 (1,255) ksi (MPa), 161 (1,110) to 388 (2,675) ksi, and 189 (1,303) to 260 (1,793) ksi (MPa), respectively. Statistical analysis indicated that the mean rut factor for the PG70-22M mixtures was significantly lower than the means for the PG76-22M and PG82-22rm mixtures. Although the mean for the PG82-22rm mixtures was algebraically lower than the mean for the PG76-22M mixtures, this difference was not statistically significant. There were a limited number of PG82-22rm mixtures (two) as compared to the PG70-22M (fourteen) and PG76-22M (eleven) mixtures, which could have contributed to these findings. It should be noted that the PG64-22 group was not included in the analysis due to lack of replicates. Thus, a decrease in the high temperature PG grade can result in lower resistance to rutting.

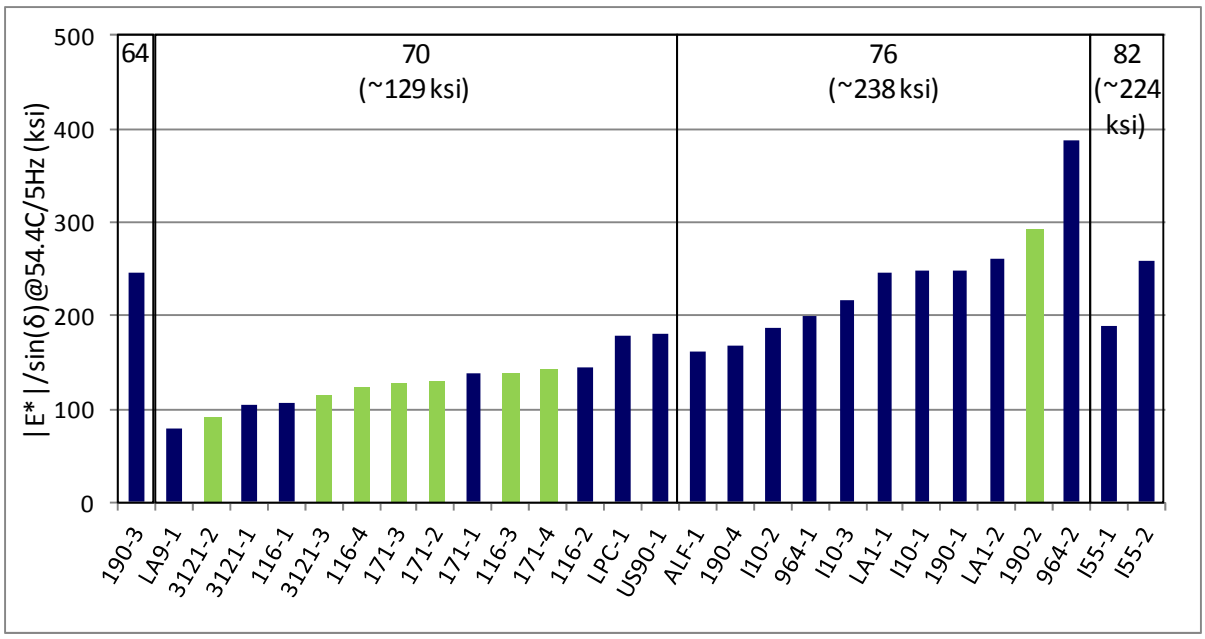

Figure 16
Mixture rut factor grouped by PG high grade

Master Curves

The dynamic modulus of asphalt mixtures obtained at various frequencies and temperatures can be combined into a "master curve" using the time-temperature superposition principle. The dynamic modulus curves at various temperatures (also called isotherms) are shifted horizontally with respect to a "reference" temperature until all the curves merge into a single "master curve", as shown in Figure 2. This master curve can be described using a sigmoidal function shown in equation (4).

Figure 17 presents the master curves for all mixtures evaluated in this study. Table 7 summarizes the ranges of the master curve parameters (δ, α+δ, β, and γ presented in equation 4). The upper and lower bounds of the master curve are described by δ and α+δ, respectively [equation 4, Figure 2]. These correspond to the dynamic modulus of asphalt mixtures at low temperature/high frequency (upper bound) and high temperature/low frequency (lower bound) testing conditions. The upper bound of the sigmoidal curve is the maximum modulus of the mixture, which is dependent on the limiting stiffness of the binder at cold temperatures [Pellinen, Witczak, AAPT 2002]. In this study all the mixtures had the same low temperature binder grade of -22ºC. Therefore, as expected, all the master curves seem to converge at the upper end (corresponding to low temperature/high frequency test condition) of the graph. At the lower bound, compressive loading at high temperature causes the aggregate influence to

be more dominant. Since there were three nominal maximum aggregate sizes included in this study (0.5 (12.5), 0.75 (19), and 1.0-in. (25-mm)), the variation in the lower bound is greater, as expected.

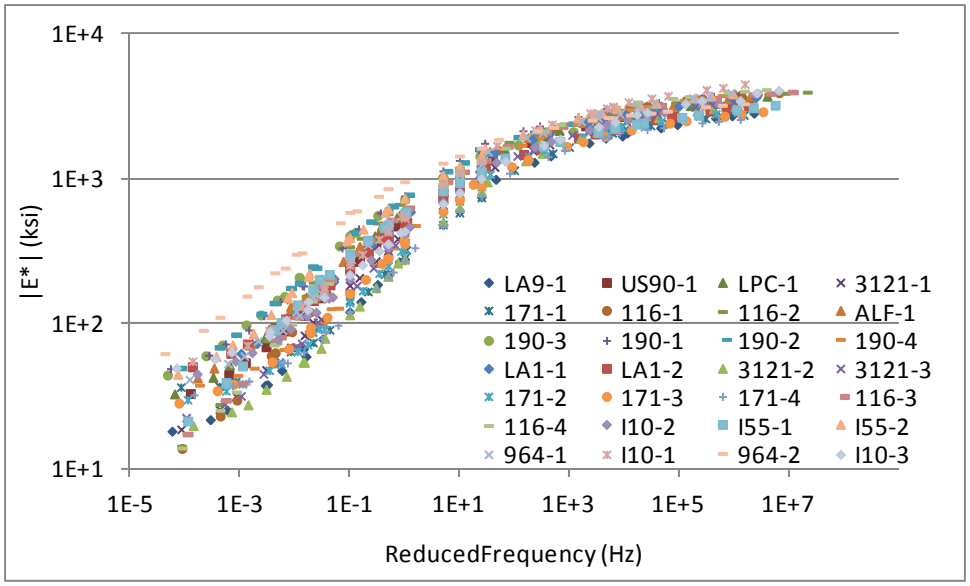

Figure 17
|E*| Master curves of all mixtures

Table 7
Ranges of master curve parameters

Parameter	Level 1	Level 2	Level 3
δ	-0.7~1.0	1.1~1.3	-0.7 ~ 1.5
$\alpha + \delta$	3.4 ~ 3.7	3.5~3.6	3.6 ~ 3.7
β	-1.51~-0.25	-0.98~-0.20	-1.47 ~ -0.21
γ	-0.71 ~ -0.44	-0.70 ~ -0.55	-0.61 ~ -0.40

Figures 18-20 present the master curves of the mixtures grouped by design levels 1, 2, and 3, respectively. It is noted that the master curves for mixtures grouped by design Level 2 (Figure 19) exhibited less variation in the lower bound region as compared to levels 1 (Figure 18) and 3 (Figure 20). This observation may be attributed to the fact that Level 2 mixtures were mostly 1.0-in. (25-mm) NMAS.

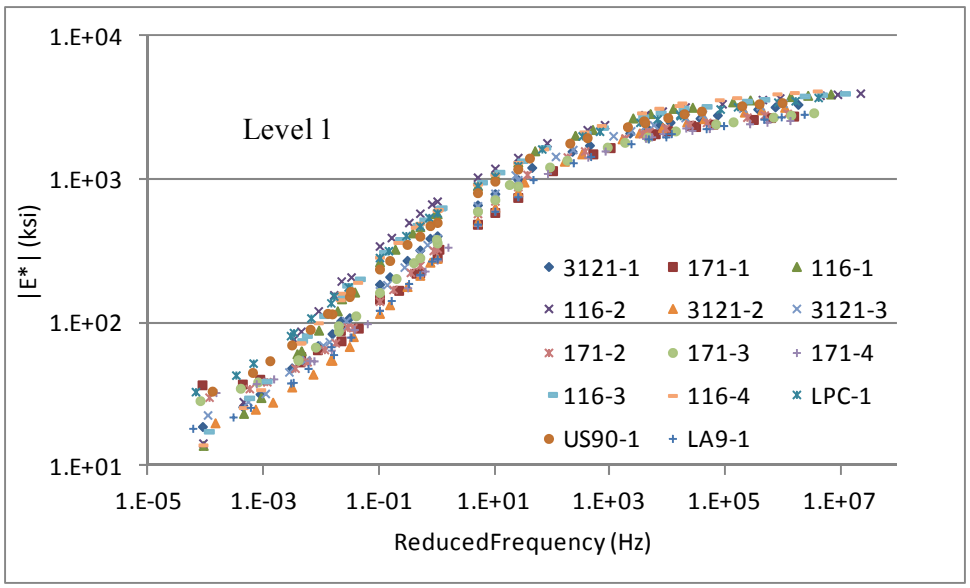

Figure 18
Master curves for Level 1 traffic mixtures

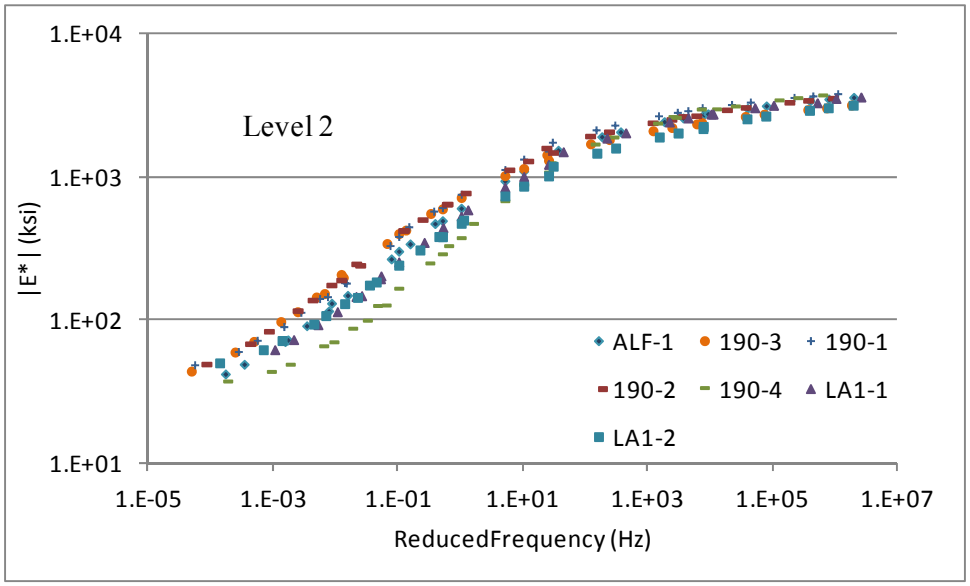

Figure 19
Master curves for Level 2 traffic mixtures

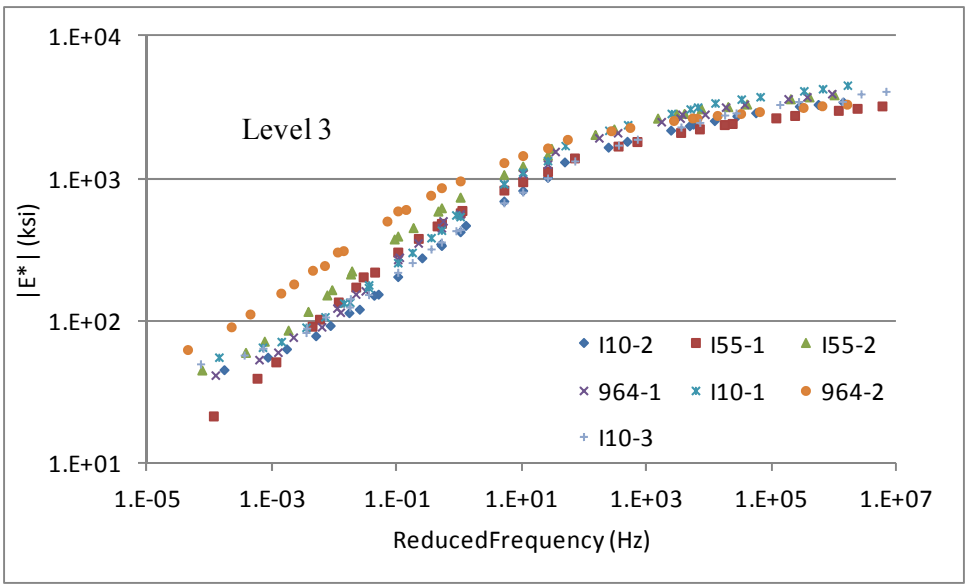

Figure 20
Master curves for Level 3 traffic mixtures

Comparison of the Dynamic Modulus Predictive Equations

Witczak's and Hirsch's are the most commonly used models to predict the dynamic modulus of asphalt mixtures. The Witczak model uses properties of the binder, aggregates, and some volumetric parameters to predict dynamic modulus. This model is presented in equation (6). In contrast, the Hirsch model only requires the complex modulus of the binder, voids in the mineral aggregate (VMA), and voids filled with asphalt (VFA). This model is presented in equation (7).

In order to evaluate the Witczak predictive equation and Hirsch model in predicting the dynamic modulus of commonly used Louisiana asphalt mixtures, the correlation of the measured and predicted dynamic modulus was assessed using goodness-of-fit statistics. The statistics include the coefficient of determination (R^2) and S_e/S_y (standard error of estimate/standard deviation). The R^2 value is a measure of accuracy of the prediction. The higher the value of R^2, the better the prediction value is. The ratio S_e/S_y is a measure of the improvement in the accuracy of the prediction due to predictive equation. The lower the ratio, more variation in the dynamic modulus values about their mean can be explained by the predictive equations, and the better the prediction will be. The R^2 value is determined using equation (14). The standard error of the estimate, (S_e), and the standard deviation, (S_y), are calculated using equations (15) and (16), respectively.

$$R^2 = 1 - \frac{(n-k)}{(n-1)}\left(\frac{S_e}{S_y}\right)^2 \quad (14)$$

$$S_e = \sqrt{\frac{\sum(y-\hat{y})^2}{(n-k)}} \quad (15)$$

$$S_y = \sqrt{\frac{\sum(y-\bar{y})^2}{(n-1)}} \quad (16)$$

where,
R^2 = coefficient of determination
S_e = standard error of estimate
S_y = standard deviation
y = measured dynamic modulus
$\hat{y}$ = predicted dynamic modulus
$\bar{y}$ = mean value of measured dynamic modulus
n = sample size
k = number of independent variables used in model

The criteria for the goodness of fit statistical parameters were given by the NCHRP project 9-19 and are presented in Table 8 *[2]*.

Table 8
Criteria for goodness of fit statistical parameters

Criteria	R^2	S_e/S_y
Excellent	≥ 0.90	≤ 0.35
Good	0.70 – 0.89	0.36 – 0.55
Fair	0.40 – 0.69	0.56 – 0.75
Poor	0.20 – 0.39	0.76 – 0.89
Very Poor	≤ 0.19	≥ 0.90

The measured and predicted |E*| values can also be compared by scatter plots of predicted vs. measured |E*|, and then performing simple linear regressions through the origin. If the data

points are distributed tightly near the "equality line," then they should have very high R^2 values. In addition to the R^2 values, slopes of the regression lines can also indicate the accuracy of the predictions; the closer the slope to the value of 1, the more parallel the prediction is to the measured |E*| curve.

Evaluation of Witczak Predictive Equation

The goodness of fit statistics were calculated separately for 26 selected mixtures designed for Level 1, Level 2, Level 3 traffic and all the mixtures together. Table 9 presents the goodness of fit statistics for all categories of mixtures. Overall, all the mixtures had good to excellent correlations. It was observed that the mixtures designed for Level 2 traffic had highest R^2 of 0.95 and the ratio Se/Sy was also least at 0.27.

Table 9
Witczak prediction goodness of fit statistics

Mixture Type	Statistical Parameter	Value	Evaluation
Level 1 Traffic Mixtures	R^2	0.84	Good
	S_e/S_y	0.55	Good
Level 2 Traffic Mixtures	R^2	0.95	Excellent
	S_e/S_y	0.27	Excellent
Level 3 Traffic Mixtures	R^2	0.92	Excellent
	S_e/S_y	0.29	Excellent
All Mixtures	R^2	0.83	Good
	S_e/S_y	0.34	Excellent

Figure 21 through Figure 24 show the comparisons made between predicted and measured dynamic modulus values for Level 1, Level 2, Level 3 and all 15 mixtures together, respectively. It was observed that the coefficient of determination (R^2) was highest for Level 2 traffic mixtures (0.95), and least (0.84) for Level 1 traffic mixtures. The slope value was the closest as 1.07 for the Level 2 traffic mixtures and the farthest as 0.66 for the Level 1 mixtures. The slope of all mixtures' prediction was 0.83, indicating a slight under-prediction, but within a tight margin.

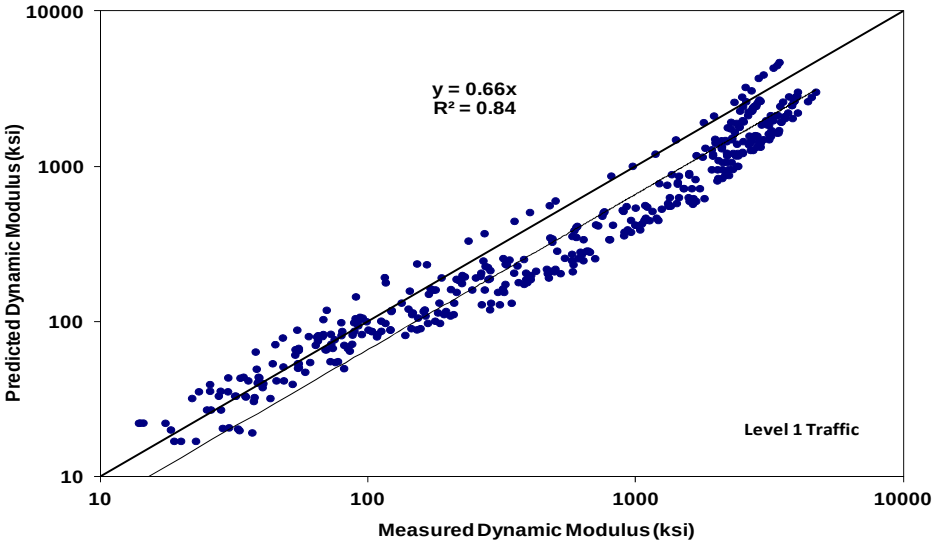

Figure 21

Witczak predictions for Level 1 traffic mixtures in log-log scale

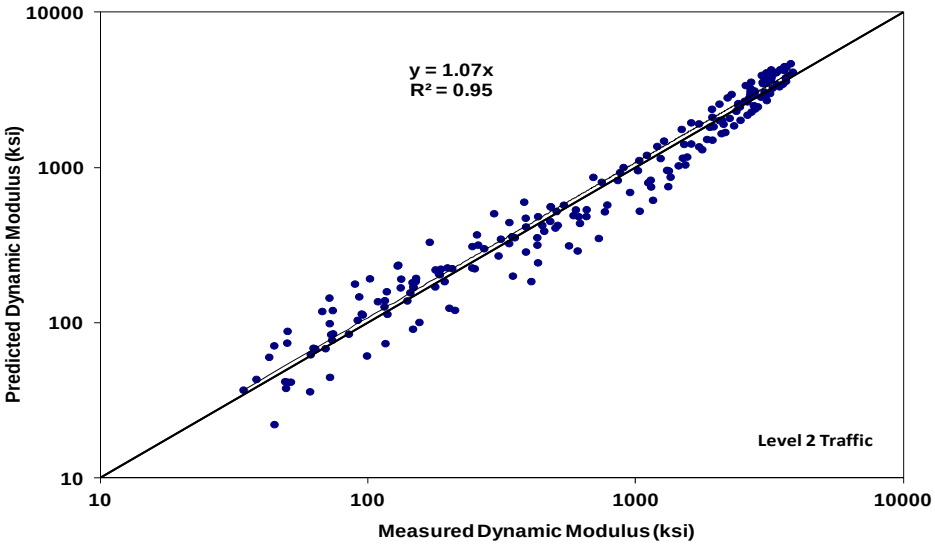

Figure 22

Witczak predictions for Level 2 traffic mixtures in log-log scale

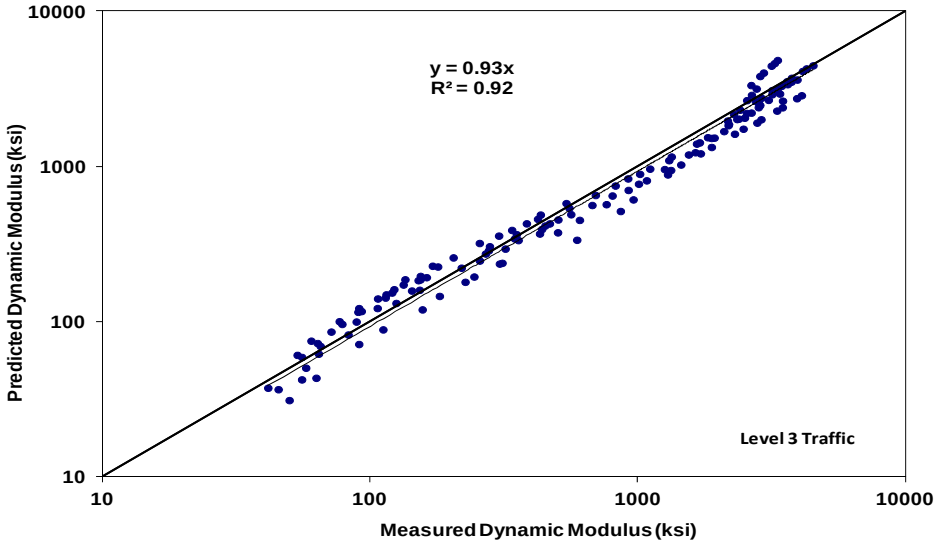

Figure 23

Witczak Predictions for Level 3 traffic mixtures in log-log scale

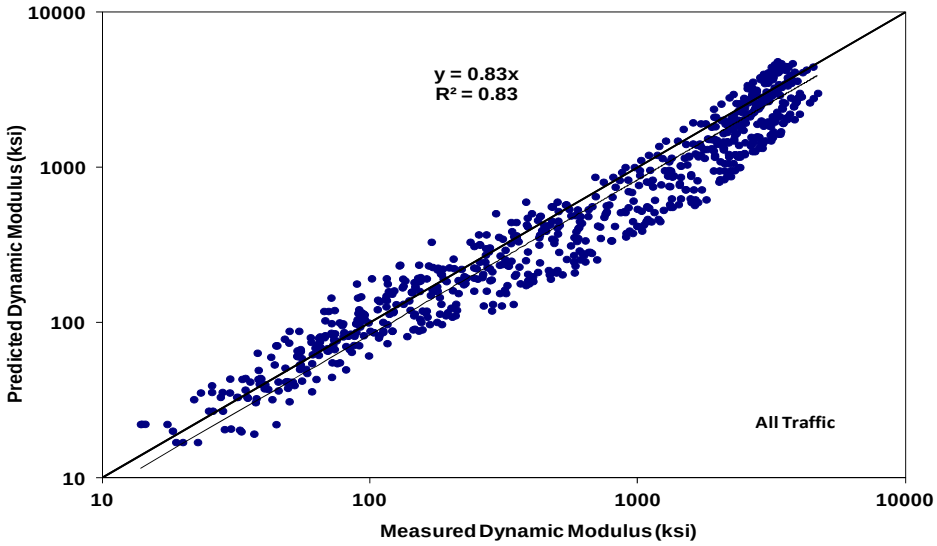

Figure 24

Witczak Predictions for all mixtures in log-log scale

Evaluation of Hirsch Model

The goodness of fit statistics were calculated separately for 26 selected mixtures designed for Level 1, Level 2, Level 3 traffic and all the mixtures together. Table 10 presents the goodness of fit statistics for all categories of mixtures for the Hirsch model predictions. It is interesting to note that all categories into which the mixtures were divided showed excellent correlation with measured dynamic modulus values. The highest value of coefficient of determination

(R^2) was observed for Level 2 traffic mixtures, which had the R^2 value of 0.97 and the ratio S_e/S_y was also least at 0.17.

Table 10
Hirsch model prediction Goodness of fit statistics

Mixture Type	Statistical Parameter	Value	Evaluation
Level 1 Traffic Mixtures	R^2	0.92	Excellent
	S_e/S_y	0.28	Excellent
Level 2 Traffic Mixtures	R^2	0.97	Excellent
	S_e/S_y	0.17	Excellent
Level 3 Traffic Mixtures	R^2	0.97	Excellent
	S_e/S_y	0.25	Excellent
All Mixtures	R^2	0.93	Excellent
	S_e/S_y	0.26	Excellent

Figure 25 through Figure 28 show the comparisons made between predicted and measured dynamic modulus values for different categories of mixtures. It was observed that the correlation was nearly the same for mixtures designed for different levels of traffic. It can be noticed from the slope value obtained for all mixtures plotted together (0.95), that generally the Hirsch model equation tends to under-predict the dynamic modulus value by a small margin.

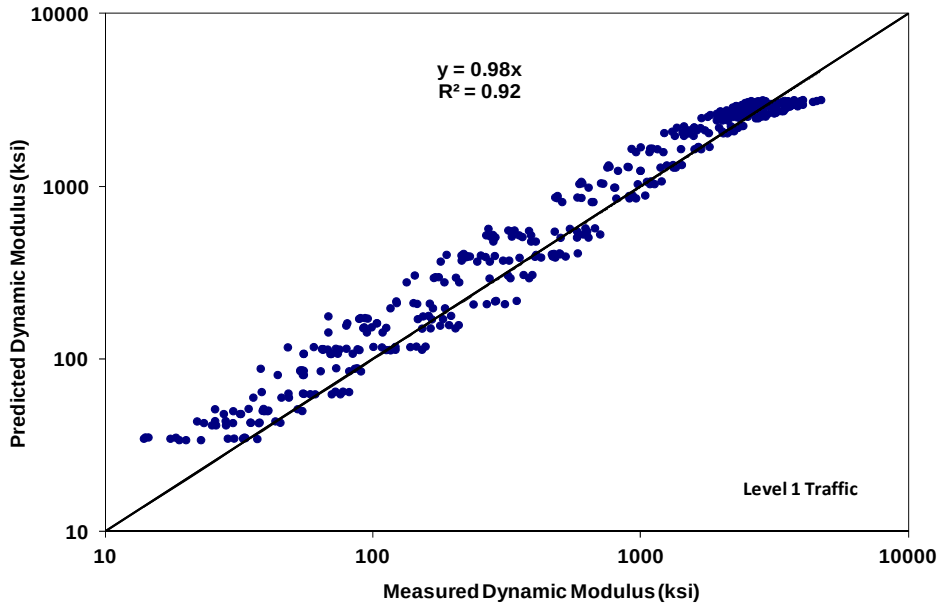

Figure 25
Hirsch model predictions for Level 1 traffic mixtures in log-log scale

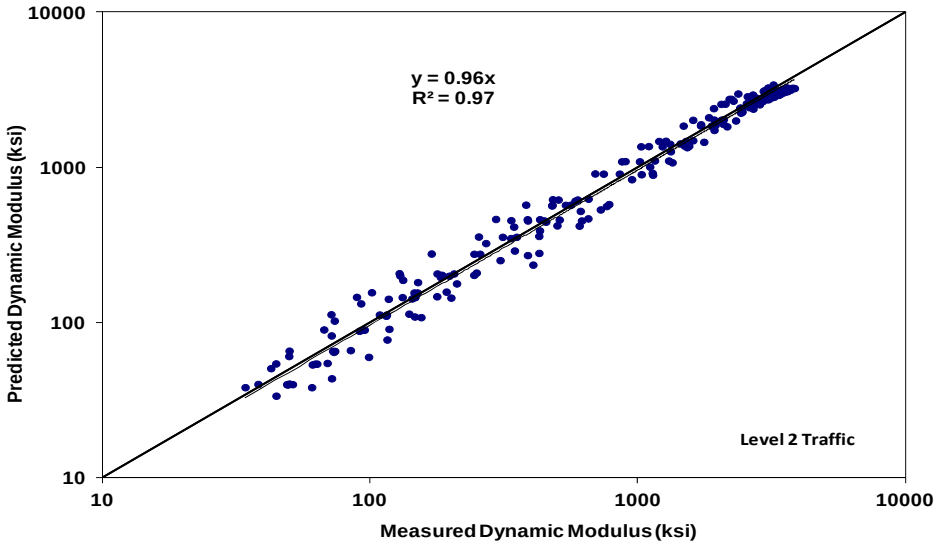

Figure 26

Hirsch model predictions for Level 2 traffic mixtures in log-log scale

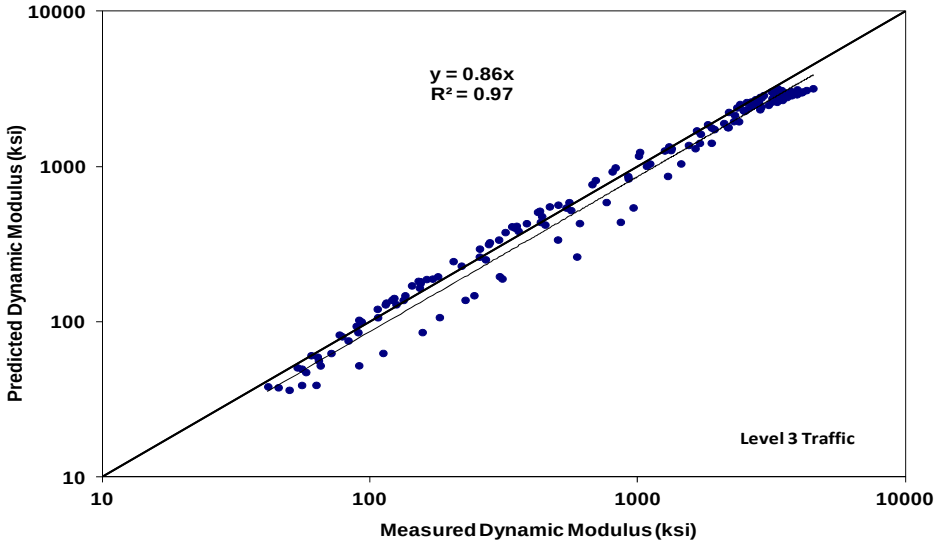

Figure 27

Hirsch model predictions for Level 3 traffic mixtures in log-log scale

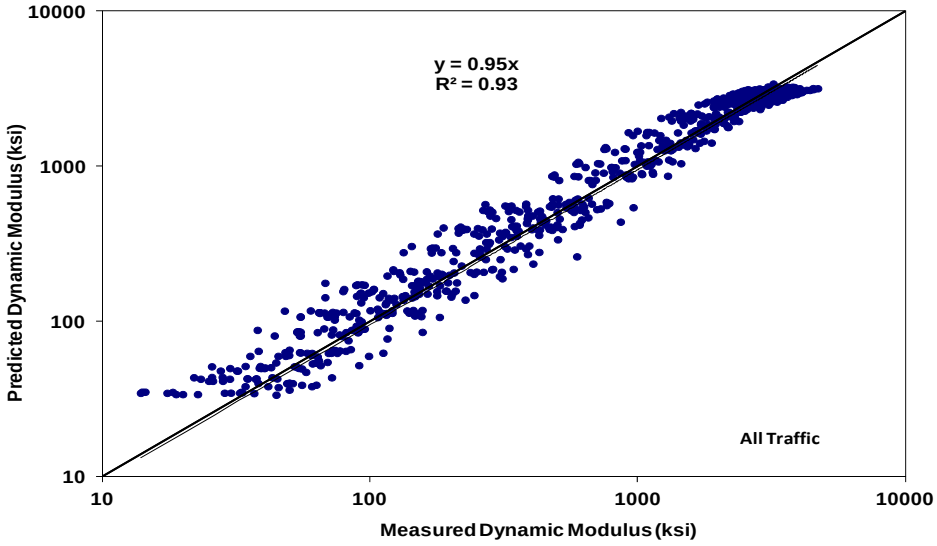

Figure 28
Hirsch model predictions for all mixtures in log-log scale

Both the Witczak predictive equation and Hirsch model performed good to excellent in predicting the measured dynamic modulus, as previously explained. Comparing the two predictive equations, the Hirsch model seems to be more accurate in estimating dynamic modulus.

Based on the accuracy of predictive equations, it appeared that the testing of the asphalt mixtures could be avoided and the predictive equation could be used to estimate dynamic modulus values from the volumetric properties of the asphalt mixtures. The results presented here are promising in terms of being able to predict the dynamic modulus, |E*|, values within a reasonable accuracy, from mixture properties, using either Witczak's predictive equation or the Hirsch model. In particular, these models are valuable for highway agencies in determining the dynamic modulus (|E*|) value for Level-2 analysis in the MEPDG. Recognizing that the dynamic modulus test is laborious, time consuming, expensive, and requires skilled personnel, the use of these prediction models can be a viable alternative in estimating the dynamic modulus, |E*|, value of asphalt mixtures.

Evaluation of MEPDG Software

The MEPDG software was developed under NCHRP Projects 1-37A (Development of the 2002 Guide for the Design of New and Rehabilitated Pavement Structures: Phase II) and 1-40D (Technical Assistance to NCHRP and NCHRP Project 1-40A: Versions 0.9 and 1.0 of the M-E Pavement Design Software). Over the years the software underwent significant

modifications, especially in the flexible pavement module *[33]*. Intellectual rights were transferred to AASHTO in 2007 and the software is now referred to as DARWin-ME (DARWin stands for Design, Analysis and Rehabilitation for Windows).

The MEPDG software allows the use of a hierarchical approach of design inputs based on the level of prediction accuracy desired. The level of accuracy provided is directly related to the testing and data collection costs. Three levels of design inputs were proposed: Level 1 provides the highest level of accuracy and requires laboratory testing; Level 2 provides an intermediate level of accuracy and requires limited laboratory testing; Level 3 provides the lowest level of accuracy and uses default values. The sensitivity analysis and local calibration performed in this study was carried out using design Level 1 to ensure the highest accuracy of results.

The sensitivity and local calibration of the rutting prediction by the MEPDG software (version 1.1) are described in the following sections.

Sensitivity of MEPDG Rutting Prediction Model

The MEPDG software requires the laboratory measured |E*| as material input for Level 1 analysis. To evaluate the effect of variations in |E*| on the predicted rut depth, a sensitivity analysis was performed. This analysis was conducted by varying the inputs to the asphalt layer, while keeping the remaining layer properties constant.

Three asphalt mixtures, LA9-1 ALF-1, and 964-2, were selected to represent low, medium, and high values of $|E^*|_{54C,\ 5Hz}$ values, respectively among the 28 mixtures evaluated. It is noted that the traffic levels for LA9-1, ALF-1, and 964-2 mixtures were Level 1, Level 2 and Level 3, respectively.

Additionally, two pavement structures (one thick, one thin) were considered in this study. Figure 29 shows the cross-sections of these two structures. The thick pavement structure consisted of four layers: a 6-in. (150-mm) asphalt concrete layer, a 6-in. crushed stone base layer, an 8-in. (200-mm) gravel subbase layer, and a subgrade layer. The thin pavement structure consisted of three layers: a 2-in. (50-mm) asphalt concrete layer, a 6-in. (150-mm) crushed stone base layer, and a subgrade layer. A 20 year design life was considered. Additional details of inputs used for the MEPDG simulations are listed in Table 11.

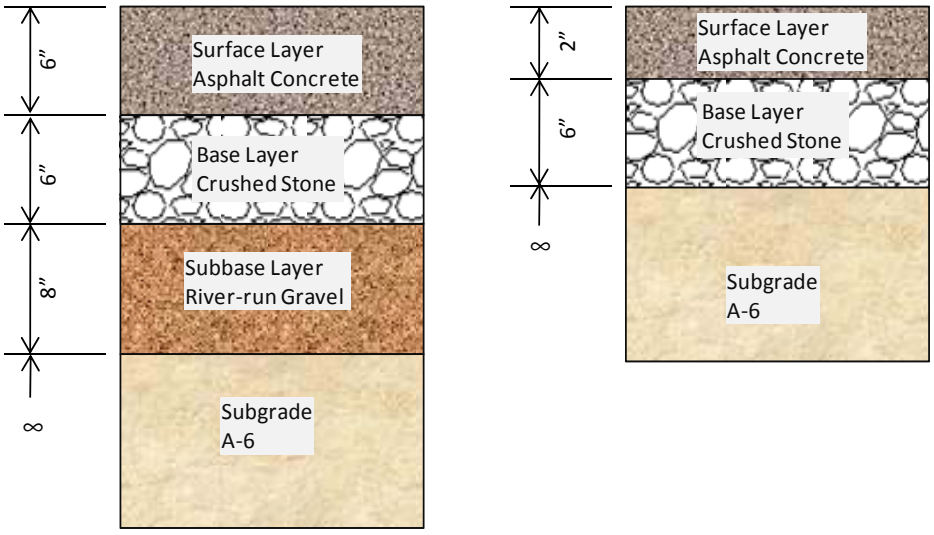

<Thick section> <Thin section>

Figure 29
Pavement structure used for MEPDG sensitivity analysis

Table 11
Input data for sensitivity analysis

Parameters	Thick Section	Thin Section
Initial Two-Way AADTT	1500	1500
Percent of Trucks in Design Lane (%)	90	90
Operational Speed (mph)	60	60
Vehicle Class Distribution	Default: Level 3	Default: Level 3
Hourly Truck Traffic Distribution	Default: Level 3	Default: Level 3
Traffic Growth Factor	4.0% Compound	4.0% Compound
Climate Data	Baton Rouge	Baton Rouge
Asphalt Concrete Thickness	6 in	2 in
Base Thickness	6 in	6 in
Base Modulus (psi)	40000	40000
Subbase Thickness	8 in	NA
Subbase Modulus (psi)	15000	NA
Subgrade Modulus (psi)	10000	10000

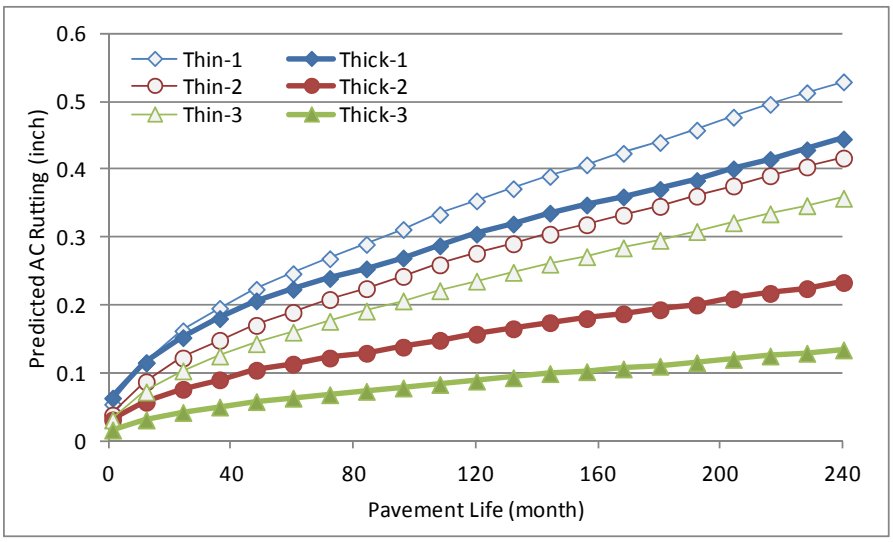

Figure 30
Asphalt layer rutting prediction results for the three traffic levels

Figure 30 presents the variation of the accumulated rut predictions of the asphalt layer over the design life. The predicted rut depths of the thin section were higher than those of the thick section. In addition, it is observed that the thick section showed higher sensitivity than the thin section. Although the thick section appeared to be more sensitive, the actual predicted rut depths were lower as compared to the thin section.

Figure 31 presents the normalized rut depth predictions at the end of 20 years of service life. The rut depths were normalized with respect to the predicted rut depth for the medium value of $|E^*|_{54C,\ 5Hz}$. It is worth noting that the mixtures with low and high values of $|E^*|_{54C,\ 5Hz}$ were approximately 0.4 and 2.0 of the mixture with medium values of $|E^*|_{54C,\ 5Hz}$, respectively.

For the thick section, this resulted in a normalized predicted asphalt layer rut depths of 1.9 and 0.6. In other words, a 60% reduction in |E*| (corresponding to the normalized ratio of 0.4) resulted in a 90% increase in rut depth (corresponding to the normalized ratio of 1.9). Similarly, a 100% increase in |E*| (corresponding to the normalized ratio of 2.0) resulted in a 40% decrease in rut depth (corresponding to the normalized ratio of 0.6).

For the thin pavement structure, variations in normalized |E*| input from 0.4 to 2.0 resulted in normalized asphalt layer rut depths of 1.3 and 0.9. In other words, a 60% reduction in |E*| (corresponding to the normalized ratio of 0.4) resulted in a 30% increase in rut depth (corresponding to the normalized ratio of 1.4). Similarly, a 100% increase in |E*| (corresponding to the normalized ratio of 2.0) resulted in a 10% decrease in rut depth (corresponding to the normalized ratio of 0.9).

In summary, as expected, the rut prediction was sensitive to the input value of the dynamic modulus. This result was expected because the rutting model selected in the M-E design guide for the asphalt concrete layer is based on an empirical relationship between the elastic strain and the plastic strain, where the computation of the elastic strains is derived from the |E*| values *[35]*.

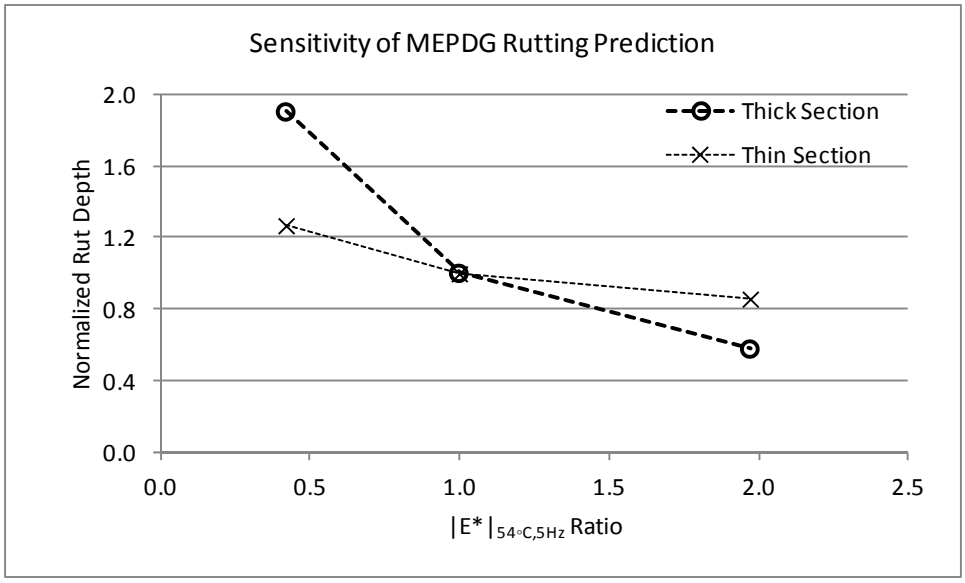

Figure 31
Normalized rutting vs. $|E^*|_{54C,5Hz}$ Ratio

Local Calibration of the Rutting Prediction Model

Performance models in the MEPDG were calibrated on a "national level" using data from test sections throughout North America *[35]*. Since materials, specifications, and policies vary across the US, the models also include "local coefficients" which could be used to calibrate the MEPDG to local conditions. The rutting prediction model used in MEPDG is presented in equation (17).

$$\frac{\varepsilon_p}{\varepsilon_r} = k_z \, \beta_{r1} \, 10^{k_1} \, T^{k_2 \beta_{r2}} \, N^{k_3 B_{r3}} \qquad (17)$$

where,

$\varepsilon_p/\varepsilon_r$ = ratio of accumulated permanent strain to elastic strain at N^{th} loading

N = number of traffic loadings

T = pavement temperature, °F

k_z = function of asphalt layer thickness for confining pressure adjustment

k_1, k_2, and k_3 = nationally calibrated model coefficients
β_{r1}, β_{r2}, and β_{r3} = local calibration coefficients

The methodology followed for the calibration of the MEPDG rutting model was a trial and error based approach. The local calibration coefficients, namely, β_{r1}, β_{r2}, and β_{r3}, were initialized to a value of 1.0 at the start of calibration. The MEPDG simulation was run then a sum of squared error (SSE) was computed for the difference between the predicted and the observed rut depths. The calibration coefficients were adjusted to reduce the error and the process was repeated until the SSE was minimized.

The calibration was performed in two phases. In the first phase, three field projects, i.e., I-10 near Egan (I10-1 and I10-2 mixtures), I-10 near Vinton (I10-3), and LA 1 near Golden Meadow (LA 1-2), were chosen to determine the local calibration coefficients. These projects provided detailed documentation on the materials for the entire structure as well as reliable field records. In the second phase, three additional field projects (I-10 near Gonzales, I-12 near Livingston, and LA 121 near Alexandria) were chosen which provided additional field rut measurements to better calibrate the rutting prediction model. The rutting measurements were obtained from LADOTD pavement management system database.

The calibration coefficients obtained after Phase II calibration are presented in Table 12. It should be noted that the calibration results are preliminary and need to be validated with additional data sets.

Figure 32 and Figure 33 present the measured and predicted rut depth measurements for Phase I and Phase II projects, respectively. The predicted rut depths were greater than the measured rut depths for the nationally calibrated model. However, the predicted and measured rut depths were in close agreement once the local calibration values of the model coefficients were implemented.

Table 12
Suggested range of calibration factors

Calibration Factors	βr1	βr2	βr3
Range	1.3-1.5	1.2-1.4	0.4-0.6
Mean	1.4	1.3	0.5

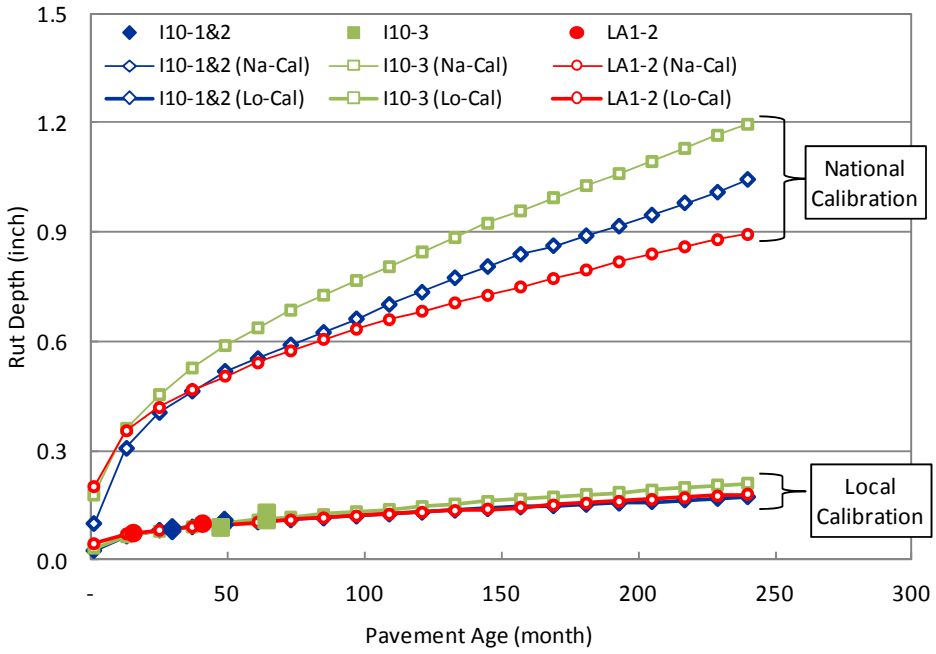

Figure 32

MEPDG predicted rutting and measured rut depth (Phase I)

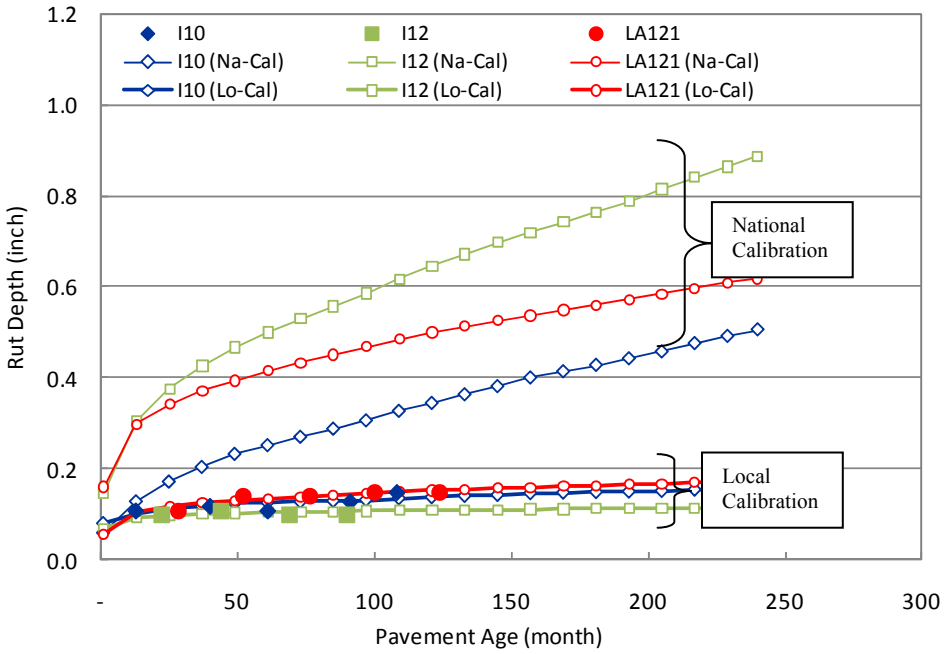

Figure 33

MEPDG predicted rutting and measured rut depth (Phase II)

Flow Number (F_N) Test Results

Figure 34 presents the mean flow number (F_N) for the mixtures evaluated in this study. High F_N values are desirable for rut-resistant mixtures.

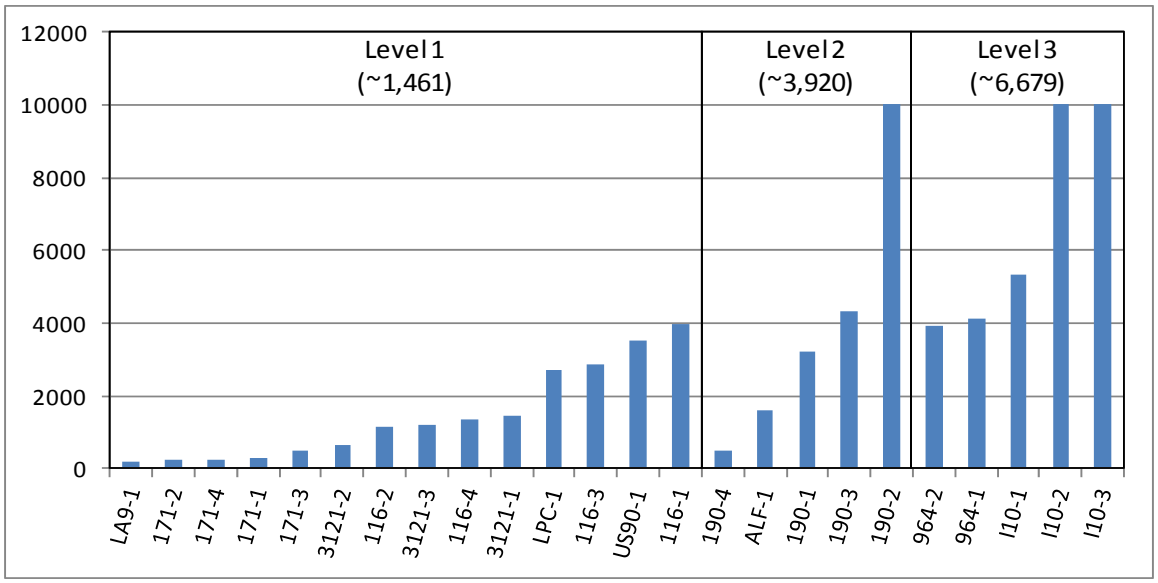

Figure 34
Flow number (F_N) test results

The average F_N values for Level 1, Level 2, and Level 3 mixtures were approximately 1461, 3920, and 6679, respectively. The Level 1, Level 2, and Level 3 F_N ranges were 195 to 3956, 486 to 10000, and 3932 to 10000, respectively.

It is worth noting that the mean F_N values increased with an increase in design level. Statistical analysis indicated that the means of all three levels were significantly different; the mean for the Level 2 mixtures was higher than the mean of the Level 1 mixtures, and the Level 3 mean was higher than the Level 2 mean.

Flow Time (F_T) Test Results

Figure 35 presents the mean flow time (F_T) for the mixtures evaluated. Higher F_T values are desirable for rut-resistant mixtures. The average F_T values for Level 1, Level 2, and Level 3 mixtures were approximately 430, 888, and 4,532, respectively. The Level 1, Level 2, and Level 3 F_T ranges were 19 to 956, 76 to 1,981, and 319 to 10,000, respectively.

It is interesting to note that the mean F_T values increased with increase in design level. However, statistical analysis indicated no significant differences among the means of Level 1, Level 2, and Level 3 mixtures.

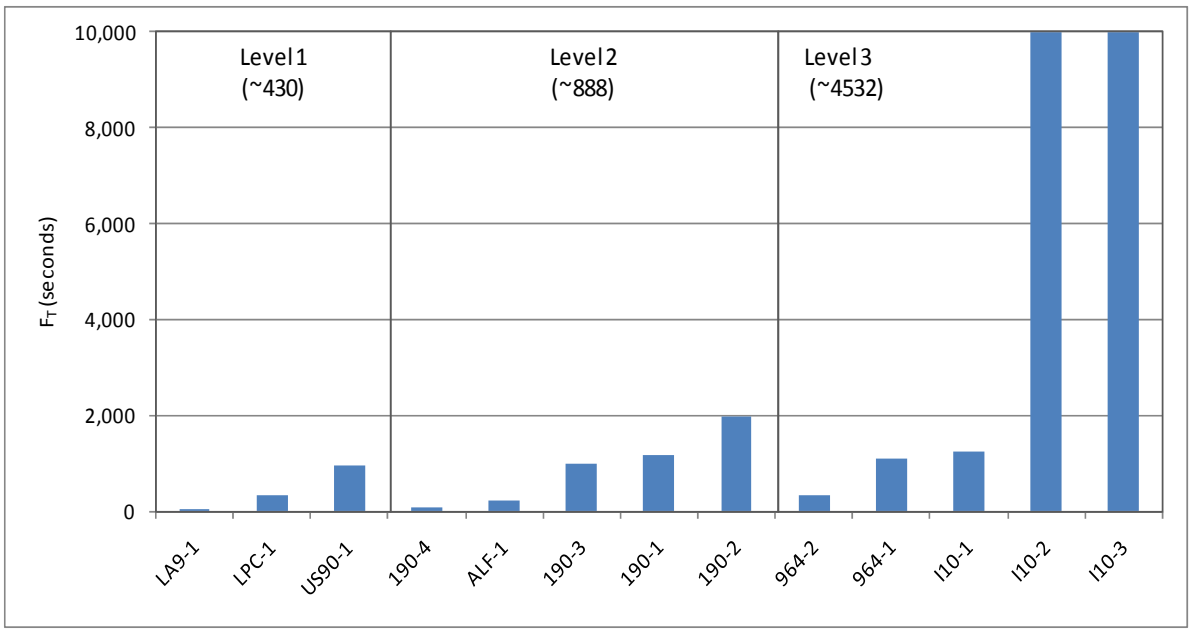

Figure 35
Flow time (F_T) test results

Loaded Wheel Tracking Device Test Results

Figure 36 presents the mean LWT rut depths for the mixtures evaluated in this study. Lower LWT rut depths at 20,000 passes indicate better rutting resistance.

The means of Level 1, Level 2, and Level 3 were 4.8, 10.0 and 3.8 mm, respectively. The Level 1, Level 2, and Level 3 LWT rut depth ranges were 2.5 to 8.37 mm, 2.05 to 21.35 mm, and 2.3 to 5.05 mm, respectively. It is observed that only three mixtures among the 24 tested considerably exceeded the 6-mm rut depth criterion at 20,000 passes. One of these mixtures (171-2 with 8.4-mm) is in the Level 1 group and the other two (190-1 and 190-3 with 14.8 and 21.4-mm respectively) were in the Level 2 group.

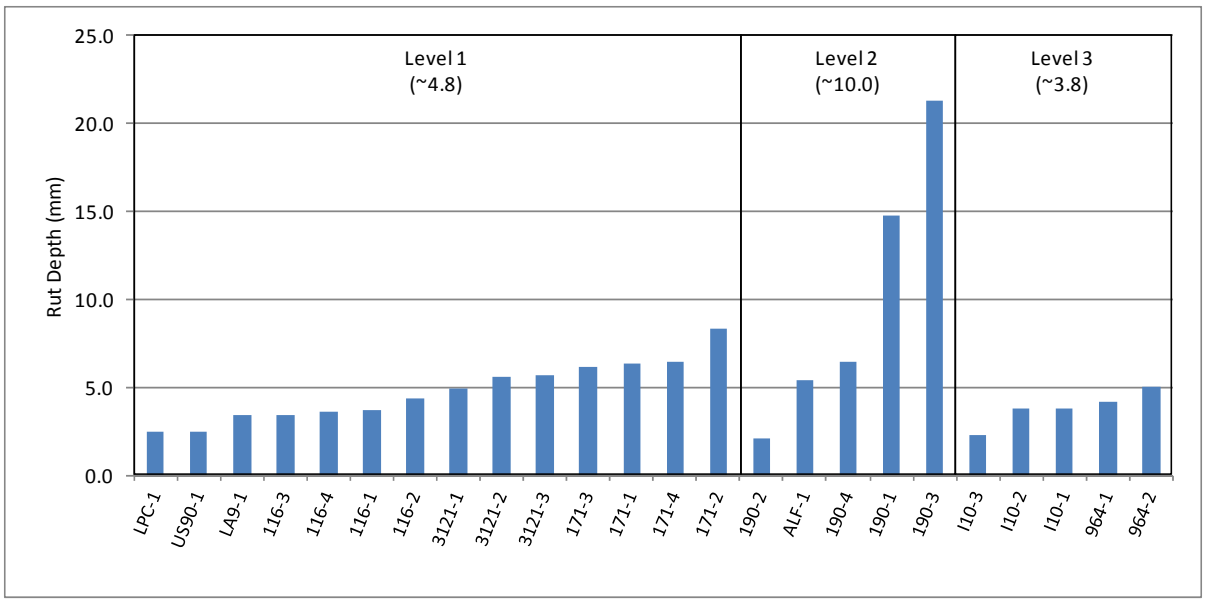

Figure 36
LWT rut depth test result

Comparison of Dynamic Moduli Obtained from Axial and Indirect Tension (IDT) Modes

A limited study was performed to compare the dynamic modulus obtained from axial and indirect tension (IDT) modes of testing. The IDT testing was performed on four mixtures at three temperatures (4.4, 25, 37.8ºC) and five frequencies (10, 5, 1, 0.5, and 0.1 Hz). The dynamic modulus was calculated as explained by Kim *[35]*.

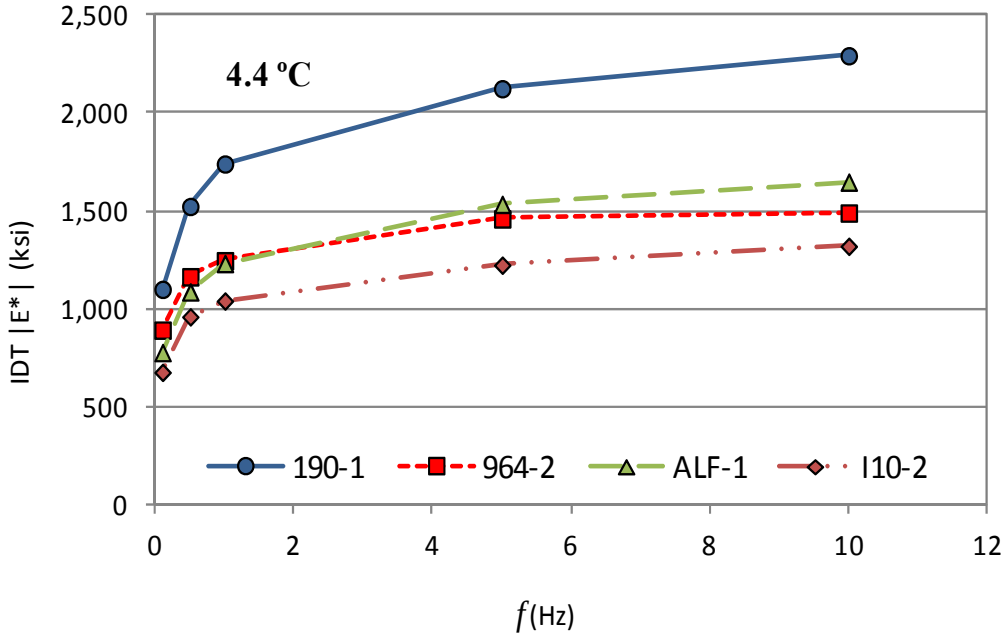

Figure 37
Dynamic modulus test results from the IDT mode at 4.4ºC

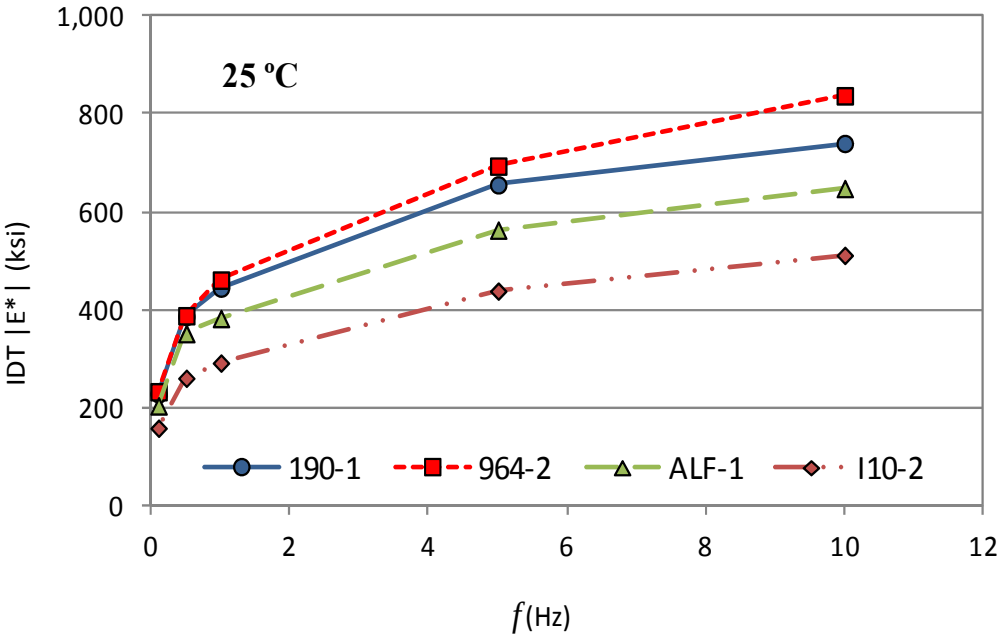

Figure 38
Dynamic modulus test results from the IDT mode at 25ºC

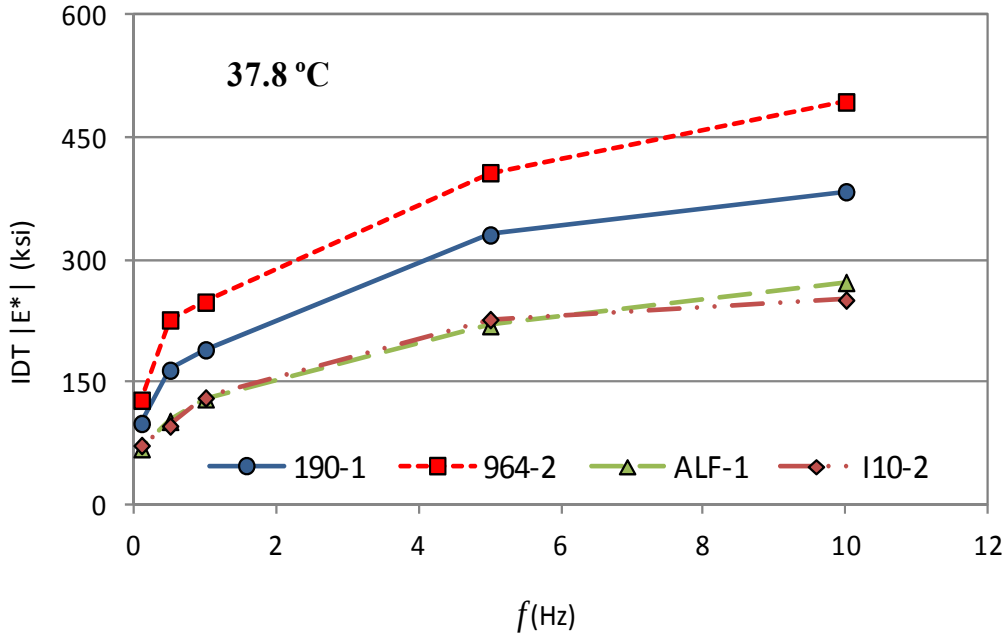

Figure 39
Dynamic modulus test results from the IDT mode at 37.8ºC

Figure 37, Figure 38, and Figure 39 present the dynamic modulus obtained from the IDT testing at 4.4, 25, and 37.8ºC. The dynamic modulus test results decreased with increase in temperature and decrease in frequency. The results followed the same trend exhibited by the dynamic modulus test results in axial mode.

Figure 40, Figure 41, Figure 42, and Figure 43 present the mean IDT and axial dynamic modulus values plotted as a function of frequency for the mixtures evaluated. The error bars indicate the standard deviation of the modulus. A statistical analysis was performed to compare two mean values of the IDT and axial dynamic moduli. The t-test procedure in SAS software was used at 95% level of confidence. The results of the analysis indicated that the IDT and axial moduli were statistically different in 35 out of the 60 cases (58 percent). Table 13 presents the mean IDT and axial modulus values and t-test results (p-values). A comparison of the modulus by temperature revealed that the IDT and axial dynamic moduli were statistically different 60 percent of the time at 4°C, 100 percent of the time at 25°C, and 15 percent of the time at 38°C.

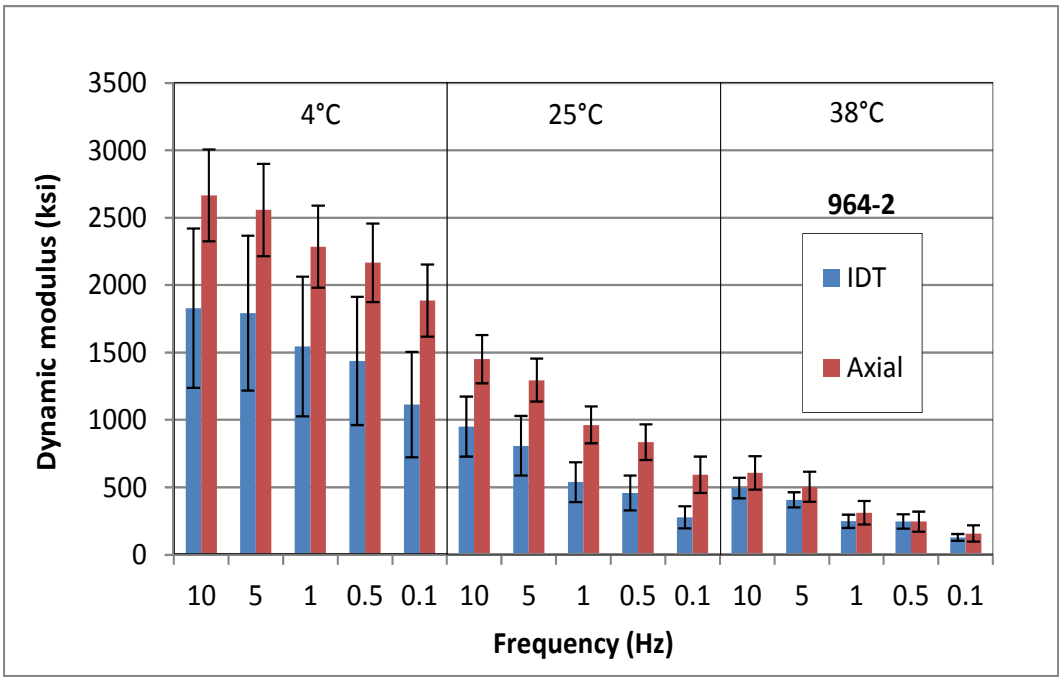

Figure 40
Mean IDT and axial modulus for 964-2

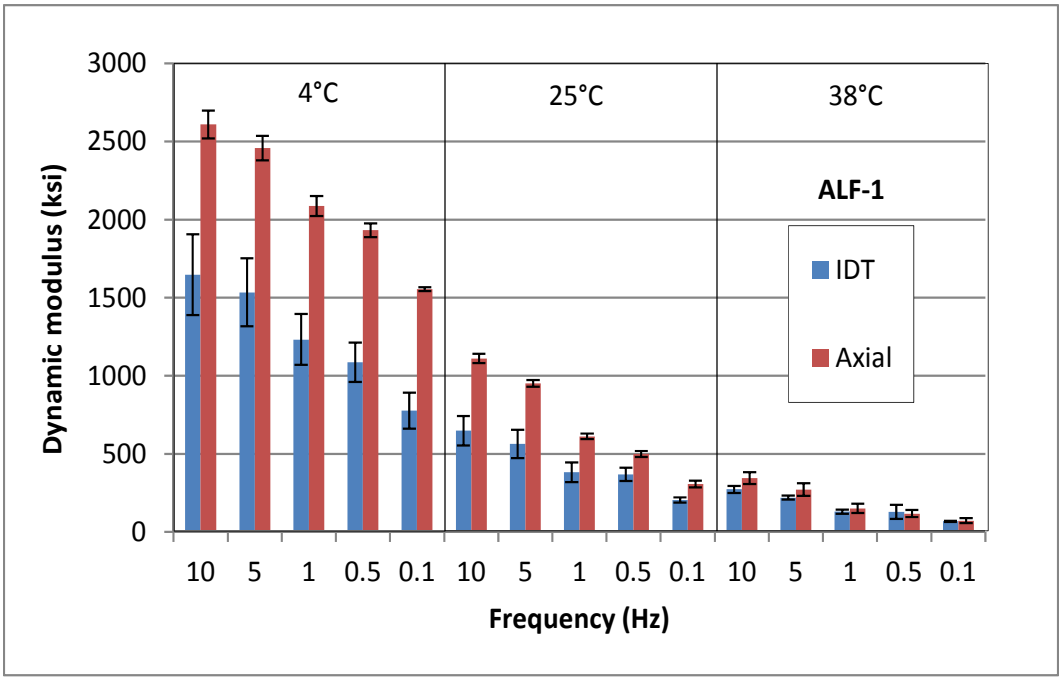

Figure 41
Mean IDT and axial modulus for ALF-1

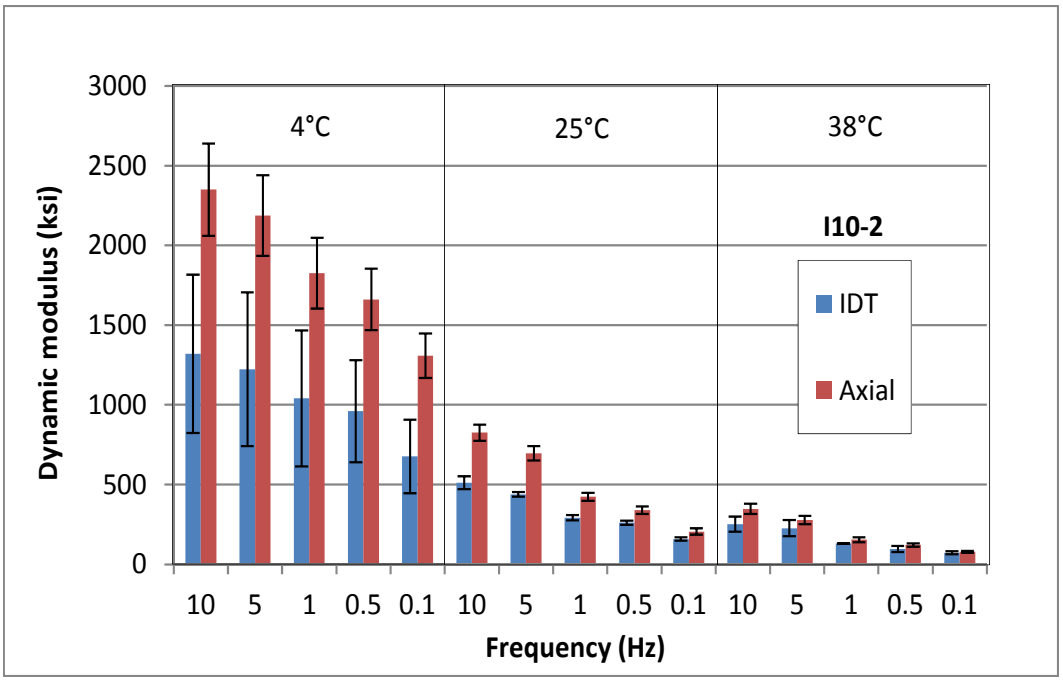

Figure 42
Mean IDT and axial modulus for I10-2

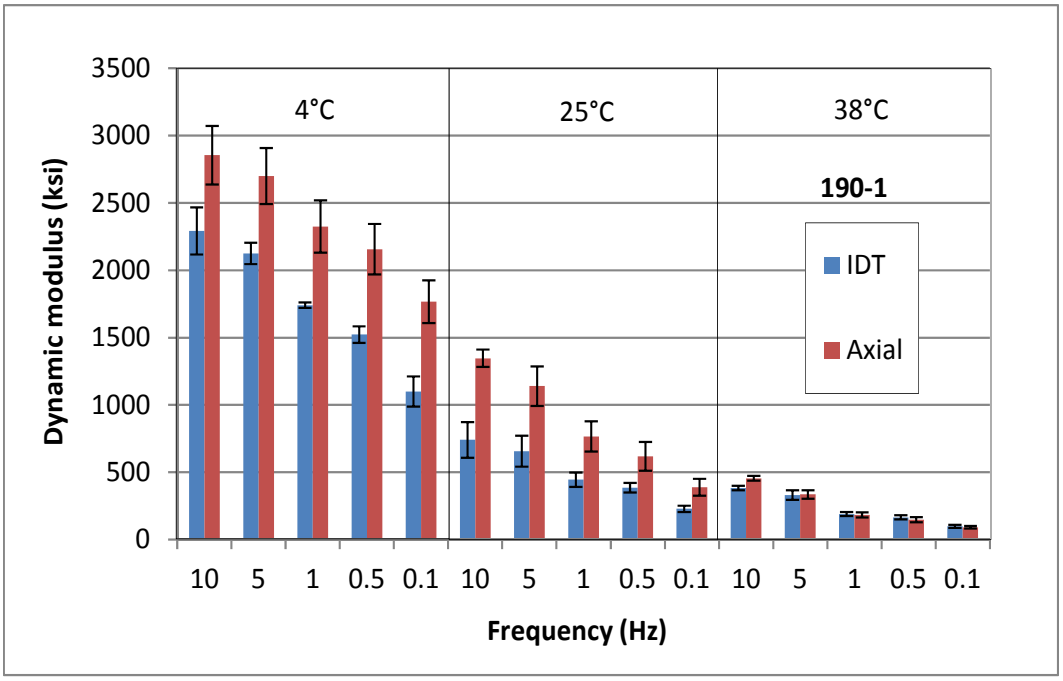

Figure 43
Mean IDT and axial modulus for 190-1

Table 13
Mean IDT and axial modulus and t-test results

Mixtures	Temperature (°C)	Frequency (Hz)	Mean Dynamic Modulus (ksi)		
			IDT	Axial	p-value
964-2	4°C	10	1831	2665	0.102
		5	1792	2558	0.118
		1	1545	2285	0.100
		0.5	1437	2167	0.087
		0.1	1114	1886	0.048
	25°C	10	949	1451	0.038
		5	808	1295	0.036
		1	538	963	0.022
		0.5	459	836	0.024
		0.1	278	593	0.026
	38°C	10	494	607	0.247
		5	407	503	0.251
		1	248	312	0.337
		0.5	246	245	0.984
		0.1	128	157	0.481
ALF-1	4°C	10	1648	2609	0.004
		5	1534	2458	0.002
		1	1232	2087	0.001
		0.5	1087	1932	0.000
		0.1	777	1554	0.007
	25°C	10	648	1111	0.001
		5	563	950	0.002
		1	382	611	0.004
		0.5	369	500	0.008
		0.1	204	307	0.011
	38°C	10	272	345	0.049
		5	220	271	0.105
		1	130	151	0.311
		0.5	128	118	0.738
		0.1	69	72	0.817

Table 13
Mean IDT and axial modulus and t-test results (continued)

I10-2	4°C	10	1320	2349	0.056
		5	1224	2188	0.056
		1	1041	1826	0.067
		0.5	960	1661	0.051
		0.1	676	1309	0.029
	25°C	10	511	825	0.001
		5	438	696	0.001
		1	291	423	0.001
		0.5	260	339	0.007
		0.1	158	205	0.023
	38°C	10	251	347	0.043
		5	227	278	0.216
		1	131	154	0.146
		0.5	96	121	0.129
		0.1	73	79	0.417
190-1	4°C	10	2293	2855	0.025
		5	2125	2700	0.011
		1	1740	2326	0.034
		0.5	1523	2157	0.005
		0.1	1100	1768	0.004
	25°C	10	740	1347	0.002
		5	656	1139	0.011
		1	445	765	0.011
		0.5	386	618	0.023
		0.1	228	388	0.014
	38°C	10	384	454	0.008
		5	331	336	0.856
		1	190	184	0.683
		0.5	165	148	0.277
		0.1	100	91	0.371

Figure 44 presents a scatter plot of the average IDT and axial dynamic modulus values. The figure also shows the line of regression and the prediction band. The prediction limits show

the variation range for a single prediction. A good correlation between the IDT and axial modulus was observed (R^2 of 0.94). It is noted that the prediction band included all but three points.

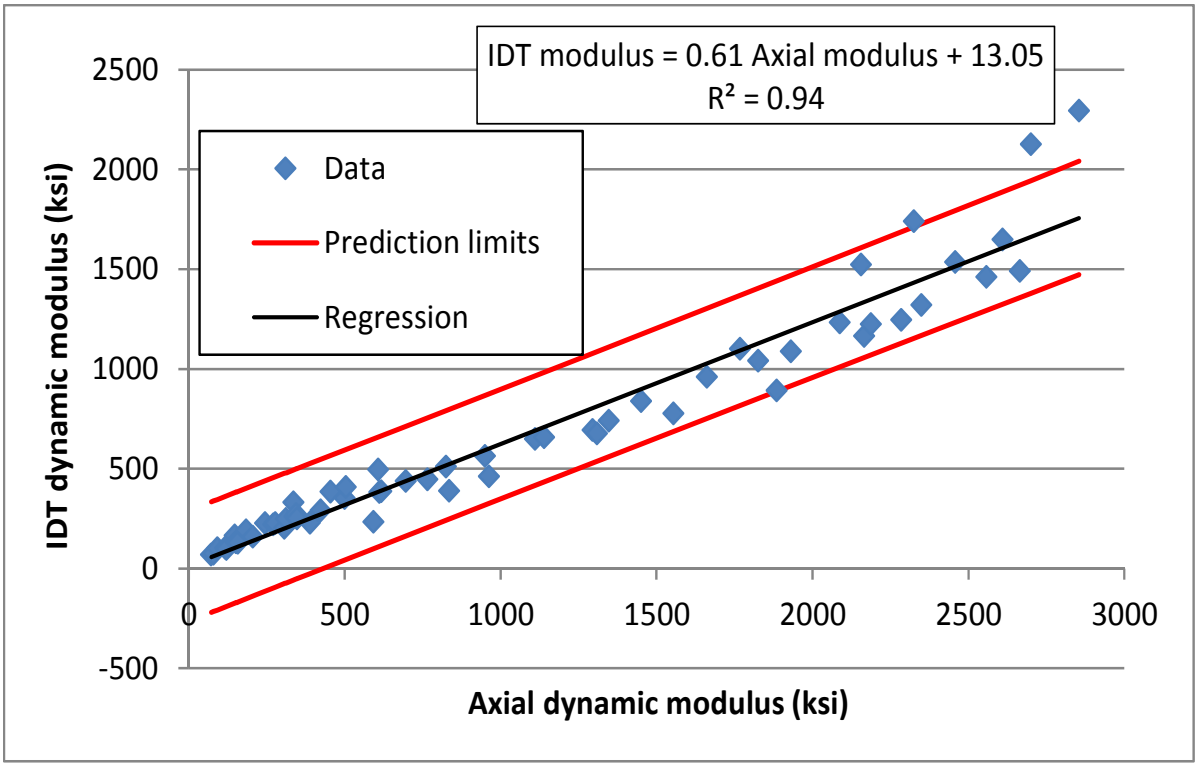

Figure 44
Scatter plot of average IDT and axial modulus values

It should be noted that the gauge length used in this study was 3 in. and the target strain level was 100-microstrain. Other researchers have used shorter gauge lengths, Kim, et.al *[16]*. It is possible that the gauge length contributed to the differences between the IDT and axial dynamic modulus. However, a strong correlation exists between the two, making prediction of one from another possible.

Developing a Catalog for Dynamic modulus (|E*|) Test Results

A catalog of dynamic modulus values for MEPDG input is presented in Tables 14 through 18. This catalog includes dynamic modulus test results at five temperatures (-10, 4.4, 25, 37.8 and 54.4ºC) and six loading frequencies (25, 10, 5, 1, 0.5, and 0.1 Hz). The dynamic modulus values were grouped by Design Levels 1 and 2, as defined in the 2006 Edition of the Louisiana Specifications for Roads and Bridges *[36]*. The dynamic modulus values are

further grouped by NMAS within each level. The dataset comprises a total of 28 mixtures, 14 for Level 1 and 14 for Level 2 categories. The mean, maximum, minimum, and standard deviation of the dynamic modulus is provided for all temperature and frequency combinations.

Table 14

Dynamic modulus (|E*|) (ksi) values at -10ºC for different frequencies

		Level 1				Level 2			
	NMAS	12.5-mm	19-mm	25-mm	All Mix	12.5-mm	19-mm	25-mm	All Mix
25 Hz	Average	3,186	4,077	3,584	3,616	3,664	3,790	3,642	3,699
	Max	3,989	4,157	3,732	4,157	4,094	3,944	4,520	4,520
	Min	2,579	3,997	3,436	2,579	3,238	3,636	3,200	3,200
	StdDev	484	113	209	269	390	218	434	347
10 Hz	Average	3,086	3,992	3,458	3,512	3,526	3,641	3,503	3,557
	Max	3,904	4,056	3,544	4,056	3,930	3,747	4,270	4,270
	Min	2,509	3,927	3,371	2,509	3,114	3,535	3,066	3,066
	StdDev	480	91	123	231	377	150	397	308
5 Hz	Average	2,996	3,919	3,362	3,426	3,412	3,532	3,380	3,441
	Max	3,832	3,971	3,459	3,971	3,781	3,630	4,132	4,132
	Min	2,448	3,867	3,266	2,448	3,013	3,435	2,950	2,950
	StdDev	481	73	136	230	356	138	385	293
1 Hz	Average	2,762	3,716	3,107	3,195	3,120	3,245	3,125	3,164
	Max	3,628	3,734	3,217	3,734	3,474	3,322	3,758	3,758
	Min	2,266	3,698	2,998	2,266	2,774	3,168	2,692	2,692
	StdDev	480	25	155	220	337	109	340	262
0.5 Hz	Average	2,656	3,613	2,986	3,085	2,984	3,113	3,004	3,033
	Max	3,524	3,614	3,098	3,614	3,312	3,178	3,612	3,612
	Min	2,200	3,612	2,874	2,200	2,670	3,047	2,571	2,571
	StdDev	474	2	158	211	319	93	327	246
0.1 Hz	Average	2,379	3,334	2,708	2,807	2,652	2,792	2,700	2,715
	Max	3,241	3,375	2,849	3,375	2,892	2,829	3,175	3,175
	Min	1,983	3,293	2,568	1,983	2,410	2,755	2,277	2,277
	StdDev	462	58	198	239	263	52	278	198

Table 15

Dynamic modulus (|E*|) (ksi) values at 4.4ºC for different frequencies

		Level 1				Level 2			
	NMAS	12.5-mm	19-mm	25-mm	All Mix	12.5-mm	19-mm	25-mm	All Mix
25 Hz	Average	2,452	3,317	2,745	2,838	2,706	2,807	2,791	2,768
	Max	3,153	3,425	2,787	3,425	3,086	2,826	3,395	3,395
	Min	1,975	3,208	2,703	1,975	2,394	2,787	2,199	2,199
	StdDev	394	153	60	202	302	28	385	238
10 Hz	Average	2,248	3,071	2,567	2,629	2,477	2,634	2,587	2,566
	Max	2,924	3,146	2,641	3,146	2,844	2,658	3,081	3,081
	Min	1,816	2,996	2,493	1,816	2,234	2,609	2,050	2,050
	StdDev	369	107	105	194	265	35	324	208
5 Hz	Average	2,084	2,874	2,418	2,459	2,314	2,483	2,430	2,409
	Max	2,741	2,922	2,503	2,922	2,657	2,509	2,863	2,863
	Min	1,682	2,827	2,333	1,682	2,109	2,458	1,922	1,922
	StdDev	354	67	120	180	242	36	300	193
1 Hz	Average	1,703	2,400	2,062	2,055	1,941	2,094	2,065	2,033
	Max	2,303	2,410	2,166	2,410	2,229	2,100	2,386	2,386
	Min	1,361	2,389	1,958	1,361	1,820	2,087	1,609	1,609
	StdDev	316	15	147	159	194	9	266	157
0.5 Hz	Average	1,539	2,191	1,903	1,878	1,778	1,932	1,908	1,873
	Max	2,103	2,227	2,014	2,227	2,039	1,933	2,180	2,180
	Min	1,221	2,154	1,792	1,221	1,661	1,931	1,482	1,482
	StdDev	296	51	157	168	176	1	255	144
0.1 Hz	Average	1,177	1,722	1,521	1,473	1,416	1,552	1,550	1,506
	Max	1,678	1,803	1,632	1,803	1,629	1,554	1,886	1,886
	Min	922	1,641	1,411	922	1,309	1,550	1,201	1,201
	StdDev	256	115	156	176	147	3	239	129

Table 16

Dynamic modulus (|E*|) (ksi) values at 25ºC for different frequencies

		Level 1				Level 2			
	NMAS	12.5-mm	19-mm	25-mm	All Mix	12.5-mm	19-mm	25-mm	All Mix
25 Hz	Average	954	1,369	1,216	1,180	1,151	1,294	1,322	1,256
	Max	1,349	1,421	1,249	1,421	1,454	1,328	1,641	1,641
	Min	749	1,318	1,183	749	1,009	1,261	1,029	1,009
	StdDev	221	73	47	113	209	47	201	152
10 Hz	Average	766	1,142	1,013	973	951	1,096	1,131	1,059
	Max	1,124	1,195	1,053	1,195	1,223	1,111	1,451	1,451
	Min	589	1,089	973	589	804	1,080	873	804
	StdDev	193	75	56	108	193	22	199	138
5 Hz	Average	632	984	856	824	817	937	966	907
	Max	958	1,037	903	1,037	1,066	951	1,295	1,295
	Min	478	931	809	478	676	923	693	676
	StdDev	173	75	67	105	179	19	202	134
1 Hz	Average	382	657	543	527	544	588	639	590
	Max	637	704	585	704	740	611	963	963
	Min	274	609	501	274	423	564	383	383
	StdDev	128	68	59	85	147	33	188	123
0.5 Hz	Average	302	539	437	426	451	476	527	485
	Max	523	581	473	581	623	500	836	836
	Min	214	496	402	214	339	451	295	295
	StdDev	110	60	50	73	132	35	174	113
0.1 Hz	Average	174	316	261	250	281	288	339	303
	Max	310	343	285	343	395	307	593	593
	Min	116	288	237	116	205	270	170	170
	StdDev	65	39	34	46	88	26	135	83

Table 17

Dynamic modulus (|E*|) (ksi) values at 37.8ºC for different frequencies

		Level 1				Level 2			
	NMAS	12.5-mm	19-mm	25-mm	All Mix	12.5-mm	19-mm	25-mm	All Mix
25 Hz	Average	384	647	509	514	522	492	589	534
	Max	629	673	543	673	597	505	764	764
	Min	264	620	476	264	431	478	481	431
	StdDev	123	37	47	69	84	19	89	64
10 Hz	Average	272	483	379	378	396	349	443	396
	Max	479	500	406	500	465	353	607	607
	Min	179	465	352	179	320	345	337	320
	StdDev	99	25	38	54	73	6	84	54
5 Hz	Average	210	379	295	295	323	276	358	319
	Max	382	393	319	393	380	280	503	503
	Min	133	365	272	133	257	271	255	255
	StdDev	81	20	33	45	64	6	77	49
1 Hz	Average	111	200	165	159	185	152	204	181
	Max	203	209	178	209	221	154	312	312
	Min	68	192	152	68	153	151	130	130
	StdDev	41	12	18	24	37	2	54	31
0.5 Hz	Average	86	151	126	121	146	120	159	142
	Max	152	157	138	157	173	123	245	245
	Min	55	145	115	55	121	117	102	102
	StdDev	29	8	16	18	27	4	43	25
0.1 Hz	Average	52	75	76	67	85	74	102	87
	Max	75	77	81	81	92	77	157	157
	Min	36	72	70	36	79	72	67	67
	StdDev	12	3	8	8	6	4	26	12

Table 18

Dynamic modulus (|E*|) (ksi) values at 54.4ºC for different frequencies

		Level 1				Level 2			
	NMAS	12.5-mm	19-mm	25-mm	All Mix	12.5-mm	19-mm	25-mm	All Mix
25 Hz	Average	105	178	160	148	181	148	207	178
	Max	182	195	166	195	224	163	305	305
	Min	68	161	154	68	143	133	129	129
	StdDev	34	24	9	22	40	21	53	38
10 Hz	Average	70	111	112	98	127	104	149	127
	Max	112	121	116	121	152	115	227	227
	Min	48	100	108	48	107	93	89	89
	StdDev	18	15	6	13	21	16	40	25
5 Hz	Average	55	80	88	74	100	82	119	100
	Max	81	87	90	90	117	91	182	182
	Min	38	73	85	38	89	74	72	72
	StdDev	12	10	3	8	12	12	32	19
1 Hz	Average	35	37	53	41	63	55	76	64
	Max	41	39	54	54	72	60	112	112
	Min	26	34	52	26	52	50	50	50
	StdDev	6	3	1	3	8	7	18	11
0.5 Hz	Average	30	27	44	34	53	48	64	55
	Max	38	28	45	45	60	54	91	91
	Min	22	26	43	22	40	43	45	40
	StdDev	6	2	1	3	9	8	13	10
0.1 Hz	Average	22	14	33	23	41	38	49	43
	Max	37	14	33	37	50	42	63	63
	Min	14	14	33	14	22	34	38	22
	StdDev	7	-	-	3	13	5	8	9

Permanent Deformation Analysis

This section compares the different tests used to predict rutting performance (permanent deformation). Table 19 presents the statistical rankings of the mixtures for the rut parameters considered in this study, namely |E*|, E*/sin(δ), F_N, and LWT rut depth. An analysis of variance procedure with 95% confidence level was used to group the mixtures' rut parameters. The letter "A" is assigned to the group with the best rut resistance, the letter "B" to the next best group, and so on. A designation such as "A/B" indicates that the group mean was not statistically different from either the "A" or "B" groups. The 22 mixtures were clustered into sub-groups based on the statistical differences in their means. There were 7 sub-groups (A-G) for the LWT tests, 8 (A-H) for the |E*| and E*/sin(δ), and 9 (A-I) for the F_N test. This indicates that the F_N test was more sensitive than the other rut parameters for the mixtures evaluated (i.e., resulting in nine sub-groups). In general, the clustering of the high, medium, and low design traffic levels was consistent with the ranking of the statistical analysis.

Table 19
Statistical ranking of rut parameters

E*		E*/sinδ		F_N		LWT	
964-2	A	964-2	A	190-2	A	190-2	A
190-2	B	190-2	B	I10-2	A	I10-3	A
I10-1	B-C	I10-1	B-C	I10-3	A	US90-1	A
I10-2	C-D	I10-3	B-D	I10-1	B	LPC-1	A-B
964-1	C-E	964-1	C-E	964-2	C	LA9-1	A-C
US90-1	C-E	I10-2	C-F	116-1	C	116-3	A-D
I10-3	C-F	US90-1	C-F	964-1	C	116-4	A-D
116-2	C-F	LPC-1	C-F	US90-1	C-D	116-1	A-D
LPC-1	C-F	190-4	C-G	116-3	D-E	I10-2	A-E
116-3	C-F	ALF-1	C-H	LPC-1	E	I10-1	A-E
ALF-1	C-G	116-2	D-H	ALF-1	F	964-1	A-F
116-4	C-H	171-4	D-H	3121-1	F	116-2	A-F
190-4	D-H	171-1	D-H	116-4	F-G	3121-1	B-F
116-1	D-H	116-3	D-H	3121-3	F-H	964-2	C-F
171-3	E-H	171-2	D-H	116-2	F-H	ALF-1	C-F
3121-3	E-H	171-3	E-H	3121-2	G-I	3121-2	C-F
3121-1	E-H	116-4	E-H	171-3	H-I	3121-3	D-F
171-4	E-H	3121-3	E-H	190-4	H-I	171-3	E-F
171-2	F-H	116-1	F-H	171-1	I	171-4	F-G
171-1	F-H	3121-1	F-H	171-4	I	171-1	F-G
3121-2	G-H	3121-2	G-H	171-2	I	190-4	F-G
LA9-1	H	LA9-1	H	LA9-1	I	171-2	G
Subgroups	8	Subgroups	8	Subgroups	9	Subgroups	7

* Blue shading indicates Level 1, green shading indicates Level 2, and orange shading indicates Level 3

In general, a fair correlation was observed between F_N and LWT test results for the mixtures evaluated; see Figure 45. This correlation was further sub-grouped by the mixtures' design traffic levels; see Figure 46. The permanent deformation of asphalt mixtures is commonly related to their viscoelastic response, which is generally modeled through a power function *[17, 18]*. It is noted that good correlations were obtained for traffic Design Levels 2 and 3, while it was fair for traffic Design Level 1. The Hamburg rut depths decreased as the F_N values increased, as expected. Note that for the comparison of F_N and LWT rut depth, the mixtures that exhibited stripping in the LWT were excluded from the analysis. This approach was adopted because the F_N test does not evaluate stripping. Figure 47 and Figure 48 present the correlations between the dynamic modulus and LWT test results. A poor correlation was observed between these two tests. However, there was a trend that exhibited a decrease in |E*| or E*/sin(δ) with an increase in LWT rut depth.

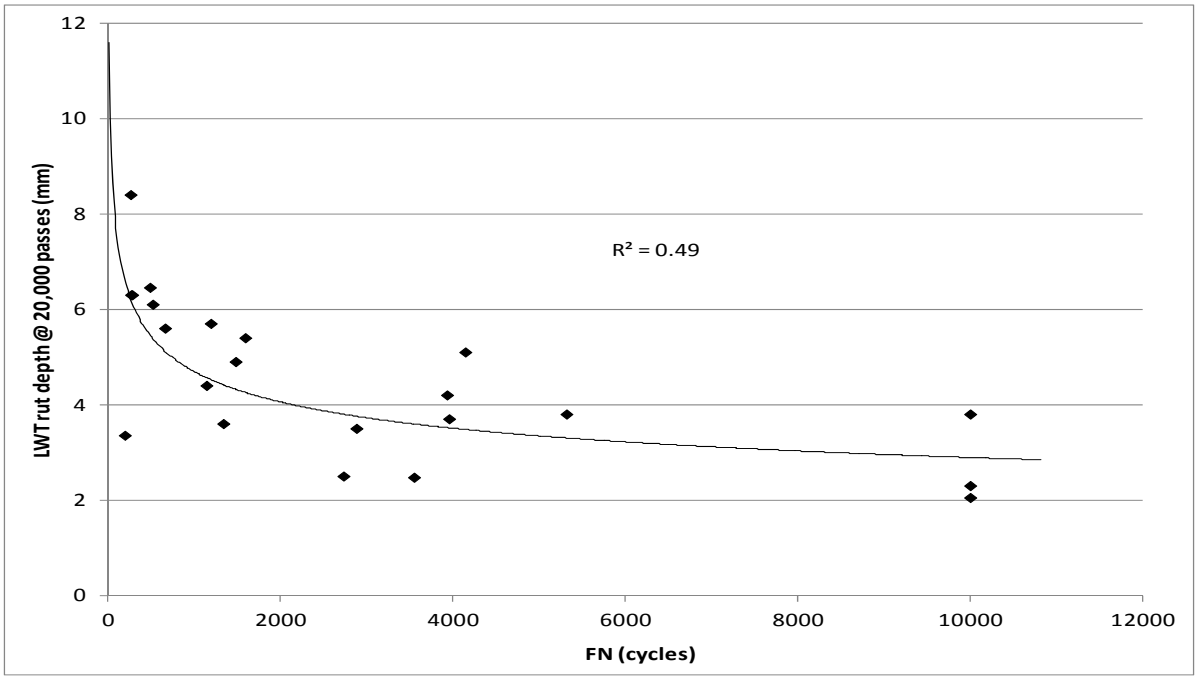

Figure 45
Correlation between LWT and F_N test results

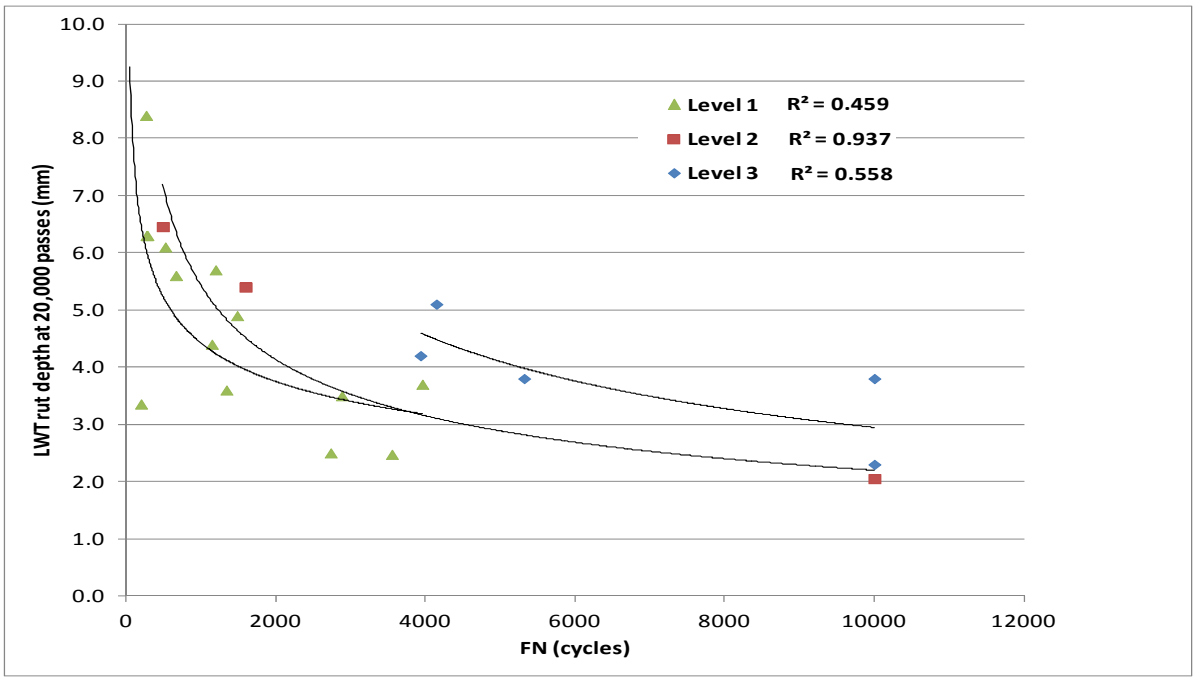

Figure 46
Correlation between LWT rut depth and F_N by levels

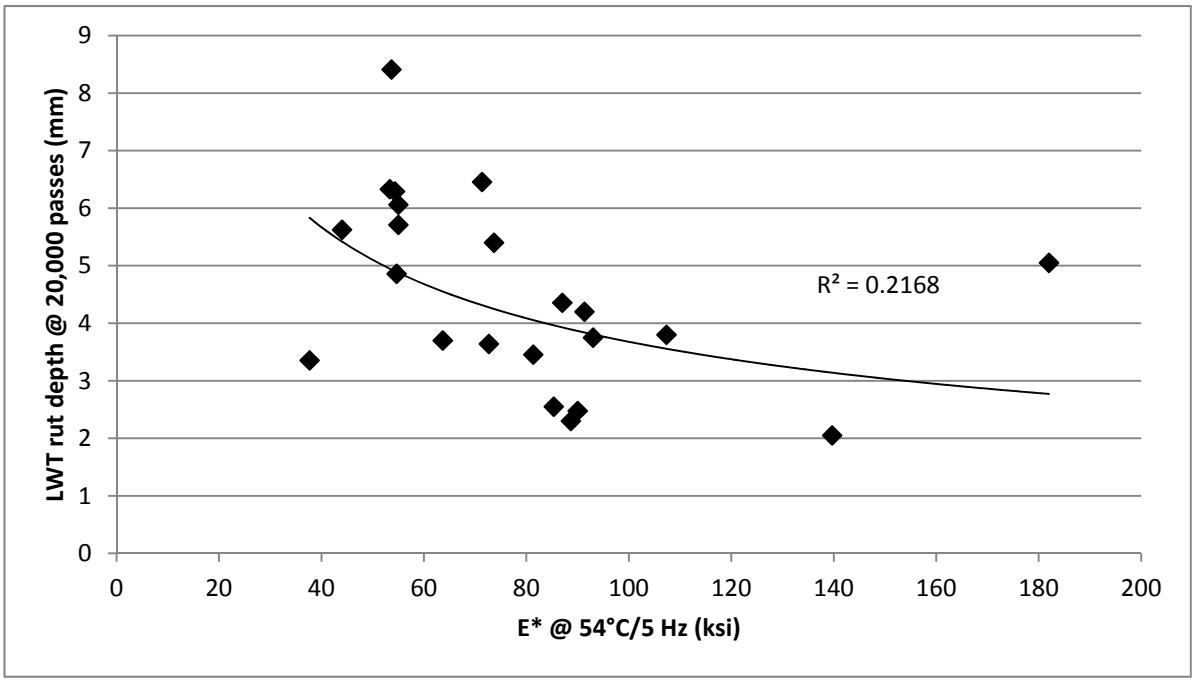

Figure 47
Correlation between LWT and |E*|

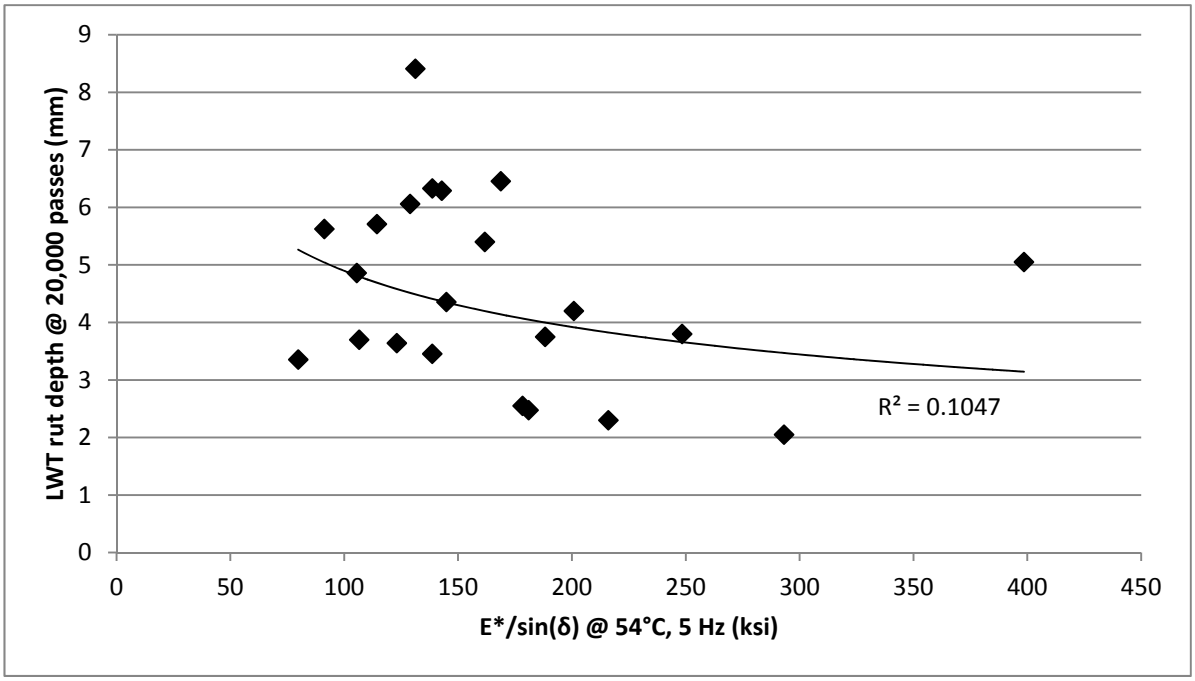

Figure 48
Correlation between LWT and E*/sin(δ)

SUMMARY AND CONCLUSIONS

Mechanical characterization testing on 28 typical Louisiana asphalt mixtures was performed. These mixtures were selected from 14 field projects, which include design Traffic Levels 1, 2, and 3. Test methods used in this study include dynamic modulus (|E*|), flow number (F_N), flow time (F_T), and LWT tests. The |E*| test results were used to develop a catalog of typical dynamic modulus values for Level 1 input in the new Mechanistic-Empirical Pavement Design Guide (MEPDG). In addition, validation of Witczak and Hirsch |E*| prediction equations, sensitivity analysis of MEPDG rutting prediction model, preliminary calibration of MEPDG rutting prediction model for use in Louisiana, comparison between uniaxial and IDT |E*|, and correlation analysis between the LWT and other asphalt mixture performance test (AMPT) methods were conducted. The following observations were made based upon the results of these analyses:

- A catalog of |E*| and phase angle values of typical Louisiana asphalt mixtures was created for the Level 1 and Level 2 traffic categories, per the Louisiana specification. It is expected that this catalog of dynamic moduli could be used for Level 1 input in the MEPDG simulations. The input instructions are described in Appendix E.
- Dynamic modulus (|E*|) appeared to be dependent on the design traffic level, nominal maximum aggregate size (NMAS), and the asphalt binder's high temperature PG grade. Mixtures designed for high volume traffic roads with larger aggregate size and higher asphalt binder grade resulted in higher |E*| values at higher temperatures.
- The rutting factor, $|E^*|/\sin(\delta)$ was found to distinguish the Level 1 traffic mixtures from the Level 2 and Level 3 mixtures for their potential rutting resistance.
- Both the Witczak and Hirsch models predicted the dynamic modulus (|E*|) values with reasonable accuracy. The MEPDG rut prediction was sensitive to changes in the dynamic modulus input values. The pavement structure with the thicker asphalt layer was more sensitive compared to the structure with the thinner asphalt layer. Dynamic modulus test results obtained from Axial and IDT modes showed no statistical differences for the majority of the mixtures tested.
- Correlations between the LWT rut depth and |E*|, $|E^*|/\sin(\delta)$, and F_N were not strong.
- A local calibration on the rutting prediction model of the MEPDG was conducted and preliminary ranges of calibration factors were presented.

RECOMMENDATIONS

This research project generated a catalog of dynamic moduli values for various asphalt mixture types. This catalog includes dynamic modulus test results at five temperatures and six loading frequencies. The dynamic modulus values were grouped by Design Levels 1 and 2, as defined in the 2006 Edition of the Louisiana Specifications for Roads and Bridges. The dynamic modulus values are further grouped by NMAS within each level. This catalog was also created as a user-friendly spreadsheet and Microsoft Access based database, which is submitted as a separate CD. It is recommended that LDOTD design engineers use this catalog as the asphalt mixtures materials input during the implementation of the MEPDG (known as Pavement-ME) design guide in Louisiana.

In addition, the rutting prediction model used in the MEPDG was calibrated based on limited number of projects. The local calibration coefficients developed in this study are recommended during the implementation of the MEPDG design guide in Louisiana.

Furthermore, it is recommended that field rut depth studies should be pursued to collect long-term rutting performance of actual field mixtures to improve MEPDG rutting predictions.

REFERENCES

1. *Guide for Mechanistic-Empirical Design of New and Rehabilitated Pavement Structures.* National Cooperative Highway Research Program (NCHRP) Report 1-37A, Transportation Research Board, National Research Council, Washington, D.C., 2004.

2. Witczak, M.W., Kaloush, K., Pellinen, T., and El-Basyouny, M., Von Quintus, H. *Simple Performance Test for Superpave Mix Design.* National Cooperative Highway Research Program (NCHRP) Report 465. Transportation Research Board, National Research Council, Washington, D.C., 2002.

3. Cominsky, R. J., Killingsworth, B.M., Anderson, R.M., Anderson, D.A., and Crockford, W. *Field Procedures and Equipment to Implement SHRP Asphalt Specifications.* National Cooperative Highway Research Program (NCHRP) Report 409. Transportation Research Board, National Research Council, Washington, D.C., 1998.

4. "Louisiana Standard Specifications for Roads and Bridges." State of Louisiana, Department of Transportation and Development, Baton Rouge, 2000 Edition.

5. *AASHTO Road Test, History and Description of Project*. Highway Research Board (HRB) Special Report 61A, 1961.

6. Huang, Y. H. *Pavement Analysis and Design*. Prentice-Hall, Inc., Englewood Cliffs, New Jersey, 1993.

7. "AASHTO Interim Guide for Design of Pavement Structures." American Association of State Highway and Transportation Officials, Washington, D.C., 1972.

8. "AASHTO Interim Guide for Design of Pavement Structures Chapter III Revised." American Association of State Highway and Transportation Officials, Washington, D.C., 1981.

9. "AASHTO Guide for Design of Pavement Structures Volume 2." American Association of State Highway and Transportation Officials, Washington, D.C., 1986.

10. "AASHTO Guide for Design of Pavement Structures 1993." American Association of State Highway and Transportation Officials. Washington, D.C., 1993.

11. Rodezno, M.C., Kaloush, K.E., and Way, G.B. "Assessment of Distress in Conventional Hot-Mix Asphalt and Asphalt-Rubber Overlays on Portland Cement Concrete

Pavements: Using the New Guide to Mechanistic-Empirical Design of Pavement Structures." *In Transportation Research Record 1929.* Transportation Research Board, National Research Council, Washington, D.C., 2005, pp. 20-27.

12. Yang, J., Wang, W., Petros, K., Sun, L., and Sherwood, J. "Test of NCHRP 1-37A Design Guide Software for New Flexible Pavements." Transportation Research Board, Annual Meeting CD-ROM, Washington, D.C., 2005.

13. Pellinen, T.K. "Investigation of the Use of Dynamic Modulus as an Indicator of Hot-Mix Asphalt Performance." Ph.D. Dissertation. Arizona State University, Tempe, AZ., May 2001.

14. Pellinen, T.K. "The Effect of Volumetric Properties on Mechanical Behavior of Asphalt Mixtures." Transportation Research Board Preprint CD-ROM, Washington, D.C., 2003.

15. Zhou, F., and Scullion, T. "Preliminary Field Validation of Simple Performance Tests for Permanent Deformation: Case Study." *In Transportation Research Record 1832.* Transportation Research Board, National Research Council, Washington, D.C., 2003, pp. 209-216.

16. Kim, Y.R., King, M., and Mostafa, M. "Typical Dynamic Moduli Values of Hot Mix Asphalt in North Carolina and Their Prediction." Transportation Research Board Annual Meeting CD-ROM, Washington, D.C., 2004.

17. Bhasin, A., Button, J.W., and Chowdhury, A. *Evaluation of Selected Laboratory Procedures and Development of Databases for HMA*. Report 0-4203-3. Texas Transportation Institute, College Station, Texas, 2005.

18. Mohammad, L.N., Wu, Z., Obulareddy, S., Cooper, S., and Abadie, C. "Permanent Deformation Analysis of Hot-Mix Asphalt Mixtures with Simple Performance Tests and 2002 Mechanistic-Empirical Pavement Design Software." *In Transportation Research Record 1970*, National Research Council, Washington, D.C., 2006, pp. 133-142.

19. Mohammad, L.N., Wu, Z., Myers, L., Cooper, S., and Abadie, C. "A Practical Look at the Simple Performance Tests: Louisiana's Experience." *Journal of the Association of Asphalt Paving Technologists*, Vol. 74, 2005, pp. 478-520.

20. Tran, N.H., and Hall, K.D. "An Examination of Strain Levels Used in the Dynamic Modulus Testing (with Discussion)." *Journal of the Association of Asphalt Paving Technologists*, Vol. 75, 2006, pp. 321-343.

21. Pellinen, T.K., Witczak, M.W. "Stress Dependent Master Curve Construction for Dynamic (Complex) Modulus (with Discussion)." *Journal of the Association of Asphalt Paving Technologists*, Vol. 71, 2002, pp. 281-309.

22. Andrei, D., Witczak, M.W., and Mirza, M.W. *Development of a Revised Predictive Model for the Dynamic (Complex) Modulus of Asphalt Mixtures*. National Cooperative Highway Research Program (NCHRP) 1-37A Inter-Report. University of Maryland, March 1999.

23. Christensen Jr., D.W., Pellinen, T., and Bonaquist, R.F. "Hirsch Model for Estimating the Modulus of Asphalt Concrete." *Journal of the Association of Asphalt Paving Technologists*, Vol.72, 2003, pp. 97-121.

24. Schwartz. C. W. "Evaluation of the Witczak Dynamic Modulus Prediction Model." Transportation Research Board Annual Meeting CD-ROM, National Research Council, Washington, D.C., 2005.

25. Kaloush, K.E., and Witczak, M.W. "Simple Performance Test for Permanent Deformation of Asphalt Mixtures." Transportation Research Board Annual Meeting CD-ROM, National research Council, Washington, D.C., 2002.

26. Kaloush, K.E., and Witczak, M.W. "Tertiary Flow Characteristics of Asphalt Mixtures (with Discussion and Closure)." *Journal of Association of Asphalt Paving Technologists*, Vol.71, 2002, pp. 248-280.

27. Kaloush, K.E., and Witczak, M.W. "Simple Performance Test for Permanent Deformation of Asphalt Mixtures." Transportation Research Board Annual Meeting CD-ROM, National Research Council, Washington, D.C., 2002.

28. Kaloush, K.E., Witczak, M.W., and Von Quintus, H. "Pursuit of the Simple Performance Test for Asphalt Mixture Rutting." *Journal of the Association of Asphalt Paving Technologists*, Vol.71, 2002, pp. 671-691.

29. Bhasin, A., Button, J.W., and Chowdhury, C. "Evaluation of Simple Performance Tests on HMA Mixtures from the South Central United States." Transportation Research Board Annual Meeting CD-ROM, National Research Council, Washington, D.C., 2003.

30. Mohammad, L.N., Wu, Z., and King, W., "Accelerated Loading Evaluation of Foamed Asphalt Treated RAP Layers in Pavement Performance." Louisiana Transportation Research Center, Baton Rouge, La, Report 475, Dec. 2013.

31. Pellinen, T.K., and Witczak, M.W. "Use of Stiffness of Hot-Mix Asphalt As A Simple Performance Test." *In Transportation Research Record 1789*. Transportation Research Board, National Research Council, Washington, D.C., 2002, pp.80-90.

32. Bhasin, A., Button, J., Chowdhury, A., and Masad, E. *Analysis of South Texas Aggregates for Use in Hot Mix Asphalt*. Research Report FHWA/TX-050-4203-4. Texas Transportation Institute, College Station, Texas, 2005.

33. Velasquez, R., Hoegh, K., Yut, I., Funk, N., Cochran, G., Marasteanu, M., and Khazanovich, L. *Implementation of the MEPDG for New and Rehabilitated Pavement Structures for Design of Concrete and Asphalt Pavements in Minnesota*. Report MN/RC 2009-06. Minnesota, 2009.

34. "Guide for the Local Calibration of the Mechanistic-Empirical Pavement Design Guide." American Association of State Highway and Transportation Officials (AASHTO), Washington, D.C., 2010.

35. Kim, Y. R., Seo, Y., King, M., Momen, M. "Dynamic Modulus Testing of Asphalt Concrete in Indirect Tension Mode." *In Transportation Research Record 1891.* Transportation Research Board, National Research Council, Washington, D.C., 2004, pp. 163-173.

36. "Louisiana Standard Specifications for Roads and Bridges." State of Louisiana, Department of Transportation and Development, Baton Rouge, 2006 Edition.

37. "Standard Test Method for Dynamic Modulus of Asphalt Mixtures." ASTM D3497, ASTM International, West Conshohocken, PA, 1979.

38. "Standard Method of Test for Determining Dynamic Modulus of Hot-Mix Asphalt Mixtures." AASHTO Designation: TP 62-03, American Association of State Highway and Transportation Officials (AASHTO), Washington, D.C., 2004.

39. Bonaquist, R.F., Christensen, D.W., and Stump III, W. "Simple Performance Tester for Superpave Mix Design: First-Article Development and Evaluation." *In Transportation Research Record 513.* Transportation Research Board, National Research Council, Washington, D.C., 2003, pp. 168.

40. Witczak, M.W., and Kaloush, K., "Performance Evaluation of Asphalt Modified Mixtures Using Superpave and P-401 Mix Gradings." Technical Report to the Maryland Department of Transportation, Maryland Port Administration, University of Maryland, College Park, Maryland, 1998.

41. Roberts, F.L., Kandhal, P.S., Brown, E.R., Lee, D.Y., and Kennedy, T.W. "Hot Mix Asphalt Materials, Mixture Design, and Construction Second Edition." NAPA Research and Educational Foundation, Lanham, MD., 1996.

42. Mohammad, L., Zhang, X., Huang, B., and Tan, Z. "Laboratory Performance Evaluation SMA, CMHB and Dense Graded Asphalt Mixtures." *Journal of the Association of Asphalt Paving Technologists*, Vol. 68, 1999, pp. 252-283.

43. Monismith, C.L., Ogawa, N., and Freeme, C.R. "Permanent Deformation Characteristics of Subgrade Soils Due To Repeated Loading." *In Transportation Research Record 537*. Transportation Research Board, National Research Council, Washington D.C., 1975, pp. 1-17.

APPENDIX

Appendix A |E*| Test Result
Appendix B Phase Angle (δ) Result
Appendix C Flow Number, Flow Time, and Loaded Wheel Tracking Test Results
Appendix D Specimen Preparation and Test Procedures
Appendix E Asphalt Layer Input Instructions to the Pavement ME Design Software

APPENDIX A
|E*| Test Result

Table A.1.1
Dynamic modulus, |E*| (ksi), test results for LA9-1 at -10ºC

	25Hz	10Hz	5Hz	1Hz	0.5Hz	0.1Hz
Sample-1	2883	2754	2643	2378	2258	1962
Sample-3	2733	2624	2539	2302	2197	1948
Sample-4	2932	2822	2723	2453	2331	2038
Average	2849	2733	2635	2378	2262	1983
Stdev	104	101	92	76	67	48
%CV	3.6	3.7	3.5	3.2	3.0	2.4

Table A.1.2
Dynamic modulus, |E*| (ksi), test results for LA9-1 at 4.4ºC

	25Hz	10Hz	5Hz	1Hz	0.5Hz	0.1Hz
Sample-1	2013	1838	1691	1360	1219	905
Sample-3	2255	2100	1955	1639	1505	1174
Sample-4	1996	1822	1681	1344	1203	914
Average	2088	1920	1776	1448	1309	998
Stdev	145	156	155	166	170	153
%CV	6.9	8.1	8.8	11.5	13.0	15.3

Table A.1.3
Dynamic modulus, |E*| (ksi), test results for LA9-1 at 25ºC

	25Hz	10Hz	5Hz	1Hz	0.5Hz	0.1Hz
Sample-1	688	533	437	244	189	105
Sample-3	883	717	588	359	282	161
Sample-4	700	547	439	237	182	100
Average	757	599	488	280	218	122
Stdev	109	102	87	69	56	34
%CV	14.4	17.1	17.7	24.5	25.6	27.8

Table A.1.4
Dynamic modulus, |E*| (ksi), test results for LA9-1 at 37.8ºC

	25Hz	10Hz	5Hz	1Hz	0.5Hz	0.1Hz
Sample-1	231	160	121	66	51	33
Sample-3	341	245	188	106	78	49
Sample-4	236	159	119	66	51	33
Average	269	188	143	79	60	38
Stdev	62	49	39	23	16	9
%CV	23.1	26.3	27.5	29.1	26.0	24.1

Table A.1.5
Dynamic modulus, |E*| (ksi), test results for LA9-1 at 54.4ºC

	25Hz	10Hz	5Hz	1Hz	0.5Hz	0.1Hz
Sample-1	53	40	32	23	20	17
Sample-3	97	66	51	33	27	21
Sample-4	54	38	30	21	19	17
Average	68	48	38	26	22	18
Stdev	25	16	12	6	4	2
%CV	36.9	32.5	30.8	25.0	19.8	12.6

Table A.2.1

Dynamic modulus, |E*| (ksi), test results for US90-1 at -10ºC

	25Hz	10Hz	5Hz	1Hz	0.5Hz	0.1Hz
Sample-5	3173	3062	2961	2690	2570	2279
Sample-6	3871	3914	3798	3513	3380	3040
Sample-11	3264	3137	3040	2790	2672	2385
Average	3436	3371	3266	2998	2874	2568
Stdev	379	472	462	449	441	412
%CV	11.0	14.0	14.1	15.0	15.4	16.1

Table A.2.2

Dynamic modulus, |E*| (ksi), test results for US90-1 at 4.4ºC

	25Hz	10Hz	5Hz	1Hz	0.5Hz	0.1Hz
Sample-5	2432	2262	2117	1754	1605	1262
Sample-6	3136	2882	2694	2274	2077	1621
Sample-11	2540	2335	2189	1845	1695	1349
Average	2703	2493	2333	1958	1792	1411
Stdev	379	339	314	278	251	187
%CV	14.0	13.6	13.5	14.2	14.0	13.3

Table A.2.3

Dynamic modulus, |E*| (ksi), test results for US90-1 at 25ºC

	25Hz	10Hz	5Hz	1Hz	0.5Hz	0.1Hz
Sample-5	1112	896	742	457	366	212
Sample-6	1317	1120	928	592	478	288
Sample-11	1120	903	757	454	362	211
Average	1183	973	809	501	402	237
Stdev	116	127	103	79	66	44
%CV	9.8	13.1	12.8	15.7	16.4	18.6

Table A.2.4

Dynamic modulus, |E*| (ksi), test results for US90-1 at 37.8ºC

	25Hz	10Hz	5Hz	1Hz	0.5Hz	0.1Hz
Sample-5	420	310	240	139	103	65
Sample-6	576	432	337	187	143	86
Sample-11	433	314	239	131	100	59
Average	476	352	272	152	115	70
Stdev	87	69	56	30	24	14
%CV	18.2	19.7	20.7	19.9	20.8	20.3

Table A.2.5

Dynamic modulus, |E*| (ksi), test results for US90-1 at 54.4ºC

	25Hz	10Hz	5Hz	1Hz	0.5Hz	0.1Hz
Sample-5	148	103	81	49	42	31
Sample-6	214	151	116	70	57	42
Sample-11	135	95	73	44	36	27
Average	166	116	90	54	45	33
Stdev	42	30	23	14	11	8
%CV	25.6	26.0	25.4	25.4	24.0	23.3

Table A.3.1

Dynamic modulus, |E*| (ksi), test results for LPC-1 at -10ºC

	25Hz	10Hz	5Hz	1Hz	0.5Hz	0.1Hz
Sample-3	3795	3470	3424	3184	3057	2887
Sample-10	3796	3657	3546	3291	3172	2875
Sample-13	3605	3506	3407	3175	3065	2783
Average	3732	3544	3459	3217	3098	2848
Stdev	110	99	76	65	64	57
%CV	2.9	2.8	2.2	2.0	2.1	2.0

Table A.3.2

Dynamic modulus, |E*| (ksi), test results for LPC-1 at 4.4ºC

	25Hz	10Hz	5Hz	1Hz	0.5Hz	0.1Hz
Sample-3	2888	2716	2566	2212	2051	1672
Sample-10	2694	2524	2392	2075	1932	1585
Sample-13	2780	2684	2551	2212	2058	1639
Average	2787	2641	2503	2166	2014	1632
Stdev	97	103	96	79	71	44
%CV	3.5	3.9	3.9	3.7	3.5	2.7

Table A.3.3

Dynamic modulus, |E*| (ksi), test results for LPC-1 at 25ºC

	25Hz	10Hz	5Hz	1Hz	0.5Hz	0.1Hz
Sample-3	1299	1101	950	625	503	306
Sample-10	1250	1030	883	560	455	274
Sample-13	1197	1027	878	569	461	276
Average	1249	1053	904	585	473	285
Stdev	51	42	40	35	26	18
%CV	4.1	4.0	4.4	6.0	5.5	6.3

Table A.3.4

Dynamic modulus, |E*| (ksi), test results for LPC-1 at 37.8ºC

	25Hz	10Hz	5Hz	1Hz	0.5Hz	0.1Hz
Sample-3	585	442	349	199	155	94
Sample-10	512	379	299	164	127	73
Sample-13	532	397	308	171	131	76
Average	543	406	319	178	138	81
Stdev	38	32	27	19	15	11
%CV	6.9	8.0	8.4	10.4	11.0	14.0

Table A.3.5

Dynamic modulus, |E*| (ksi), test results for LPC-1 at 54.4ºC

	25Hz	10Hz	5Hz	1Hz	0.5Hz	0.1Hz
Sample-3	166	117	92	55	46	34
Sample-10	153	109	86	53	43	33
Sample-13	142	97	78	49	41	32
Average	154	108	85	52	43	33
Stdev	12	10	7	3	3	1
%CV	7.8	9.3	8.2	5.8	5.8	3.0

Table A.4.1

Dynamic modulus, |E*| (ksi), test results for 3121-1 at -10ºC

	25Hz	10Hz	5Hz	1Hz	0.5Hz	0.1Hz
Sample-1	3476	3350	3235	2938	2804	2483
Sample-2	3180	3026	2908	2615	2477	2285
Sample-3	3370	3251	3152	2878	2752	2469
Average	3342	3209	3098	2811	2677	2412
Stdev	150	166	170	172	176	111
%CV	4.5	5.2	5.5	6.1	6.6	4.6

Table A.4.2

Dynamic modulus, |E*| (ksi), test results for 3121-1 at 4.4ºC

	25Hz	10Hz	5Hz	1Hz	0.5Hz	0.1Hz
Sample-1	2539	2299	2126	1746	1583	1223
Sample-2	2550	2300	2130	1749	1584	1192
Sample-3	2436	2230	2069	1705	1550	1223
Average	2508	2277	2108	1733	1572	1213
Stdev	63	40	34	25	19	18
%CV	2.5	1.8	1.6	1.4	1.2	1.4

Table A.4.3

Dynamic modulus, |E*| (ksi), test results for 3121-1 at 25ºC

	25Hz	10Hz	5Hz	1Hz	0.5Hz	0.1Hz
Sample-1	1001	806	674	417	335	199
Sample-2	964	757	628	381	302	168
Sample-3	1026	822	690	415	329	190
Average	997	795	664	405	322	185
Stdev	31	34	32	20	18	16
%CV	3.1	4.3	4.8	5.0	5.5	8.5

Table A.4.4

Dynamic modulus, |E*| (ksi), test results for 3121-1 at 37.8ºC

	25Hz	10Hz	5Hz	1Hz	0.5Hz	0.1Hz
Sample-1	395	283	213	111	86	48
Sample-2	374	253	199	103	79	46
Sample-3	397	281	216	110	87	51
Average	389	272	209	108	84	48
Stdev	13	17	9	4	4	2
%CV	3.3	6.1	4.3	4.0	4.6	4.6

Table A.4.5

Dynamic modulus, |E*| (ksi), test results for 3121-1 at 54.4ºC

	25Hz	10Hz	5Hz	1Hz	0.5Hz	0.1Hz
Sample-1	106	73	57	31	25	18
Sample-2	95	62	49	28	23	17
Sample-3	109	72	58	37	29	22
Average	103	69	55	32	26	19
Stdev	7	6	5	5	3	3
%CV	7.3	8.5	8.6	14.9	13.0	15.6

Table A.5.1
Dynamic modulus, |E*| (ksi), test results for 3121-2 at -10ºC

	25Hz	10Hz	5Hz	1Hz	0.5Hz	0.1Hz
Sample-1	2974	2891	2808	2556	2443	2204
Sample-2	3358	3193	3066	2747	2599	2217
Sample-3	3227	3099	2975	2658	2513	2151
Average	3186	3061	2950	2654	2518	2191
Stdev	195	155	131	96	78	35
%CV	6.1	5.1	4.4	3.6	3.1	1.6

Table A.5.2
Dynamic modulus, |E*| (ksi), test results for 3121-2 at 4.4ºC

	25Hz	10Hz	5Hz	1Hz	0.5Hz	0.1Hz
Sample-1	2374	2168	2001	1612	1452	1094
Sample-2	2295	2059	1854	1435	1266	899
Sample-3	2255	2102	1906	1481	1297	883
Average	2308	2110	1921	1509	1338	959
Stdev	61	55	75	92	99	117
%CV	2.6	2.6	3.9	6.1	7.4	12.2

Table A.5.3
Dynamic modulus, |E*| (ksi), test results for 3121-2 at 25ºC

	25Hz	10Hz	5Hz	1Hz	0.5Hz	0.1Hz
Sample-1	1000	819	659	370	289	164
Sample-2	730	530	425	229	168	87
Sample-3	732	563	440	244	185	97
Average	820	637	508	281	214	116
Stdev	155	158	131	77	66	42
%CV	18.9	24.9	25.8	27.5	30.7	36.2

Table A.5.4
Dynamic modulus, |E*| (ksi), test results for 3121-2 at 37.8ºC

	25Hz	10Hz	5Hz	1Hz	0.5Hz	0.1Hz
Sample-1	312	221	167	89	72	47
Sample-2	232	149	111	55	45	30
Sample-3	249	166	122	60	48	30
Average	264	179	133	68	55	36
Stdev	42	38	30	18	15	10
%CV	16.0	21.1	22.5	26.9	26.9	27.8

Table A.5.5
Dynamic modulus, |E*| (ksi), test results for 3121-2 at 54.4ºC

	25Hz	10Hz	5Hz	1Hz	0.5Hz	0.1Hz
Sample-1	101	70	54	32	28	21
Sample-2	75	52	39	26	25	20
Sample-3	64	43	39	25	22	19
Average	80	55	44	28	25	20
Stdev	19	14	9	4	3	1
%CV	24.1	25.0	19.9	13.2	11.7	6.5

Table A.6.1

Dynamic modulus, |E*| (ksi), test results for 3121-3 at -10ºC

	25Hz	10Hz	5Hz	1Hz	0.5Hz	0.1Hz
Sample-1	3348	3213	3097	2794	2660	2319
Sample-2	3665	3523	3410	3112	2974	2621
Sample-3	3177	3043	2922	2618	2479	2147
Average	3397	3260	3143	2841	2704	2362
Stdev	247	243	247	251	251	240
%CV	7.3	7.5	7.9	8.8	9.3	10.2

Table A.6.2

Dynamic modulus, |E*| (ksi), test results for 3121-3 at 4.4ºC

	25Hz	10Hz	5Hz	1Hz	0.5Hz	0.1Hz
Sample-1	2491	2265	2086	1689	1511	1112
Sample-2	2586	2346	2167	1753	1580	1183
Sample-3	2134	1940	1803	1411	1251	932
Average	2404	2184	2019	1618	1448	1076
Stdev	238	215	191	182	174	129
%CV	9.9	9.8	9.5	11.3	12.0	12.0

Table A.6.3

Dynamic modulus, |E*| (ksi), test results for 3121-3 at 25ºC

	25Hz	10Hz	5Hz	1Hz	0.5Hz	0.1Hz
Sample-1	945	768	616	365	287	159
Sample-2	1086	886	743	444	351	193
Sample-3	954	748	606	358	279	150
Average	995	801	655	389	305	167
Stdev	79	74	76	48	39	23
%CV	7.9	9.3	11.6	12.2	12.9	13.6

Table A.6.4
Dynamic modulus, |E*| (ksi), test results for 3121-3 at 37.8ºC

	25Hz	10Hz	5Hz	1Hz	0.5Hz	0.1Hz
Sample-1	385	256	190	97	76	46
Sample-2	370	271	205	105	81	49
Sample-3	298	208	158	82	65	41
Average	351	245	184	95	74	45
Stdev	46	33	24	11	8	4
%CV	13.1	13.5	12.9	11.9	11.0	9.6

Table A.6.5
Dynamic modulus, |E*| (ksi), test results for 3121-3 at 54.4ºC

	25Hz	10Hz	5Hz	1Hz	0.5Hz	0.1Hz
Sample-1	109	73	61	35	29	22
Sample-2	112	76	57	33	29	24
Sample-3	89	61	47	29	27	22
Average	103	70	55	32	28	23
Stdev	13	8	7	3	1	1
%CV	12.5	11.5	13.6	9.0	3.3	5.3

Table A.7.1
Dynamic modulus, |E*| (ksi), test results for 171-1 at -10ºC

	25Hz	10Hz	5Hz	1Hz	0.5Hz	0.1Hz
Sample-1	2913	2849	2772	2574	2475	2214
Sample-2	2737	2674	2577	2415	2326	2034
Sample-3	2660	2592	2521	2314	2224	2013
Average	2770	2705	2623	2434	2342	2087
Stdev	130	131	132	131	127	110
%CV	4.7	4.9	5.0	5.4	5.4	5.3

Table A.7.2
Dynamic modulus, |E*| (ksi), test results for 171-1 at 4.4ºC

	25Hz	10Hz	5Hz	1Hz	0.5Hz	0.1Hz
Sample-1	2611	2390	2225	1835	1662	1265
Sample-2	2278	2091	1949	1600	1454	1140
Sample-3	2270	2077	1929	1571	1415	1054
Average	2386	2186	2034	1668	1510	1153
Stdev	195	176	165	145	133	106
%CV	8.2	8.1	8.1	8.7	8.8	9.2

Table A.7.3
Dynamic modulus, |E*| (ksi), test results for 171-1 at 25ºC

	25Hz	10Hz	5Hz	1Hz	0.5Hz	0.1Hz
Sample-1	812	630	527	305	235	122
Sample-2	715	553	458	265	206	180
Sample-3	721	583	477	287	230	135
Average	749	589	487	286	224	146
Stdev	55	39	35	20	16	30
%CV	7.3	6.5	7.3	7.0	6.9	20.8

Table A.7.4
Dynamic modulus, |E*| (ksi), test results for 171-1 at 37.8ºC

	25Hz	10Hz	5Hz	1Hz	0.5Hz	0.1Hz
Sample-1	328	221	168	89	71	47
Sample-2	340	232	178	98	84	81
Sample-3	309	213	160	88	70	46
Average	326	222	168	92	75	58
Stdev	15	10	9	6	8	20
%CV	4.8	4.5	5.3	6.1	10.4	34.1

Table A.7.5
Dynamic modulus, |E*| (ksi), test results for 171-1 at 54.4ºC

	25Hz	10Hz	5Hz	1Hz	0.5Hz	0.1Hz
Sample-1	89	64	55	41	39	35
Sample-2	86	64	53	40	37	46
Sample-3	91	66	52	39	36	30
Average	89	65	53	40	37	37
Stdev	2	1	1	1	2	8
%CV	2.6	2.0	2.1	2.4	5.1	21.3

Table A.8.1

Dynamic modulus, |E*| (ksi), test results for 171-2 at -10ºC

	25Hz	10Hz	5Hz	1Hz	0.5Hz	0.1Hz
Sample-1	2914	2865	2774	2575	2503	2267
Sample-2	2960	2874	2772	2543	2453	2178
Sample-3	2796	2706	2617	2392	2307	2036
Average	2890	2815	2721	2503	2421	2160
Stdev	84	94	90	98	102	117
%CV	2.9	3.4	3.3	3.9	4.2	5.4

Table A.8.2

Dynamic modulus, |E*| (ksi), test results for 171-2 at 4.4ºC

	25Hz	10Hz	5Hz	1Hz	0.5Hz	0.1Hz
Sample-1	2405	2204	2045	1670	1529	1177
Sample-2	2160	1962	1816	1474	1329	980
Sample-3	2301	2115	1962	1599	1443	1091
Average	2289	2094	1941	1581	1434	1083
Stdev	123	123	116	99	101	99
%CV	5.4	5.9	6.0	6.3	7.0	9.1

Table A.8.3

Dynamic modulus, |E*| (ksi), test results for 171-2 at 25ºC

	25Hz	10Hz	5Hz	1Hz	0.5Hz	0.1Hz
Sample-1	913	726	594	343	266	156
Sample-2	934	736	608	341	259	138
Sample-3	829	666	535	304	232	131
Average	892	709	579	330	252	141
Stdev	55	38	39	22	18	13
%CV	6.2	5.4	6.7	6.7	7.0	9.2

Table A.8.4
Dynamic modulus, |E*| (ksi), test results for 171-2 at 37.8ºC

	25Hz	10Hz	5Hz	1Hz	0.5Hz	0.1Hz
Sample-1	325	232	175	95	73	49
Sample-2	312	213	165	88	70	48
Sample-3	322	230	173	95	74	48
Average	320	225	171	93	73	48
Stdev	7	10	6	4	2	1
%CV	2.1	4.7	3.3	4.3	2.9	1.2

Table A.8.5
Dynamic modulus, |E*| (ksi), test results for 171-2 at 54.4ºC

	25Hz	10Hz	5Hz	1Hz	0.5Hz	0.1Hz
Sample-1	90	62	51	36	31	26
Sample-2	104	72	59	43	39	34
Sample-3	85	62	51	38	35	31
Average	93	65	54	39	35	30
Stdev	10	6	5	4	4	4
%CV	10.6	9.2	9.0	9.5	11.1	13.8

Table A.9.1

Dynamic modulus, |E*| (ksi), Test Results for 171-3 at -10ºC

	25Hz	10Hz	5Hz	1Hz	0.5Hz	0.1Hz
Sample-1	3050	2930	2846	2633	2543	2243
Sample-2	2862	2753	2662	2483	2405	2192
Sample-3	2851	2754	2659	2465	2367	2116
Average	2921	2812	2723	2527	2438	2184
Stdev	112	102	107	92	92	64
%CV	3.8	3.6	3.9	3.7	3.8	2.9

Table A.9.2

Dynamic modulus, |E*| (ksi), test results for 171-3 at 4.4ºC

	25Hz	10Hz	5Hz	1Hz	0.5Hz	0.1Hz
Sample-1	2182	1985	1821	1481	1335	1001
Sample-2	2013	1890	1775	1465	1326	1044
Sample-3	1734	1576	1453	1140	1006	724
Average	1976	1817	1683	1362	1222	923
Stdev	226	214	201	193	188	174
%CV	11.4	11.8	11.9	14.1	15.4	18.8

Table A.9.3

Dynamic modulus, |E*| (ksi) test results for 171-3 at 25ºC

	25Hz	10Hz	5Hz	1Hz	0.5Hz	0.1Hz
Sample-1	943	742	614	358	279	159
Sample-2	971	803	665	411	334	189
Sample-3	782	624	519	313	241	140
Average	899	723	599	361	285	163
Stdev	102	91	74	49	46	25
%CV	11.3	12.6	12.4	13.6	16.3	15.3

Table A.9.4
Dynamic modulus, |E*| (ksi), test results for 171-3 at 37.8ºC

	25Hz	10Hz	5Hz	1Hz	0.5Hz	0.1Hz
Sample-1	381	255	202	113	89	57
Sample-2	411	283	215	121	95	59
Sample-3	354	251	194	101	78	50
Average	382	263	204	112	87	55
Stdev	29	17	10	10	8	5
%CV	7.5	6.6	5.1	8.8	9.5	8.8

Table A.9.5
Dynamic modulus, |E*| (ksi) test results for 171-3 at 54.4ºC

	25Hz	10Hz	5Hz	1Hz	0.5Hz	0.1Hz
Sample-1	94	66	54	38	35	27
Sample-2	102	73	60	43	39	34
Sample-3	90	63	51	35	31	25
Average	95	68	55	39	35	29
Stdev	6	5	4	4	4	5
%CV	6.4	7.4	8.1	11.3	11.9	16.4

Table A.10.1

Dynamic modulus, |E*| (ksi), test results for 171-4 at -10ºC

	25Hz	10Hz	5Hz	1Hz	0.5Hz	0.1Hz
Sample-1	2411	2345	2271	2113	2073	1882
Sample-2	2622	2556	2482	2285	2192	1945
Sample-3	2710	2632	2594	2406	2341	2132
Average	2581	2511	2449	2268	2202	1986
Stdev	154	149	164	147	134	130
%CV	6.0	5.9	6.7	6.5	6.1	6.5

Table A.10.2

Dynamic modulus, |E*| (ksi), test results for 171-4 at 4.4ºC

	25Hz	10Hz	5Hz	1Hz	0.5Hz	0.1Hz
Sample-1	2192	2014	1881	1547	1403	1080
Sample-2	2403	2195	2032	1654	1496	1153
Sample-3	2265	2066	1904	1541	1399	1075
Average	2286	2092	1939	1581	1432	1103
Stdev	107	93	81	64	55	44
%CV	4.7	4.5	4.2	4.0	3.8	4.0

Table A.10.3

Dynamic modulus, |E*| (ksi), test results for 171-4 at 25ºC

	25Hz	10Hz	5Hz	1Hz	0.5Hz	0.1Hz
Sample-1	756	613	481	275	212	121
Sample-2	734	552	453	261	203	117
Sample-3	798	646	501	287	225	130
Average	763	604	478	274	214	122
Stdev	32	48	25	13	11	7
%CV	4.3	7.9	5.1	4.6	5.2	5.7

Table A.10.4
Dynamic modulus, |E*| (ksi), test results for 171-4 at 37.8ºC

	25Hz	10Hz	5Hz	1Hz	0.5Hz	0.1Hz
Sample-1	358	236	182	106	85	58
Sample-2	316	217	163	93	74	50
Sample-3	337	236	182	97	79	56
Average	337	230	176	99	79	55
Stdev	21	11	11	6	5	4
%CV	6.4	4.9	6.2	6.5	6.7	7.3

Table A.10.5
Dynamic modulus, |E*| (ksi), test results for 171-4 at 54.4ºC

	25Hz	10Hz	5Hz	1Hz	0.5Hz	0.1Hz
Sample-1	92	66	55	42	39	34
Sample-2	91	66	56	42	39	34
Sample-3	86	61	52	38	35	30
Average	90	64	54	41	38	33
Stdev	3	3	2	2	2	2
%CV	3.4	4.8	4.1	4.9	5.5	7.1

Table A.11.1
Dynamic modulus, |E*| (ksi), test results for 116-1 at -10ºC

	25Hz	10Hz	5Hz	1Hz	0.5Hz	0.1Hz
Sample-1	4057	3964	3883	3650	3530	3197
Sample-2	3819	3755	3699	3533	3445	3195
Sample-3	4110	3993	3893	3617	3478	3108
Average	3995	3904	3825	3600	3484	3167
Stdev	155	130	109	60	43	51
%CV	3.9	3.3	2.9	1.7	1.2	1.6

Table A.11.2
Dynamic modulus, |E*| (ksi), test results for 116-1 at 4.4ºC

	25Hz	10Hz	5Hz	1Hz	0.5Hz	0.1Hz
Sample-1	3250	2977	2766	2286	2060	1596
Sample-2	2988	2750	2563	2131	1940	1504
Sample-3	3154	2915	2724	2278	2089	1656
Average	3131	2881	2684	2232	2030	1585
Stdev	133	118	107	87	79	77
%CV	4.2	4.1	4.0	3.9	3.9	4.8

Table A.11.3
Dynamic modulus, |E*| (ksi), test results for 116-1 at 25ºC

	25Hz	10Hz	5Hz	1Hz	0.5Hz	0.1Hz
Sample-1	1306	1084	926	580	459	252
Sample-2	1271	996	821	516	423	232
Sample-3	1392	1161	970	636	522	313
Average	1323	1080	906	577	468	266
Stdev	62	83	76	60	50	42
%CV	4.7	7.7	8.4	10.4	10.8	16.0

Table A.11.4
Dynamic modulus, |E*| (ksi), test results for 116-1 at 37.8ºC

	25Hz	10Hz	5Hz	1Hz	0.5Hz	0.1Hz
Sample-1	565	401	303	148	108	55
Sample-2	526	376	286	139	101	49
Sample-3	642	494	388	205	154	78
Average	577	424	326	164	121	61
Stdev	59	62	54	36	28	16
%CV	10.2	14.8	16.7	21.9	23.5	25.8

Table A.11.5
Dynamic modulus, |E*| (ksi), test results for 116-1 at 54.4ºC

	25Hz	10Hz	5Hz	1Hz	0.5Hz	0.1Hz
Sample-1	146	84	60	28	21	13
Sample-2	131	78	56	27	21	13
Sample-3	163	104	75	36	27	15
Average	147	89	64	30	23	14
Stdev	16	14	10	5	3	1
%CV	11.0	15.5	16.3	16.0	14.4	9.9

Table A.12.1

Dynamic modulus, |E*| (ksi), test results for 116-2 at -10ºC

	25Hz	10Hz	5Hz	1Hz	0.5Hz	0.1Hz
Sample-1	4087	4002	3927	3719	3612	3321
Sample-2	3961	3886	3822	3643	3552	3304
Sample-3	4031	3963	3906	3747	3666	3445
Average	4026	3950	3885	3703	3610	3356
Stdev	63	59	56	54	57	77
%CV	1.6	1.5	1.4	1.5	1.6	2.3

Table A.12.2

Dynamic modulus, |E*| (ksi), test results for 116-2 at 4.4ºC

	25Hz	10Hz	5Hz	1Hz	0.5Hz	0.1Hz
Sample-1	3196	2988	2821	2401	2212	1785
Sample-2	3137	2945	2781	2379	2198	1777
Sample-3	3291	3055	2877	2452	2270	1847
Average	3208	2996	2827	2410	2227	1803
Stdev	78	55	48	38	38	39
%CV	2.4	1.9	1.7	1.6	1.7	2.1

Table A.12.3

Dynamic modulus, |E*| (ksi), test results for 116-2 at 25ºC

	25Hz	10Hz	5Hz	1Hz	0.5Hz	0.1Hz
Sample-1	1442	1197	1036	683	557	326
Sample-2	1399	1179	1026	691	575	337
Sample-3	1422	1207	1050	740	611	367
Average	1421	1195	1037	704	581	343
Stdev	21	14	12	31	28	21
%CV	1.5	1.2	1.1	4.4	4.7	6.2

Table A.12.4
Dynamic modulus, |E*| (ksi), test results for 116-2 at 37.8ºC

	25Hz	10Hz	5Hz	1Hz	0.5Hz	0.1Hz
Sample-1	662	485	371	191	143	70
Sample-2	648	481	383	201	150	73
Sample-3	710	535	425	234	178	89
Average	673	500	393	209	157	77
Stdev	33	30	29	22	18	10
%CV	4.9	6.0	7.3	10.6	11.8	13.1

Table A.12.5
Dynamic modulus, |E*| (ksi), test results for 116-2 at 54.4ºC

	25Hz	10Hz	5Hz	1Hz	0.5Hz	0.1Hz
Sample-1	188	114	81	36	26	13
Sample-2	204	125	90	39	28	14
Sample-3	194	124	90	41	30	16
Average	195	121	87	39	28	14
Stdev	8	6	5	3	2	1
%CV	4.2	5.1	5.7	7.0	8.2	10.0

Table A.13.1
Dynamic modulus, |E*| (ksi), test results for 116-3 at -10ºC

	25Hz	10Hz	5Hz	1Hz	0.5Hz	0.1Hz
Sample-1	3820	3724	3641	3409	3291	2972
Sample-2	3825	3749	3683	3497	3400	3133
Sample-3	4355	4252	4165	3923	3801	3476
Average	4000	3909	3830	3610	3498	3194
Stdev	308	298	291	275	269	257
%CV	7.7	7.6	7.6	7.6	7.7	8.1

Table A.13.2
Dynamic modulus, |E*| (ksi), test results for 116-3 at 4.4ºC

	25Hz	10Hz	5Hz	1Hz	0.5Hz	0.1Hz
Sample-1	2981	2763	2586	2151	1938	1523
Sample-2	3095	2862	2683	2259	2075	1655
Sample-3	3382	3146	2955	2499	2296	1856
Average	3153	2924	2741	2303	2103	1678
Stdev	207	199	191	178	181	168
%CV	6.6	6.8	7.0	7.7	8.6	10.0

Table A.13.3
Dynamic modulus, |E*| (ksi), test results for 116-3 at 25ºC

	25Hz	10Hz	5Hz	1Hz	0.5Hz	0.1Hz
Sample-1	1221	998	846	548	448	259
Sample-2	1382	1167	1006	668	541	322
Sample-3	1445	1208	1023	694	580	349
Average	1349	1124	958	637	523	310
Stdev	115	111	98	78	68	46
%CV	8.6	9.9	10.2	12.3	13.0	14.8

Table A.13.4
Dynamic modulus, |E*| (ksi), test results for 116-3 at 37.8ºC

	25Hz	10Hz	5Hz	1Hz	0.5Hz	0.1Hz
Sample-1	553	416	328	170	126	60
Sample-2	643	484	384	202	151	77
Sample-3	692	537	434	237	180	89
Average	629	479	382	203	152	75
Stdev	71	60	53	34	27	15
%CV	11.2	12.6	13.9	16.6	17.7	19.2

Table A.13.5
Dynamic modulus, |E*| (ksi), test results for 116-3 at 54.4ºC

	25Hz	10Hz	5Hz	1Hz	0.5Hz	0.1Hz
Sample-1	147	90	65	32	25	15
Sample-2	180	110	79	38	30	18
Sample-3	220	136	100	47	35	20
Average	182	112	81	39	30	17
Stdev	36	23	18	7	5	3
%CV	19.9	20.4	21.5	18.9	17.8	14.7

Table A.14.1
Dynamic modulus, |E*| (ksi), test results for 116-4 at -10ºC

	25Hz	10Hz	5Hz	1Hz	0.5Hz	0.1Hz
Sample-1	3839	3770	3710	3538	3448	3199
Sample-2	4348	4225	4121	3840	3702	3339
Sample-3	5932	5608	5347	4695	4396	3679
Average	4707	4534	4393	4024	3849	3406
Stdev	1092	957	852	600	491	246
%CV	23.2	21.1	19.4	14.9	12.8	7.2

Table A.14.2
Dynamic modulus, |E*| (ksi), test results for 116-4 at 4.4ºC

	25Hz	10Hz	5Hz	1Hz	0.5Hz	0.1Hz
Sample-1	3156	2933	2744	2294	2093	1661
Sample-2	3267	2998	2788	2315	2105	1652
Sample-3	3852	3509	3233	2559	2265	1609
Average	3425	3146	2922	2389	2154	1641
Stdev	374	316	271	147	96	28
%CV	10.9	10.0	9.3	6.2	4.4	1.7

Table A.14.3
Dynamic modulus, |E*| (ksi), test results for 116-4 at 25ºC

	25Hz	10Hz	5Hz	1Hz	0.5Hz	0.1Hz
Sample-1	1243	1045	913	588	469	268
Sample-2	1301	1069	919	608	508	295
Sample-3	1410	1152	961	631	511	300
Average	1318	1089	931	609	496	288
Stdev	85	56	26	21	24	17
%CV	6.4	5.2	2.8	3.5	4.7	6.1

Table A.14.4
Dynamic modulus, |E*| (ksi), test results for 116-4 at 37.8ºC

	25Hz	10Hz	5Hz	1Hz	0.5Hz	0.1Hz
Sample-1	595	443	346	177	131	62
Sample-2	597	449	356	189	144	72
Sample-3	668	503	392	210	160	83
Average	620	465	365	192	145	72
Stdev	42	33	24	17	15	10
%CV	6.7	7.1	6.5	8.9	10.0	14.1

Table A.14.5
Dynamic modulus, |E*| (ksi), test results for 116-4 at 54.4ºC

	25Hz	10Hz	5Hz	1Hz	0.5Hz	0.1Hz
Sample-1	144	83	60	28	21	13
Sample-2	161	103	76	37	28	15
Sample-3	178	115	82	38	28	15
Average	161	100	73	34	26	14
Stdev	17	16	12	6	4	1
%CV	10.5	16.0	16.1	16.3	15.0	9.4

Table A.15.1

Dynamic modulus, |E*| (ksi), test results for 190-1 at -10ºC

	25Hz	10Hz	5Hz	1Hz	0.5Hz	0.1Hz
Sample-22	3635	3472	3418	3163	3043	2755
Sample-28	3930	3821	3708	3444	3319	3002
Sample-33	3997	3862	3755	3489	3357	3037
Average	3854	3718	3627	3365	3240	2931
Stdev	193	214	183	177	171	154
%CV	5.0	5.8	5.0	5.2	5.3	5.2

Table A.15.2

Dynamic modulus, |E*| (ksi), test results for 190-1 at 4.4ºC

	25Hz	10Hz	5Hz	1Hz	0.5Hz	0.1Hz
Sample-22	2864	2603	2461	2101	1941	1585
Sample-28	3165	2989	2826	2442	2269	1868
Sample-33	3212	2972	2814	2434	2260	1851
Average	3080	2855	2700	2326	2157	1768
Stdev	189	218	207	195	187	159
%CV	6.1	7.6	7.7	8.4	8.7	9.0

Table A.15.3

Dynamic modulus, |E*| (ksi), test results for 190-1 at 25ºC

	25Hz	10Hz	5Hz	1Hz	0.5Hz	0.1Hz
Sample-22	1416	1315	1020	672	520	338
Sample-28	1630	1422	1302	889	730	458
Sample-33	1543	1304	1096	735	604	369
Average	1530	1347	1139	765	618	388
Stdev	108	65	146	112	106	62
%CV	7.0	4.8	12.8	14.6	17.1	16.0

Table A.15.4

Dynamic modulus, |E*| (ksi), test results for 190-1 at 37.8ºC

	25Hz	10Hz	5Hz	1Hz	0.5Hz	0.1Hz
Sample-22	494	435	301	162	127	81
Sample-28	651	470	345	188	152	94
Sample-33	608	458	362	201	164	99
Average	584	454	336	184	148	91
Stdev	81	18	31	20	19	9
%CV	13.9	3.9	9.4	10.8	12.8	10.2

Table A.15.5

Dynamic modulus, |E*| (ksi), test results for 190-1 at 54.4ºC

	25Hz	10Hz	5Hz	1Hz	0.5Hz	0.1Hz
Sample-22	155	117	91	59	51	42
Sample-28	211	152	122	79	68	57
Sample-33	190	162	132	82	64	49
Average	185	144	115	73	61	49
Stdev	28	24	21	13	9	8
%CV	15.3	16.4	18.6	17.0	14.6	15.2

Table A.16.1
Dynamic modulus, |E*| (ksi), test results for 190-2 at -10ºC

	25Hz	10Hz	5Hz	1Hz	0.5Hz	0.1Hz
Sample-2	3636	3515	3387	3062	2915	2596
Sample-4	3846	3686	3606	3369	3258	2959
Sample-11	3279	3175	3082	2846	2741	2479
Average	3587	3459	3358	3092	2971	2678
Stdev	287	260	263	263	263	250
%CV	8.0	7.5	7.8	8.5	8.8	9.3

Table A.16.2
Dynamic modulus, |E*| (ksi), test results for 190-2 at 4.4ºC

	25Hz	10Hz	5Hz	1Hz	0.5Hz	0.1Hz
Sample-2	2493	2325	2196	1872	1727	1390
Sample-4	2880	2719	2590	2287	2153	1829
Sample-11	2750	2605	2461	2119	1969	1608
Average	2708	2550	2416	2093	1950	1609
Stdev	197	203	201	209	214	220
%CV	7.3	7.9	8.3	10.0	11.0	13.6

Table A.16.3
Dynamic modulus, |E*| (ksi), test results for 190-2 at 25ºC

	25Hz	10Hz	5Hz	1Hz	0.5Hz	0.1Hz
Sample-2	1366	1208	1045	689	559	334
Sample-4	1656	1460	1306	955	814	576
Sample-11	1465	1253	1055	701	586	375
Average	1496	1307	1135	781	653	428
Stdev	148	134	148	150	140	130
%CV	9.9	10.3	13.0	19.2	21.4	30.3

Table A.16.4
Dynamic modulus, |E*| (ksi), test results for 190-2 at 37.8ºC

	25Hz	10Hz	5Hz	1Hz	0.5Hz	0.1Hz
Sample-2	534	399	309	168	129	80
Sample-4	779	654	563	349	280	170
Sample-11	650	478	412	217	170	104
Average	654	510	428	245	193	118
Stdev	123	131	128	93	78	47
%CV	18.7	25.6	29.9	38.2	40.4	39.6

Table A.16.5
Dynamic modulus, |E*| (ksi), test results for 190-2 at 54.4ºC

	25Hz	10Hz	5Hz	1Hz	0.5Hz	0.1Hz
Sample-2	177	124	96	60	51	40
Sample-4	357	258	204	122	98	65
Sample-11	216	152	119	72	59	45
Average	250	178	140	85	69	50
Stdev	95	71	57	33	25	13
%CV	38.0	39.6	40.8	38.5	35.8	26.6

Table A.17.1

Dynamic modulus, |E*| (ksi), test results for 190-3 at -10ºC

	25Hz	10Hz	5Hz	1Hz	0.5Hz	0.1Hz
Sample-28	3812	3614	3513	3272	3153	2858
Sample-29	2714	2634	2558	2369	2285	2075
Sample-30	3104	2951	2872	2673	2580	2351
Average	3210	3066	2981	2771	2673	2428
Stdev	557	500	487	459	441	397
%CV	17.3	16.3	16.3	16.6	16.5	16.4

Table A.17.2

Dynamic modulus, |E*| (ksi), test results for 190-3 at 4.4ºC

	25Hz	10Hz	5Hz	1Hz	0.5Hz	0.1Hz
Sample-28	2554	2408	2287	1980	1850	1550
Sample-29	2229	2106	1997	1743	1628	1376
Sample-30	2330	2202	2089	1807	1688	1404
Average	2371	2239	2125	1844	1722	1443
Stdev	167	154	148	123	115	93
%CV	7.0	6.9	7.0	6.6	6.7	6.5

Table A.17.3

Dynamic modulus, |E*| (ksi), test results for 190-3 at 25ºC

	25Hz	10Hz	5Hz	1Hz	0.5Hz	0.1Hz
Sample-28	1511	1291	1161	827	694	469
Sample-29	1204	1076	950	673	566	385
Sample-30	1246	1107	987	680	557	366
Average	1320	1158	1033	727	606	407
Stdev	167	116	113	87	77	55
%CV	12.6	10.0	10.9	12.0	12.7	13.5

Table A.17.4
Dynamic modulus, |E*| (ksi), test results for 190-3 at 37.8ºC

	25Hz	10Hz	5Hz	1Hz	0.5Hz	0.1Hz
Sample-28	640	514	424	253	191	122
Sample-29	518	395	317	181	146	94
Sample-30	529	383	301	169	129	81
Average	562	431	348	201	156	99
Stdev	68	73	67	46	32	21
%CV	12.0	16.8	19.2	22.7	20.6	21.1

Table A.17.5
Dynamic modulus, |E*| (ksi), test results for 190-3 at 54.4ºC

	25Hz	10Hz	5Hz	1Hz	0.5Hz	0.1Hz
Sample-28	258	186	145	88	73	51
Sample-29	183	132	105	66	58	43
Sample-30	192	123	97	62	51	40
Average	211	147	116	72	61	45
Stdev	41	34	26	14	11	6
%CV	19.6	23.2	22.7	19.2	17.9	13.4

Table A.18.1
Dynamic modulus, |E*| (ksi), test results for 190-4 at -10ºC

	25Hz	10Hz	5Hz	1Hz	0.5Hz	0.1Hz
Sample-1	3543	3371	3267	2957	2822	2524
Sample-3	3634	3514	3400	3101	2956	2621
Sample-4	4181	3996	3844	3472	3302	2891
Average	3786	3627	3504	3177	3026	2678
Stdev	345	328	302	266	248	190
%CV	9.1	9.0	8.6	8.4	8.2	7.1

Table A.18.2
Dynamic modulus, |E*| (ksi), test results for 190-4 at 4.4ºC

	25Hz	10Hz	5Hz	1Hz	0.5Hz	0.1Hz
Sample-1	3214	2599	2323	1856	1658	1242
Sample-3	2726	2489	2300	1838	1647	1220
Sample-4	3127	2847	2610	2092	1855	1358
Average	3022	2645	2411	1929	1720	1273
Stdev	260	183	173	142	117	74
%CV	8.6	6.9	7.2	7.3	6.8	5.8

Table A.18.3
Dynamic modulus, |E*| (ksi), test results for 190-4 at 25ºC

	25Hz	10Hz	5Hz	1Hz	0.5Hz	0.1Hz
Sample-1	1107	953	720	394	307	180
Sample-3	1008	789	646	346	266	154
Sample-4	1182	955	714	407	313	175
Average	1099	899	693	383	295	170
Stdev	87	95	41	32	25	14
%CV	8.0	10.5	5.9	8.3	8.5	8.4

Table A.18.4
Dynamic modulus, |E*| (ksi), test results for 190-4 at 37.8ºC

	25Hz	10Hz	5Hz	1Hz	0.5Hz	0.1Hz
Sample-1	512	382	291	142	109	69
Sample-3	406	277	215	112	89	62
Sample-4	527	351	258	135	106	71
Average	481	337	255	130	102	67
Stdev	66	54	38	16	11	4
%CV	13.7	15.9	14.9	12.3	10.4	6.7

Table A.18.5
Dynamic modulus, |E*| (ksi), test results for 190-4 at 54.4ºC

	25Hz	10Hz	5Hz	1Hz	0.5Hz	0.1Hz
Sample-1	142	93	75	51	44	38
Sample-3	124	91	74	53	49	42
Sample-4	120	83	65	46	41	35
Average	129	89	72	50	45	38
Stdev	12	5	5	4	4	4
%CV	9.1	5.7	7.6	7.8	8.7	10.0

Table A.19.1
Dynamic modulus, |E*| (ksi), test results for ALF-1 at -10ºC

	25Hz	10Hz	5Hz	1Hz	0.5Hz	0.1Hz
Sample-1	3747	3651	3552	3280	3155	2856
Sample-4	3458	3358	3263	3005	2893	2617
Sample-8	3703	3596	3489	3219	3093	2794
Average	3636	3535	3435	3168	3047	2756
Stdev	156	156	152	144	137	124
%CV	4.3	4.4	4.4	4.6	4.5	4.5

Table A.19.2
Dynamic modulus, |E*| (ksi), test results for ALF-1 at 4.4ºC

	25Hz	10Hz	5Hz	1Hz	0.5Hz	0.1Hz
Sample-1	2868	2687	2528	2139	1965	1541
Sample-4	2615	2511	2373	2015	1883	1557
Sample-8	2878	2630	2472	2108	1947	1564
Average	2787	2609	2458	2087	1932	1554
Stdev	149	90	78	65	43	12
%CV	5.3	3.4	3.2	3.1	2.2	0.8

Table A.19.3
Dynamic modulus, |E*| (ksi), test results for ALF-1 at 25ºC

	25Hz	10Hz	5Hz	1Hz	0.5Hz	0.1Hz
Sample-1	1339	1118	959	597	482	282
Sample-4	1283	1078	926	606	499	322
Sample-8	1360	1137	966	631	519	316
Average	1327	1111	950	611	500	307
Stdev	40	30	21	18	19	22
%CV	3.0	2.7	2.2	2.9	3.7	7.0

Table A.19.4
Dynamic modulus, |E*| (ksi), test results for ALF-1 at 37.8ºC

	25Hz	10Hz	5Hz	1Hz	0.5Hz	0.1Hz
Sample-1	447	301	224	118	91	54
Sample-4	492	363	298	170	134	81
Sample-8	496	371	292	165	128	80
Average	478	345	271	151	118	72
Stdev	27	38	41	29	23	15
%CV	5.7	11.1	15.1	19.0	19.8	21.4

Table A.19.5
Dynamic modulus, |E*| (ksi), test results for ALF-1 at 54.4ºC

	25Hz	10Hz	5Hz	1Hz	0.5Hz	0.1Hz
Sample-1	112	77	61	42	36	30
Sample-4	144	101	81	53	45	35
Sample-8	142	99	79	54	46	37
Average	133	92	74	50	42	34
Stdev	18	13	11	7	6	4
%CV	13.5	14.4	15.0	13.4	13.0	10.6

Table A.20. 1

Dynamic modulus, |E*| (ksi), test results for LA1-1 at -10ºC

	25Hz	10Hz	5Hz	1Hz	0.5Hz	0.1Hz
Sample-7	3310	3252	3060	2946	2832	2542
Sample-8	3850	3752	3488	3332	3214	2964
Sample-9	3784	3706	3432	3298	3166	2824
Average	3648	3570	3327	3192	3071	2777
Stdev	295	276	233	214	208	215
%CV	8.1	7.7	7.0	6.7	6.8	7.7

Table A.20.2

Dynamic modulus, |E*| (ksi), test results for LA1-1 at 4.4ºC

	25Hz	10Hz	5Hz	1Hz	0.5Hz	0.1Hz
Sample-7	2458	2269	2127	1767	1619	1285
Sample-8	2998	2865	2670	2243	2065	1652
Sample-9	2865	2689	2534	2144	1981	1605
Average	2774	2608	2444	2051	1888	1514
Stdev	281	306	283	251	237	200
%CV	10.1	11.7	11.6	12.2	12.6	13.2

Table A.20.3

Dynamic modulus, |E*| (ksi), test results for LA1-1 at 25ºC

	25Hz	10Hz	5Hz	1Hz	0.5Hz	0.1Hz
Sample-7	1111	902	765	480	385	234
Sample-8	1175	977	814	485	380	217
Sample-9	1424	1173	988	649	528	322
Average	1237	1017	856	538	431	258
Stdev	165	140	117	96	84	56
%CV	13.4	13.8	13.7	17.9	19.5	21.9

Table A.20.4
Dynamic modulus, |E*| (ksi), test results for LA1-1 at 37.8ºC

	25Hz	10Hz	5Hz	1Hz	0.5Hz	0.1Hz
Sample-7	522	397	315	180	139	86
Sample-8	594	431	336	185	140	88
Sample-9	673	512	407	227	172	109
Average	596	447	353	197	150	94
Stdev	76	59	48	26	19	13
%CV	12.7	13.2	13.7	13.1	12.5	13.5

Table A.20.5
Dynamic modulus, |E*| (ksi), test results for LA1-1 at 54.4ºC

	25Hz	10Hz	5Hz	1Hz	0.5Hz	0.1Hz
Sample-7	167	118	93	61	52	38
Sample-8	223	160	125	79	66	53
Sample-9	228	165	129	82	70	56
Average	206	148	116	74	63	49
Stdev	34	26	20	11	9	10
%CV	16.4	17.5	17.1	15.3	15.1	19.7

Table A.21.1
Dynamic modulus, |E*| (ksi), test results for LA1-2 at -10ºC

	25Hz	10Hz	5Hz	1Hz	0.5Hz	0.1Hz
Sample-8	3382	3260	3130	2886	2756	2476
Sample-9	3085	2946	2822	2548	2436	2130
Sample-12	3134	3005	2897	2642	2520	2224
Average	3200	3070	2950	2692	2571	2277
Stdev	159	167	161	174	166	179
%CV	5.0	5.4	5.4	6.5	6.5	7.9

Table A.21.2
Dynamic modulus, |E*| (ksi), test results for LA1-2 at 4.4ºC

	25Hz	10Hz	5Hz	1Hz	0.5Hz	0.1Hz
Sample-8	2164	1981	1851	1543	1415	1133
Sample-9	2390	2232	2105	1790	1663	1374
Sample-12	2044	1937	1811	1493	1367	1096
Average	2199	2050	1922	1609	1482	1201
Stdev	176	159	160	159	159	151
%CV	8.0	7.8	8.3	9.9	10.7	12.5

Table A.21.3
Dynamic modulus, |E*| (ksi), test results for LA1-2 at 25ºC

	25Hz	10Hz	5Hz	1Hz	0.5Hz	0.1Hz
Sample-8	1022	866	743	493	408	262
Sample-9	972	882	752	471	377	241
Sample-12	1093	870	741	475	378	232
Average	1029	873	745	480	387	245
Stdev	61	8	6	11	17	15
%CV	5.9	0.9	0.7	2.4	4.5	6.1

Table A.21.4
Dynamic modulus, |E*| (ksi), test results for LA1-2 at 37.8ºC

	25Hz	10Hz	5Hz	1Hz	0.5Hz	0.1Hz
Sample-8	504	391	315	184	144	92
Sample-9	561	429	346	208	163	105
Sample-12	452	345	278	169	132	88
Average	505	388	313	187	146	95
Stdev	54	42	34	20	16	9
%CV	10.7	10.8	10.9	10.6	10.9	9.3

Table A.21.5
Dynamic modulus, |E*| (ksi), test results for LA1-2 at 54.4ºC

	25Hz	10Hz	5Hz	1Hz	0.5Hz	0.1Hz
Sample-8	182	134	107	70	60	47
Sample-9	169	129	108	73	65	53
Sample-12	184	134	111	75	65	54
Average	178	132	109	73	63	51
Stdev	8	3	2	2	3	4
%CV	4.7	2.3	1.6	3.3	4.5	6.8

Table A.22.1

Dynamic modulus, |E*| (ksi), test results for I10-1 at -10ºC

	25Hz	10Hz	5Hz	1Hz	0.5Hz	0.1Hz
Sample-4	3240	3111	3003	2720	2642	2296
Sample-6	5173	4662	4520	4068	3880	3348
Sample-12	5148	5036	4873	4486	4313	3881
Average	4520	4270	4132	3758	3612	3175
Stdev	1109	1021	993	923	867	807
%CV	24.5	23.9	24.0	24.6	24.0	25.4

Table A.22.2

Dynamic modulus, |E*| (ksi), test results for I10-1 at 4.4ºC

	25Hz	10Hz	5Hz	1Hz	0.5Hz	0.1Hz
Sample-4	2479	2327	2216	1847	1692	1360
Sample-6	3813	3371	3082	2549	2296	1750
Sample-12	3892	3544	3290	2762	2552	2001
Average	3395	3081	2863	2386	2180	1704
Stdev	794	658	570	478	442	323
%CV	23.4	21.4	19.9	20.0	20.3	19.0

Table A.22.3

Dynamic modulus, |E*| (ksi), test results for I10-1 at 25ºC

	25Hz	10Hz	5Hz	1Hz	0.5Hz	0.1Hz
Sample-4	1167	965	819	478	389	225
Sample-6	1266	1047	851	497	404	240
Sample-12	1578	1322	1090	648	508	305
Average	1337	1111	920	541	434	257
Stdev	215	187	148	93	65	42
%CV	16.0	16.8	16.1	17.2	14.9	16.4

Table A.22.4
Dynamic modulus, |E*| (ksi), test results for I10-1 at 37.8ºC

	25Hz	10Hz	5Hz	1Hz	0.5Hz	0.1Hz
Sample-4	502	343	270	150	122	81
Sample-6	532	387	304	169	128	84
Sample-12	630	424	334	195	156	106
Average	555	384	303	172	135	90
Stdev	67	40	32	22	18	14
%CV	12.1	10.5	10.5	13.0	13.5	15.0

Table A.22.5
Dynamic modulus, |E*| (ksi), test results for I10-1 at 54.4ºC

	25Hz	10Hz	5Hz	1Hz	0.5Hz	0.1Hz
Sample-4	153	117	97	65	60	49
Sample-6	155	116	94	63	59	51
Sample-12	230	167	131	87	77	67
Average	179	134	107	72	65	56
Stdev	44	29	21	13	10	10
%CV	24.4	22.0	19.2	18.6	15.4	17.6

Table A.23.1

Dynamic modulus, |E*| (ksi), test results for I10-2 at -10ºC

	25Hz	10Hz	5Hz	1Hz	0.5Hz	0.1Hz
Sample-2	4178	4007	3926	3537	3396	2975
Sample-7	3323	3203	3064	2729	2547	2182
Sample-8	2847	2736	2679	2427	2319	2074
Average	3449	3315	3223	2898	2754	2410
Stdev	674	643	639	574	568	492
%CV	19.6	19.4	19.8	19.8	20.6	20.4

Table A.23.2

Dynamic modulus, |E*| (ksi), test results for I10-2 at 4.4ºC

	25Hz	10Hz	5Hz	1Hz	0.5Hz	0.1Hz
Sample-2	2791	2512	2319	1965	1778	1385
Sample-7	2736	2520	2349	1944	1768	1394
Sample-8	2129	2016	1897	1570	1438	1148
Average	2552	2349	2188	1826	1661	1309
Stdev	367	289	253	222	193	140
%CV	14.4	12.3	11.5	12.2	11.6	10.7

Table A.23.3

Dynamic modulus, |E*| (ksi), test results for I10-2 at 25ºC

	25Hz	10Hz	5Hz	1Hz	0.5Hz	0.1Hz
Sample-2	1048	845	700	426	336	200
Sample-7	1043	864	739	446	364	227
Sample-8	964	767	650	398	317	188
Average	1018	825	696	423	339	205
Stdev	47	51	45	24	24	20
%CV	4.6	6.2	6.4	5.7	7.0	9.7

Table A.23.4
Dynamic modulus, |E*| (ksi), test results for I10-2 at 37.8ºC

	25Hz	10Hz	5Hz	1Hz	0.5Hz	0.1Hz
Sample-2	458	335	275	148	121	77
Sample-7	519	383	304	172	132	86
Sample-8	429	323	254	142	110	73
Average	469	347	278	154	121	79
Stdev	46	32	25	16	11	7
%CV	9.8	9.1	9.0	10.3	9.1	8.5

Table A.23.5
Dynamic modulus, |E*| (ksi), test results for I10-2 at 54.4ºC

	25Hz	10Hz	5Hz	1Hz	0.5Hz	0.1Hz
Sample-2	150	107	85	56	49	39
Sample-7	164	130	108	75	64	53
Sample-8	140	106	86	60	54	45
Average	151	114	93	64	56	46
Stdev	12	14	13	10	8	7
%CV	8.0	11.9	14.0	15.7	13.7	15.4

Table A.24.1

Dynamic modulus, |E*| (ksi), test results for I55-1 at -10ºC

	25Hz	10Hz	5Hz	1Hz	0.5Hz	0.1Hz
Sample-1	3499	3397	3304	3069	2964	2684
Sample-2	3002	2925	2840	2615	2516	2275
Sample-3	3214	3018	2894	2638	2530	2356
Average	3238	3114	3013	2774	2670	2438
Stdev	250	250	253	256	255	216
%CV	7.7	8.0	8.4	9.2	9.5	8.9

Table A.24.2

Dynamic modulus, |E*| (ksi), test results for I55-1 at 4.4ºC

	25Hz	10Hz	5Hz	1Hz	0.5Hz	0.1Hz
Sample-1	2381	2224	2103	1814	1686	1391
Sample-2	2091	1950	1840	1578	1465	1201
Sample-3	2710	2528	2385	2069	1923	1597
Average	2394	2234	2109	1820	1691	1396
Stdev	310	289	272	245	229	198
%CV	12.9	12.9	12.9	13.5	13.5	14.2

Table A.24.3

Dynamic modulus, |E*| (ksi), test results for I55-1 at 25ºC

	25Hz	10Hz	5Hz	1Hz	0.5Hz	0.1Hz
Sample-1	1182	1009	884	616	518	327
Sample-2	945	789	685	457	382	232
Sample-3	1241	1055	922	652	554	355
Average	1123	951	830	575	485	305
Stdev	157	142	127	103	90	64
%CV	14.0	15.0	15.3	18.0	18.7	21.0

Table A.24.4
Dynamic modulus, |E*| (ksi), test results for I55-1 at 37.8ºC

	25Hz	10Hz	5Hz	1Hz	0.5Hz	0.1Hz
Sample-1	587	457	372	215	169	91
Sample-2	566	440	362	210	166	87
Sample-3	637	498	406	237	184	98
Average	597	465	380	221	173	92
Stdev	36	30	23	14	10	5
%CV	6.1	6.5	6.1	6.6	5.8	5.8

Table A.24.5
Dynamic modulus, |E*| (ksi), test results for I55-1 at 54.4ºC

	25Hz	10Hz	5Hz	1Hz	0.5Hz	0.1Hz
Sample-1	202	134	103	52	41	22
Sample-2	210	140	105	53	41	22
Sample-3	200	134	101	50	38	20
Average	204	136	103	52	40	22
Stdev	5	4	2	2	2	1
%CV	2.5	2.6	2.1	3.0	4.5	4.6

Table A.25.1

Dynamic modulus, |E*| (ksi), test results for I55-2 at -10ºC

	25Hz	10Hz	5Hz	1Hz	0.5Hz	0.1Hz
Sample-1	4153	4033	3920	3620	3480	3130
Sample-2	3755	3619	3504	3204	3070	2738
Sample-3	3717	3582	3472	3184	3051	2729
Average	3875	3744	3632	3336	3201	2866
Stdev	242	250	250	246	242	229
%CV	6.2	6.7	6.9	7.4	7.6	8.0

Table A.25.2

Dynamic modulus, |E*| (ksi), test results for I55-2 at 4.4ºC

	25Hz	10Hz	5Hz	1Hz	0.5Hz	0.1Hz
Sample-1	3248	2997	2789	2324	2120	1678
Sample-2	3029	2782	2602	2173	1977	1570
Sample-3	2981	2753	2579	2191	2021	1639
Average	3086	2844	2657	2229	2039	1629
Stdev	142	133	115	83	73	55
%CV	4.6	4.7	4.3	3.7	3.6	3.4

Table A.25.3

Dynamic modulus, |E*| (ksi), test results for I55-2 at 25ºC

	25Hz	10Hz	5Hz	1Hz	0.5Hz	0.1Hz
Sample-1	1442	1189	999	673	569	359
Sample-2	1475	1249	1098	758	630	398
Sample-3	1446	1231	1101	790	671	428
Average	1454	1223	1066	740	623	395
Stdev	18	31	58	60	52	35
%CV	1.2	2.5	5.4	8.1	8.3	8.8

Table A.25.4
Dynamic modulus, |E*| (ksi), Test Results for I55-2 at 37.8ºC

	25Hz	10Hz	5Hz	1Hz	0.5Hz	0.1Hz
Sample-1	582	444	368	208	156	79
Sample-2	596	457	380	216	169	88
Sample-3	594	457	380	216	172	91
Average	591	453	376	213	166	86
Stdev	7	8	7	5	8	6
%CV	1.3	1.7	1.9	2.3	4.9	7.1

Table A.25.5
Dynamic modulus, |E*| (ksi), test results for I55-2 at 54.4ºC

	25Hz	10Hz	5Hz	1Hz	0.5Hz	0.1Hz
Sample-1	225	150	114	69	59	44
Sample-2	244	170	133	81	66	48
Sample-3	204	137	103	67	56	44
Average	224	152	117	72	60	45
Stdev	20	16	15	8	5	2
%CV	9.0	10.8	12.8	10.8	8.0	4.7

Table A.26.1

Dynamic modulus, |E*| (ksi), test results for I10-3 at -10ºC

	25Hz	10Hz	5Hz	1Hz	0.5Hz	0.1Hz
Sample-4	4500	4302	4156	3811	3610	3172
Sample-5	4362	4250	4076	3776	3619	3132
Sample-6	3421	3239	3110	2836	2707	2372
Average	4094	3930	3781	3474	3312	2892
Stdev	587	599	582	553	524	451
%CV	14.3	15.2	15.4	15.9	15.8	15.6

Table A.26.2

Dynamic modulus, |E*| (ksi), test results for I10-3 at 4.4ºC

	25Hz	10Hz	5Hz	1Hz	0.5Hz	0.1Hz
Sample-4	3115	2779	2590	2103	1916	1470
Sample-5	3106	2722	2513	2068	1874	1465
Sample-6	2154	1941	1805	1492	1363	1054
Average	2792	2481	2303	1888	1718	1330
Stdev	552	468	433	343	308	239
%CV	19.8	18.9	18.8	18.2	17.9	18.0

Table A.26.3

Dynamic modulus, |E*| (ksi), test results for I10-3 at 25ºC

	25Hz	10Hz	5Hz	1Hz	0.5Hz	0.1Hz
Sample-4	1145	897	760	501	410	256
Sample-5	966	793	657	415	331	193
Sample-6	915	722	611	400	334	210
Average	1009	804	676	439	358	220
Stdev	121	88	76	55	45	33
%CV	12.0	10.9	11.3	12.4	12.5	14.8

Table A.26.4
Dynamic modulus, |E*| (ksi), test results for I10-3 at 37.8ºC

	25Hz	10Hz	5Hz	1Hz	0.5Hz	0.1Hz
Sample-4	470	348	281	170	142	94
Sample-5	428	313	248	146	118	81
Sample-6	394	300	241	144	116	74
Average	431	320	257	153	125	83
Stdev	38	25	21	14	14	10
%CV	8.8	7.8	8.3	9.4	11.5	12.2

Table A.26.5
Dynamic modulus, |E*| (ksi), test results for I10-3 at 54.4ºC

	25Hz	10Hz	5Hz	1Hz	0.5Hz	0.1Hz
Sample-4	157	114	97	75	68	62
Sample-5	127	96	78	53	46	37
Sample-6	146	110	91	65	59	51
Average	143	107	89	64	58	50
Stdev	15	9	10	11	11	13
%CV	10.6	8.9	11.0	17.1	19.2	25.1

Table A.27.1

Dynamic modulus, |E*| (ksi), test results for 964-1 at -10ºC

	25Hz	10Hz	5Hz	1Hz	0.5Hz	0.1Hz
Sample-3	3597	3234	3102	2809	2672	2341
Sample-4	3943	3790	3666	3359	3214	2855
Sample-6	4292	4218	4122	3798	3647	3292
Average	3944	3747	3630	3322	3178	2829
Stdev	348	494	511	495	489	477
%CV	8.8	13.2	14.1	14.9	15.4	16.8

Table A.27.2

Dynamic modulus, |E*| (ksi), test results for 964-1 at 4.4ºC

	25Hz	10Hz	5Hz	1Hz	0.5Hz	0.1Hz
Sample-3	2744	2594	2435	2045	1889	1498
Sample-4	2616	2458	2316	1916	1750	1407
Sample-6	3120	2920	2775	2338	2160	1744
Average	2827	2658	2509	2100	1933	1550
Stdev	262	238	238	216	209	174
%CV	9.3	8.9	9.5	10.3	10.8	11.2

Table A.27.3

Dynamic modulus, |E*| (ksi), test results for 964-1 at 25ºC

	25Hz	10Hz	5Hz	1Hz	0.5Hz	0.1Hz
Sample-3	1189	1019	859	526	423	243
Sample-4	1177	972	826	493	394	237
Sample-6	1417	1248	1083	672	536	332
Average	1261	1080	923	564	451	270
Stdev	135	148	140	95	75	53
%CV	10.7	13.7	15.2	16.9	16.6	19.7

Table A.27.4
Dynamic modulus, |E*| (ksi), test results for 964-1 at 37.8ºC

	25Hz	10Hz	5Hz	1Hz	0.5Hz	0.1Hz
Sample-3	452	299	247	124	96	59
Sample-4	446	320	247	130	102	64
Sample-6	616	440	345	209	171	107
Average	505	353	280	155	123	77
Stdev	97	76	57	47	41	26
%CV	19.1	21.6	20.3	30.6	33.5	33.9

Table A.27.5
Dynamic modulus, |E*| (ksi), test results for 964-1 at 54.4ºC

	25Hz	10Hz	5Hz	1Hz	0.5Hz	0.1Hz
Sample-3	145	102	81	54	48	38
Sample-4	164	115	88	59	51	39
Sample-6	179	128	105	67	61	47
Average	163	115	91	60	54	42
Stdev	17	13	13	7	7	5
%CV	10.3	11.2	13.7	10.8	12.2	11.6

Table A.28.1

Dynamic modulus, |E*| (ksi), test results for 964-2 at -10ºC

	25Hz	10Hz	5Hz	1Hz	0.5Hz	0.1Hz
Sample-25	3324	3228	3148	2946	2853	2619
Sample-26	3686	3606	3516	3294	3201	2978
Sample-27	2979	2902	2812	2622	2538	2363
Average	3330	3246	3159	2954	2864	2653
Stdev	354	352	352	336	332	309
%CV	10.6	10.9	11.1	11.4	11.6	11.6

Table A.28.2

Dynamic modulus, |E*| (ksi), test results for 964-2 at 4.4ºC

	25Hz	10Hz	5Hz	1Hz	0.5Hz	0.1Hz
Sample-25	2683	2540	2410	2121	1992	1684
Sample-26	3125	3051	2949	2636	2503	2189
Sample-27	2520	2405	2314	2097	2005	1785
Average	2776	2665	2557	2285	2167	1886
Stdev	313	341	342	305	291	267
%CV	11.3	12.8	13.4	13.3	13.4	14.2

Table A.28.3

Dynamic modulus, |E*| (ksi), test results for 964-2 at 25ºC

	25Hz	10Hz	5Hz	1Hz	0.5Hz	0.1Hz
Sample-25	1481	1267	1118	807	687	448
Sample-26	1834	1623	1427	1024	881	614
Sample-27	1608	1464	1340	1057	939	716
Average	1641	1451	1295	963	836	593
Stdev	179	179	160	136	132	135
%CV	10.9	12.3	12.3	14.1	15.8	22.8

Table A.28.4
Dynamic modulus, |E*| (ksi), test results for 964-2 at 37.8ºC

	25Hz	10Hz	5Hz	1Hz	0.5Hz	0.1Hz
Sample-25	603	466	378	219	167	101
Sample-26	851	660	541	323	251	150
Sample-27	838	695	591	394	318	221
Average	764	607	503	312	245	157
Stdev	139	123	111	88	76	60
%CV	18.2	20.3	22.1	28.1	30.8	38.2

Table A.28.5
Dynamic modulus, |E*| (ksi), test results for 964-2 at 54.4ºC

	25Hz	10Hz	5Hz	1Hz	0.5Hz	0.1Hz
Sample-25	212	151	119	72	59	41
Sample-26	312	224	172	102	83	56
Sample-27	390	307	255	161	132	91
Average	305	228	182	112	91	63
Stdev	89	78	68	45	37	26
%CV	29.2	34.3	37.6	40.6	40.8	41.0

APPENDIX B

Phase Angle (δ) Result

Table B.1.1

Phase angle, δ (degrees), test results for LA9-1 at -10ºC

	25Hz	10Hz	5Hz	1Hz	0.5Hz	0.1Hz
Sample-1	3.5	4.1	5.1	6.9	7.6	9.4
Sample-3	3.2	3.6	4.6	6.2	6.8	8.3
Sample-4	3.5	4.1	5.1	6.8	7.5	9.4
Average	3.4	3.9	4.9	6.6	7.3	9.0
Stdev	0.2	0.3	0.3	0.4	0.5	0.6
%CV	5.7	6.8	5.4	5.6	6.3	6.7

Table B.1.2

Phase angle, δ (degrees), test results for LA9-1 at 4.4ºC

	25Hz	10Hz	5Hz	1Hz	0.5Hz	0.1Hz
Sample-1	4.7	9.2	10.8	14.2	15.7	19.8
Sample-3	5.3	8.0	9.4	12.2	13.5	16.9
Sample-4	5.7	9.6	11.2	14.7	16.3	20.2
Average	5.2	8.9	10.5	13.7	15.2	19.0
Stdev	0.5	0.8	1.0	1.3	1.5	1.8
%CV	9.1	9.4	9.2	9.6	9.6	9.5

Table B.1.3

Phase angle, δ (degrees), test results for LA9-1 at 25ºC

	25Hz	10Hz	5Hz	1Hz	0.5Hz	0.1Hz
Sample-1	21.6	25.0	27.3	32.4	33.3	32.8
Sample-3	19.6	22.8	25.1	30.1	31.7	32.6
Sample-4	21.9	25.9	28.3	33.4	34.1	32.8
Average	21.0	24.6	26.9	32.0	33.1	32.7
Stdev	1.3	1.6	1.6	1.7	1.2	0.1

%CV	6.1	6.4	6.1	5.2	3.7	0.4

Table B.1.4

Phase angle, δ (degrees), test results for LA9-1 at 37.8ºC

	25Hz	10Hz	5Hz	1Hz	0.5Hz	0.1Hz
Sample-1	30.8	32.9	33.1	31.2	29.6	23.9
Sample-3	29.8	31.7	32.3	30.7	30.3	25.5
Sample-4	31.7	34.0	34.3	31.2	29.5	23.3
Average	30.7	32.8	33.2	31.0	29.8	24.2
Stdev	1.0	1.1	1.0	0.3	0.4	1.1
%CV	3.2	3.5	3.0	1.0	1.5	4.7

Table B.1.5

Phase angle, δ (degrees), test results for LA9-1 at 54.4ºC

	25Hz	10Hz	5Hz	1Hz	0.5Hz	0.1Hz
Sample-1	30.8	27.8	26.6	21.0	18.7	14.9
Sample-3	33.6	31.7	29.5	24.5	22.3	17.2
Sample-4	31.4	28.4	27.8	21.5	19.4	15.8
Average	31.9	29.3	28.0	22.3	20.1	16.0
Stdev	1.4	2.1	1.5	1.9	1.9	1.2
%CV	4.5	7.1	5.2	8.4	9.4	7.2

Table B.2.1

Phase angle, δ (degrees), test results for US90-1 at -10ºC

	25Hz	10Hz	5Hz	1Hz	0.5Hz	0.1Hz
Sample-5	2.5	3.8	4.8	6.4	7.0	8.8
Sample-6	1.6	2.6	3.6	5.0	5.5	6.9
Sample-11	2.5	3.1	4.0	5.4	6.0	7.4
Average	2.2	3.2	4.1	5.6	6.2	7.7
Stdev	0.5	0.6	0.6	0.7	0.8	1.0
%CV	24.2	19.0	14.2	13.2	12.5	12.5

Table B.2.2

Phase angle, δ (degrees), test results for US90-1 at 4.4ºC

	25Hz	10Hz	5Hz	1Hz	0.5Hz	0.1Hz
Sample-5	5.3	8.0	9.4	12.3	13.6	16.9
Sample-6	4.6	7.1	8.5	11.2	12.5	15.8
Sample-11	4.7	7.1	8.5	11.2	12.4	15.4
Average	4.9	7.4	8.8	11.6	12.8	16.0
Stdev	0.4	0.5	0.5	0.6	0.7	0.8
%CV	7.6	6.8	5.8	5.4	5.4	4.9

Table B.2.3

Phase angle, δ (degrees), test results for US90-1 at 25ºC

	25Hz	10Hz	5Hz	1Hz	0.5Hz	0.1Hz
Sample-5	16.3	20.4	22.8	28.4	29.9	31.6
Sample-6	16.3	19.5	21.6	26.8	28.5	30.4
Sample-11	16.2	20.4	22.9	28.8	30.4	32.3
Average	16.3	20.1	22.4	28.0	29.6	31.5
Stdev	0.1	0.6	0.7	1.0	1.0	1.0
%CV	0.4	2.8	3.1	3.6	3.3	3.1

Table B.2.4

Phase angle, δ (degrees), test results for US90-1 at 37.8ºC

	25Hz	10Hz	5Hz	1Hz	0.5Hz	0.1Hz
Sample-5	27.1	29.7	30.9	30.6	28.3	25.3
Sample-6	25.9	28.7	30.1	31.3	31.2	27.3
Sample-11	27.8	30.4	31.7	31.7	31.3	27.4
Average	26.9	29.6	30.9	31.2	30.3	26.7
Stdev	1.0	0.9	0.8	0.5	1.7	1.2
%CV	3.7	2.9	2.5	1.7	5.7	4.4

Table B.2.5

Phase angle, δ (degrees), test results for US90-1 at 54.4ºC

	25Hz	10Hz	5Hz	1Hz	0.5Hz	0.1Hz
Sample-5	31.4	30.5	29.1	25.6	23.5	19.4
Sample-6	31.3	31.3	30.5	26.6	24.3	18.8
Sample-11	31.9	31.0	29.6	25.9	23.6	19.0
Average	31.5	30.9	29.7	26.0	23.8	19.1
Stdev	0.3	0.4	0.7	0.5	0.5	0.3
%CV	1.0	1.3	2.4	2.0	1.9	1.6

Table B.3.1

Phase angle, δ (degrees), test results for LPC-1 at -10ºC

	25Hz	10Hz	5Hz	1Hz	0.5Hz	0.1Hz
Sample-3	1.4	2.4	3.3	4.6	5.2	6.0
Sample-10	1.6	2.7	3.6	4.9	5.4	6.6
Sample-13	1.5	2.4	3.4	4.7	5.2	6.3
Average	1.5	2.5	3.4	4.7	5.3	6.3
Stdev	0.1	0.2	0.2	0.2	0.1	0.3

%CV	6.7	6.9	4.8	3.8	2.6	4.7

Table B.3.2

Phase angle, δ (degrees), test results for LPC-1 at 4.4ºC

	25Hz	10Hz	5Hz	1Hz	0.5Hz	0.1Hz
Sample-3	3.5	6.1	7.2	9.5	10.5	13.5
Sample-10	3.5	5.8	7.0	9.2	10.3	13.1
Sample-13	4.9	5.8	7.1	9.4	10.4	13.3
Average	4.0	5.9	7.1	9.4	10.4	13.3
Stdev	0.8	0.2	0.1	0.1	0.1	0.2
%CV	21.3	2.7	1.5	1.5	1.2	1.3

Table B.3.3

Phase angle, δ (degrees), test results for LPC-1 at 25ºC

	25Hz	10Hz	5Hz	1Hz	0.5Hz	0.1Hz
Sample-3	15.4	18.5	20.8	26.1	27.5	30.2
Sample-10	15.5	18.8	21.2	26.9	28.4	30.2
Sample-13	15.9	19.0	21.4	26.8	28.5	30.9
Average	15.6	18.8	21.1	26.6	28.1	30.4
Stdev	0.3	0.3	0.3	0.4	0.6	0.4
%CV	1.8	1.3	1.5	1.6	2.0	1.4

Table B.3.4

Phase angle, δ (degrees), test results for LPC-1 at 37.8ºC

	25Hz	10Hz	5Hz	1Hz	0.5Hz	0.1Hz
Sample-3	24.2	27.2	28.8	30.6	30.3	26.9
Sample-10	26.3	30.3	31.8	35.1	35.0	31.1
Sample-13	25.7	28.6	30.4	31.8	31.3	27.2
Average	25.4	28.7	30.3	32.5	32.2	28.4

Stdev	1.1	1.6	1.5	2.3	2.5	2.4
%CV	4.2	5.5	4.9	7.2	7.7	8.3

Table B.3.5

Phase angle, δ (degrees), test results for LPC-1 at 54.4ºC

	25Hz	10Hz	5Hz	1Hz	0.5Hz	0.1Hz
Sample-3	31.0	29.8	28.5	24.8	22.9	18.0
Sample-10	31.6	30.6	28.7	24.4	22.1	17.3
Sample-13	31.1	30.5	28.6	24.1	21.9	17.4
Average	31.2	30.3	28.6	24.4	22.3	17.5
Stdev	0.3	0.4	0.1	0.3	0.5	0.4
%CV	1.0	1.4	0.4	1.3	2.4	2.2

Table B.4.1

Phase angle, δ (degrees), test results for 3121-1 at -10ºC

	25Hz	10Hz	5Hz	1Hz	0.5Hz	0.1Hz
Sample-1	1.7	3.6	4.6	6.1	6.7	8.2
Sample-2	2.5	4.7	5.7	7.4	8.0	8.9
Sample-3	1.9	3.2	4.1	5.6	6.2	7.5
Average	2.0	3.8	4.8	6.4	7.0	8.2
Stdev	0.4	0.8	0.8	0.9	1.0	0.7
%CV	20.2	19.9	17.1	14.2	13.8	8.5

Table B.4.2

Phase angle, δ (degrees), test results for 3121-1 at 4.4ºC

	25Hz	10Hz	5Hz	1Hz	0.5Hz	0.1Hz
Sample-1	5.8	8.5	10.0	12.9	14.2	17.1
Sample-2	6.0	8.7	10.1	13.1	14.5	17.6
Sample-3	5.8	8.5	9.9	12.9	14.2	17.1
Average	5.8	8.6	10.0	13.0	14.3	17.3
Stdev	0.1	0.1	0.1	0.1	0.2	0.3
%CV	2.0	0.9	1.0	1.0	1.3	1.8

Table B.4.3

Phase angle, δ (degrees), test results for 3121-1 at 25ºC

	25Hz	10Hz	5Hz	1Hz	0.5Hz	0.1Hz
Sample-1	17.1	20.8	23.2	28.2	29.6	30.8
Sample-2	18.1	21.8	24.1	29.0	30.3	31.8
Sample-3	17.8	21.7	24.1	29.9	31.6	33.0
Average	17.7	21.5	23.8	29.0	30.5	31.9
Stdev	0.5	0.6	0.5	0.9	1.0	1.1
%CV	2.9	2.7	2.2	3.0	3.4	3.5

Table B.4.4

Phase angle, δ (degrees), test results for 3121-1 at 37.8ºC

	25Hz	10Hz	5Hz	1Hz	0.5Hz	0.1Hz
Sample-1	26.8	29.9	31.2	32.8	32.2	29.1
Sample-2	27.7	30.6	31.5	32.3	31.4	27.2
Sample-3	27.4	30.2	31.1	32.2	30.6	26.7
Average	27.3	30.2	31.3	32.4	31.4	27.7
Stdev	0.4	0.3	0.2	0.3	0.8	1.3
%CV	1.5	1.1	0.7	1.0	2.6	4.6

Table B.4.5

Phase angle, δ (degrees), test results for 3121-1 at 54.4ºC

	25Hz	10Hz	5Hz	1Hz	0.5Hz	0.1Hz
Sample-1	33.9	34.3	32.5	29.0	26.2	20.8
Sample-2	33.4	33.8	32.0	27.9	25.2	19.8
Sample-3	31.2	31.1	29.5	24.3	22.7	18.1
Average	32.8	33.1	31.3	27.1	24.7	19.5
Stdev	1.4	1.7	1.6	2.4	1.8	1.3
%CV	4.4	5.2	5.1	9.0	7.2	6.9

Table B.5.1

Phase angle, δ (degrees), test results for 3121-2 at -10ºC

	25Hz	10Hz	5Hz	1Hz	0.5Hz	0.1Hz
Sample-1	1.2	3.5	4.4	6.0	6.6	8.1
Sample-2	1.9	4.3	5.3	7.1	7.9	10.0
Sample-3	1.9	4.3	5.3	7.2	8.0	10.3
Average	1.7	4.0	5.0	6.8	7.5	9.4
Stdev	0.4	0.4	0.5	0.7	0.8	1.2
%CV	25.9	11.1	10.1	10.2	10.7	12.9

Table B.5.2

Phase angle, δ (degrees), test results for 3121-2 at 4.4ºC

	25Hz	10Hz	5Hz	1Hz	0.5Hz	0.1Hz
Sample-1	6.4	9.2	10.7	14.0	15.4	18.9
Sample-2	7.6	10.6	12.6	16.7	18.6	22.8
Sample-3	7.8	11.0	12.8	16.8	18.6	22.5
Average	7.3	10.3	12.0	15.8	17.5	21.4
Stdev	0.8	0.9	1.2	1.6	1.8	2.2
%CV	10.4	9.2	9.7	9.9	10.4	10.1

Table B.5.3

Phase angle, δ (degrees), test results for 3121-2 at 25ºC

	25Hz	10Hz	5Hz	1Hz	0.5Hz	0.1Hz
Sample-1	17.8	21.4	23.8	28.7	30.0	30.4
Sample-2	22.7	27.1	29.0	32.9	33.8	31.7
Sample-3	23.0	26.6	28.8	32.4	32.6	31.3
Average	21.1	25.0	27.2	31.3	32.1	31.1
Stdev	2.9	3.1	2.9	2.3	2.0	0.6
%CV	13.9	12.6	10.8	7.4	6.2	2.1

Table B.5.4

Phase angle, δ (degrees), test results for 3121-2 at 37.8ºC

	25Hz	10Hz	5Hz	1Hz	0.5Hz	0.1Hz
Sample-1	28.0	30.2	31.0	30.6	29.1	24.1
Sample-2	32.0	34.1	33.9	32.8	30.0	24.3
Sample-3	31.6	33.8	33.9	32.9	30.4	24.7
Average	30.6	32.7	32.9	32.1	29.8	24.4
Stdev	2.2	2.2	1.7	1.3	0.7	0.3
%CV	7.2	6.6	5.2	4.1	2.3	1.3

Table B.5.5

Phase angle, δ (degrees), test results for 3121-2 at 54.4ºC

	25Hz	10Hz	5Hz	1Hz	0.5Hz	0.1Hz
Sample-1	31.5	30.9	29.5	26.1	23.4	18.1
Sample-2	31.3	29.0	27.0	20.6	17.2	12.6
Sample-3	33.8	31.4	29.9	22.6	19.0	13.7
Average	32.2	30.5	28.8	23.1	19.9	14.8
Stdev	1.4	1.3	1.6	2.8	3.2	2.9
%CV	4.4	4.2	5.5	12.1	16.0	19.6

Table B.6.1

Phase angle, δ (degrees), test results for 3121-3 at -10ºC

	25Hz	10Hz	5Hz	1Hz	0.5Hz	0.1Hz
Sample-1	2.1	4.2	5.2	6.9	7.5	9.2
Sample-2	1.2	3.3	4.3	5.8	6.4	7.9
Sample-3	1.9	4.2	5.3	6.9	7.7	9.5
Average	1.7	3.9	4.9	6.6	7.2	8.9
Stdev	0.4	0.5	0.5	0.6	0.7	0.8
%CV	25.6	12.6	11.0	9.8	9.5	9.6

Table B.6.2

Phase angle, δ (degrees), test results for 3121-3 at 4.4ºC

	25Hz	10Hz	5Hz	1Hz	0.5Hz	0.1Hz
Sample-1	6.3	8.9	10.4	13.7	15.2	18.7
Sample-2	6.1	8.8	10.3	13.7	15.2	18.8
Sample-3	7.7	10.6	12.3	15.9	17.4	21.1
Average	6.7	9.4	11.0	14.4	15.9	19.5
Stdev	0.9	1.0	1.1	1.3	1.3	1.4
%CV	13.3	11.1	10.0	9.1	8.2	7.1

Table B.6.3

Phase angle, δ (degrees), test results for 3121-3 at 25ºC

	25Hz	10Hz	5Hz	1Hz	0.5Hz	0.1Hz
Sample-1	19.3	22.9	25.2	30.4	31.6	32.5
Sample-2	18.1	21.3	23.8	29.0	30.4	31.2
Sample-3	19.2	22.7	24.9	29.9	30.9	31.0
Average	18.9	22.3	24.7	29.7	31.0	31.6
Stdev	0.7	0.9	0.8	0.7	0.6	0.8
%CV	3.8	4.0	3.1	2.3	1.9	2.6

Table B.6.4

Phase angle, (δ) (degrees), test results for 3121-3 at 37.8ºC

	25Hz	10Hz	5Hz	1Hz	0.5Hz	0.1Hz
Sample-1	28.2	31.2	32.3	32.8	31.3	26.6
Sample-2	29.0	30.8	32.0	33.2	31.8	27.0
Sample-3	28.8	30.7	31.1	30.5	28.9	24.0
Average	28.7	30.9	31.8	32.2	30.7	25.8
Stdev	0.4	0.3	0.6	1.5	1.6	1.7
%CV	1.4	0.9	1.9	4.6	5.1	6.4

Table B.6.5

Phase angle, δ (degrees), test results for 3121-3 at 54.4ºC

	25Hz	10Hz	5Hz	1Hz	0.5Hz	0.1Hz
Sample-1	32.7	31.8	28.7	25.3	22.7	17.2
Sample-2	31.8	31.1	29.5	25.9	22.9	16.7
Sample-3	30.7	29.5	28.0	23.3	20.5	16.0
Average	31.7	30.8	28.7	24.8	22.0	16.6
Stdev	1.0	1.2	0.7	1.4	1.3	0.6
%CV	3.1	3.7	2.5	5.5	5.9	3.6

Table B.7.1

Phase angle, δ (degrees), test results for 171-1 at -10ºC

	25Hz	10Hz	5Hz	1Hz	0.5Hz	0.1Hz
Sample-1	1.1	2.8	3.4	4.9	5.4	6.8
Sample-2	0.8	2.3	3.3	5.0	5.6	7.1
Sample-3	1.0	2.7	3.6	5.1	5.6	7.0
Average	1.0	2.6	3.4	5.0	5.5	7.0
Stdev	0.1	0.3	0.1	0.1	0.1	0.1
%CV	15.5	11.7	3.5	2.0	2.1	1.9

Table B.7.2

Phase angle, δ (degrees), test results for 171-1 at 4.4ºC

	25Hz	10Hz	5Hz	1Hz	0.5Hz	0.1Hz
Sample-1	8.0	9.5	10.6	13.4	14.8	18.6
Sample-2	8.0	9.4	10.5	13.2	14.6	18.3
Sample-3	8.6	10.0	11.1	14.0	15.5	19.2
Average	8.2	9.6	10.7	13.6	15.0	18.7
Stdev	0.3	0.3	0.4	0.4	0.5	0.5
%CV	3.7	3.4	3.3	3.2	3.2	2.6

Table B.7.3

Phase angle, δ (degrees), test results for 171-1 at 25ºC

	25Hz	10Hz	5Hz	1Hz	0.5Hz	0.1Hz
Sample-1	17.4	20.8	23.2	26.3	26.8	29.7
Sample-2	19.5	23.1	25.3	29.8	30.3	28.3
Sample-3	20.0	23.4	25.8	30.6	31.4	30.8
Average	18.9	22.4	24.8	28.9	29.5	29.6
Stdev	1.4	1.4	1.4	2.3	2.4	1.3
%CV	7.4	6.4	5.6	7.9	8.1	4.2

Table B.7.4

Phase angle, δ (degrees), test results for 171-1 at 37.8ºC

	25Hz	10Hz	5Hz	1Hz	0.5Hz	0.1Hz
Sample-1	30.5	33.1	33.4	30.2	28.5	20.8
Sample-2	29.3	31.2	31.1	28.6	26.6	20.9
Sample-3	29.8	31.8	32.2	28.9	26.8	19.7
Average	29.9	32.0	32.2	29.2	27.3	20.4
Stdev	0.6	1.0	1.1	0.9	1.1	0.6
%CV	2.1	3.0	3.5	3.0	4.0	3.1

Table B.7.5

Phase angle, δ (degrees), test results for 171-1 at 54.4ºC

	25Hz	10Hz	5Hz	1Hz	0.5Hz	0.1Hz
Sample-1	28.4	25.2	21.8	15.9	13.8	10.5
Sample-2	28.1	25.0	21.6	16.3	14.1	10.9
Sample-3	30.2	27.8	24.9	19.8	16.5	13.2
Average	28.9	26.0	22.7	17.3	14.8	11.5
Stdev	1.1	1.6	1.9	2.1	1.5	1.5
%CV	3.9	6.0	8.2	12.3	10.0	12.6

Table B.8.1

Phase angle, δ (degrees), test results for 171-2 at -10ºC

	25Hz	10Hz	5Hz	1Hz	0.5Hz	0.1Hz
Sample-1	0.6	2.1	2.8	4.2	4.6	5.8
Sample-2	0.8	2.5	3.2	4.8	5.3	6.7
Sample-3	0.3	2.1	3.0	4.5	5.0	6.4
Average	0.6	2.2	3.0	4.5	4.9	6.3
Stdev	0.3	0.2	0.2	0.3	0.3	0.5
%CV	46.3	10.9	7.8	6.7	6.7	7.3

Table B.8.2

Phase angle, δ (degrees), test results for 171-2 at 4.4ºC

	25Hz	10Hz	5Hz	1Hz	0.5Hz	0.1Hz
Sample-1	8.5	9.9	11.0	13.8	15.2	18.9
Sample-2	5.2	7.6	9.0	12.3	13.6	16.9
Sample-3	8.2	9.6	10.7	13.6	15.0	18.9
Average	7.3	9.1	10.3	13.2	14.6	18.2
Stdev	1.8	1.3	1.1	0.8	0.9	1.2
%CV	25.2	13.8	10.5	6.4	6.0	6.5

Table B.8.3

Phase angle, δ (degrees), test results for 171-2 at 25ºC

	25Hz	10Hz	5Hz	1Hz	0.5Hz	0.1Hz
Sample-1	19.9	23.9	26.3	31.3	32.1	31.2
Sample-2	19.5	24.0	26.4	31.6	32.8	32.1
Sample-3	20.4	24.2	26.6	31.4	32.8	30.8
Average	19.9	24.0	26.4	31.4	32.6	31.4
Stdev	0.4	0.1	0.2	0.2	0.4	0.7
%CV	2.2	0.5	0.7	0.5	1.3	2.2

Table B.8.4

Phase angle, δ (degrees), test results for 171-2 at 37.8ºC

	25Hz	10Hz	5Hz	1Hz	0.5Hz	0.1Hz
Sample-1	30.5	32.3	32.8	30.3	28.3	22.3
Sample-2	31.5	33.5	33.8	31.5	28.3	21.0
Sample-3	29.6	31.7	32.0	29.7	27.3	20.9
Average	30.5	32.5	32.9	30.5	28.0	21.4
Stdev	1.0	0.9	0.9	0.9	0.6	0.8
%CV	3.2	2.8	2.7	3.1	2.0	3.6

Table B.8.5

Phase angle, δ (degrees), test results for 171-2 at 54.4ºC

	25Hz	10Hz	5Hz	1Hz	0.5Hz	0.1Hz
Sample-1	31.2	29.0	25.9	19.5	17.0	13.8
Sample-2	29.5	27.3	24.2	17.8	15.3	11.5
Sample-3	29.0	25.5	22.6	16.5	13.9	9.8
Average	29.9	27.2	24.2	17.9	15.4	11.7
Stdev	1.2	1.8	1.6	1.5	1.5	2.0
%CV	3.9	6.5	6.8	8.4	10.0	17.2

Table B.9.1

Phase angle, δ (degrees), test results for 171-3 at -10ºC

	25Hz	10Hz	5Hz	1Hz	0.5Hz	0.1Hz
Sample-1	1.3	3.1	3.7	5.3	5.8	7.4
Sample-2	0.8	2.8	3.5	4.9	5.5	6.7
Sample-3	0.5	2.2	3.1	4.6	5.0	6.3
Average	0.9	2.7	3.5	4.9	5.4	6.8
Stdev	0.4	0.4	0.3	0.4	0.4	0.5
%CV	48.5	16.0	8.5	7.1	7.4	7.9

Table B.9.2

Phase angle, δ (degrees), test results for 171-3 at 4.4ºC

	25Hz	10Hz	5Hz	1Hz	0.5Hz	0.1Hz
Sample-1	5.0	7.5	8.9	12.0	13.3	17.0
Sample-2	4.3	6.8	8.1	10.9	12.1	15.4
Sample-3	5.7	8.3	9.6	12.5	14.0	17.6
Average	5.0	7.5	8.9	11.8	13.1	16.7
Stdev	0.7	0.7	0.8	0.8	1.0	1.1
%CV	13.6	9.8	8.5	7.2	7.4	6.8

Table B.9.3

Phase angle, δ (degrees), test results for 171-3 at 25ºC

	25Hz	10Hz	5Hz	1Hz	0.5Hz	0.1Hz
Sample-1	18.6	22.7	25.0	30.3	31.6	30.2
Sample-2	18.0	21.7	24.1	28.8	30.4	30.4
Sample-3	19.8	23.2	25.6	30.1	31.5	30.1
Average	18.8	22.5	24.9	29.7	31.2	30.2
Stdev	0.9	0.7	0.7	0.8	0.7	0.1
%CV	4.7	3.3	2.9	2.8	2.2	0.4

Table B.9.4

Phase angle, δ (degrees), test results for 171-3 at 37.8ºC

	25Hz	10Hz	5Hz	1Hz	0.5Hz	0.1Hz
Sample-1	28.9	31.5	31.8	29.9	27.2	21.8
Sample-2	28.2	30.7	31.6	30.2	29.5	22.8
Sample-3	28.4	31.0	31.3	30.4	28.2	21.7
Average	28.5	31.0	31.5	30.2	28.3	22.1
Stdev	0.4	0.4	0.2	0.3	1.2	0.6
%CV	1.3	1.2	0.8	0.9	4.1	2.8

Table B.9.5

Phase angle, δ (degrees), test results for 171-3 at 54.4ºC

	25Hz	10Hz	5Hz	1Hz	0.5Hz	0.1Hz
Sample-1	30.6	28.3	25.6	20.0	17.6	13.8
Sample-2	29.2	26.9	24.3	18.2	15.8	11.6
Sample-3	30.9	28.7	26.1	20.7	17.8	13.7
Average	30.2	28.0	25.3	19.6	17.0	13.1
Stdev	0.9	0.9	0.9	1.3	1.1	1.2
%CV	3.0	3.3	3.6	6.6	6.5	9.4

Table B.10.1

Phase angle, δ (degrees), test results for 171-4 at -10ºC

	25Hz	10Hz	5Hz	1Hz	0.5Hz	0.1Hz
Sample-1	1.3	2.9	3.8	5.3	5.8	6.8
Sample-2	2.1	3.6	4.3	6.0	6.6	8.2
Sample-3	1.1	2.7	3.4	4.8	5.2	6.6
Average	1.5	3.1	3.8	5.3	5.9	7.2
Stdev	0.5	0.5	0.5	0.6	0.7	0.9
%CV	36.6	15.6	12.8	11.3	11.5	12.5

Table B.10.2

Phase angle, δ (degrees), test results for 171-4 at 4.4ºC

	25Hz	10Hz	5Hz	1Hz	0.5Hz	0.1Hz
Sample-1	8.2	9.5	10.6	13.3	14.7	18.4
Sample-2	8.1	9.6	10.7	13.5	15.0	18.8
Sample-3	8.1	9.5	10.6	13.3	14.7	18.4
Average	8.1	9.5	10.6	13.4	14.8	18.6
Stdev	0.0	0.1	0.1	0.1	0.2	0.2
%CV	0.6	0.6	0.6	1.0	1.2	1.3

Table B.10.3

Phase angle, δ (degrees), test results for 171-4 at 25ºC

	25Hz	10Hz	5Hz	1Hz	0.5Hz	0.1Hz
Sample-1	17.4	21.1	22.8	26.8	27.6	27.5
Sample-2	18.4	22.6	25.4	29.3	30.3	28.5
Sample-3	18.6	22.0	23.6	27.9	28.6	27.3
Average	18.2	21.9	23.9	28.0	28.8	27.8
Stdev	0.6	0.8	1.3	1.3	1.3	0.6
%CV	3.5	3.5	5.6	4.5	4.6	2.3

Table B.10.4

Phase angle, δ (degrees), test results for 171-4 at 37.8ºC

	25Hz	10Hz	5Hz	1Hz	0.5Hz	0.1Hz
Sample-1	28.6	30.7	31.0	28.8	25.8	19.6
Sample-2	30.7	32.6	32.9	29.8	27.4	20.5
Sample-3	29.6	31.4	31.3	29.6	26.6	19.9
Average	29.6	31.5	31.7	29.4	26.6	20.0
Stdev	1.1	1.0	1.1	0.5	0.8	0.5
%CV	3.6	3.0	3.3	1.8	3.0	2.3

Table B.10.5

Phase angle, δ (degrees), test results for 171-4 at 54.4ºC

	25Hz	10Hz	5Hz	1Hz	0.5Hz	0.1Hz
Sample-1	28.4	25.6	22.7	16.9	15.1	11.3
Sample-2	27.5	24.6	21.0	15.5	13.3	9.8
Sample-3	29.0	26.4	23.7	18.4	15.3	12.5
Average	28.3	25.5	22.5	16.9	14.6	11.2
Stdev	0.7	0.9	1.3	1.4	1.1	1.4
%CV	2.6	3.5	6.0	8.5	7.8	12.3

Table B.11.1

Phase angle, δ (degrees), test results for 116-1 at -10ºC

	25Hz	10Hz	5Hz	1Hz	0.5Hz	0.1Hz
Sample-1	0.4	2.4	3.1	4.4	4.9	6.2
Sample-2	0.2	2.4	2.9	4.1	4.7	6.1
Sample-3	0.8	2.2	2.8	4.3	4.8	6.3
Average	0.5	2.3	2.9	4.3	4.8	6.2
Stdev	0.3	0.1	0.1	0.1	0.1	0.1
%CV	68.7	5.1	4.6	3.2	2.0	1.3

Table B.11.2

Phase angle, δ (degrees), test results for 116-1 at 4.4ºC

	25Hz	10Hz	5Hz	1Hz	0.5Hz	0.1Hz
Sample-1	7.6	9.0	10.0	12.7	13.9	17.4
Sample-2	7.7	8.9	9.9	12.5	13.8	17.2
Sample-3	7.1	8.3	9.2	11.5	12.5	15.4
Average	7.5	8.7	9.7	12.2	13.4	16.7
Stdev	0.3	0.4	0.4	0.6	0.8	1.1
%CV	4.1	4.0	4.3	5.3	5.9	6.4

Table B.11.3

Phase angle, δ (degrees), test results for 116-1 at 25ºC

	25Hz	10Hz	5Hz	1Hz	0.5Hz	0.1Hz
Sample-1	21.7	23.9	25.5	29.3	30.3	32.6
Sample-2	21.1	23.9	25.6	29.7	30.7	33.0
Sample-3	19.4	21.9	23.5	27.4	28.5	31.4
Average	20.7	23.3	24.9	28.8	29.8	32.3
Stdev	1.2	1.2	1.2	1.3	1.2	0.8
%CV	5.8	5.0	4.7	4.4	4.0	2.5

Table B.11.4

Phase angle, δ (degrees), test results for 116-1 at 37.8ºC

	25Hz	10Hz	5Hz	1Hz	0.5Hz	0.1Hz
Sample-1	30.9	32.8	33.5	34.8	34.6	33.7
Sample-2	30.9	32.9	33.6	34.9	34.7	33.9
Sample-3	28.7	30.9	31.8	33.9	33.9	34.1
Average	30.2	32.2	32.9	34.5	34.4	33.9
Stdev	1.3	1.1	1.0	0.5	0.4	0.2
%CV	4.2	3.5	3.1	1.6	1.2	0.5

Table B.11.5

Phase angle, δ (degrees), test results for 116-1 at 54.4ºC

	25Hz	10Hz	5Hz	1Hz	0.5Hz	0.1Hz
Sample-1	37.0	38.4	37.2	34.2	31.9	27.0
Sample-2	36.7	37.9	36.6	33.5	31.0	25.7
Sample-3	36.1	37.4	36.4	34.1	32.2	28.1
Average	36.6	37.9	36.7	33.9	31.7	26.9
Stdev	0.5	0.5	0.4	0.3	0.6	1.2
%CV	1.3	1.3	1.2	1.0	2.0	4.4

Table B.12.1

Phase angle, δ (degrees), test results for 116-2 at -10ºC

	25Hz	10Hz	5Hz	1Hz	0.5Hz	0.1Hz
Sample-1	0.4	1.9	2.3	3.3	3.7	4.7
Sample-2	0.4	1.9	2.3	3.4	3.8	5.0
Sample-3	0.2	1.6	2.0	3.1	3.5	4.7
Average	0.3	1.8	2.2	3.3	3.7	4.8
Stdev	0.1	0.2	0.1	0.2	0.1	0.2
%CV	44.3	9.8	5.7	5.1	3.6	3.9

Table B.12.2

Phase angle, δ (degrees), test results for 116-2 at 4.4ºC

	25Hz	10Hz	5Hz	1Hz	0.5Hz	0.1Hz
Sample-1	6.7	7.9	8.8	11.0	12.0	15.0
Sample-2	7.0	8.1	8.9	11.0	12.1	15.1
Sample-3	7.6	8.6	9.3	11.3	12.3	14.9
Average	7.1	8.2	9.0	11.1	12.1	15.0
Stdev	0.4	0.3	0.3	0.2	0.2	0.1
%CV	6.2	4.1	3.3	1.8	1.3	0.6

Table B.12.3

Phase angle, δ (degrees), test results for 116-2 at 25ºC

	25Hz	10Hz	5Hz	1Hz	0.5Hz	0.1Hz
Sample-1	19.4	21.5	22.9	26.6	27.6	30.5
Sample-2	18.6	20.5	22.0	25.7	26.9	30.1
Sample-3	17.8	20.1	21.7	25.6	26.6	29.5
Average	18.6	20.7	22.2	25.9	27.0	30.0
Stdev	0.8	0.7	0.6	0.5	0.5	0.5
%CV	4.2	3.5	2.8	2.1	2.0	1.7

Table B.12.4

Phase angle, δ (degrees), test results for 116-2 at 37.8ºC

	25Hz	10Hz	5Hz	1Hz	0.5Hz	0.1Hz
Sample-1	28.3	30.1	31.1	33.1	33.2	33.5
Sample-2	28.6	30.6	31.6	33.5	33.4	33.1
Sample-3	26.9	29.1	30.3	32.7	32.9	33.3
Average	27.9	30.0	31.0	33.1	33.2	33.3
Stdev	0.9	0.8	0.6	0.4	0.3	0.2
%CV	3.2	2.5	2.1	1.2	0.8	0.7

Table B.12.5

Phase angle, δ (degrees), test results for 116-2 at 54.4ºC

	25Hz	10Hz	5Hz	1Hz	0.5Hz	0.1Hz
Sample-1	36.2	38.3	37.7	36.6	35.6	32.7
Sample-2	35.8	37.5	36.7	35.5	34.4	31.5
Sample-3	35.9	37.3	36.4	34.6	32.9	29.0
Average	36.0	37.7	37.0	35.6	34.3	31.1
Stdev	0.2	0.5	0.7	1.0	1.3	1.9
%CV	0.6	1.4	1.8	2.8	3.9	6.0

Table B.13.1

Phase angle, δ (degrees), test results for 116-3 at -10ºC

	25Hz	10Hz	5Hz	1Hz	0.5Hz	0.1Hz
Sample-1	0.2	2.2	2.6	3.8	4.3	5.6
Sample-2	0.4	2.1	2.8	4.2	4.6	6.2
Sample-3	0.4	2.0	2.8	4.0	4.5	5.9
Average	0.3	2.1	2.7	4.0	4.5	5.9
Stdev	0.1	0.1	0.1	0.2	0.2	0.3
%CV	41.9	4.5	3.2	3.9	3.5	4.7

Table B.13.2

Phase angle, δ (degrees), test results for 116-3 at 4.4ºC

	25Hz	10Hz	5Hz	1Hz	0.5Hz	0.1Hz
Sample-1	7.8	9.0	9.9	12.2	13.4	16.4
Sample-2	7.8	8.9	9.8	12.2	13.2	16.2
Sample-3	6.3	7.6	8.4	10.6	11.6	14.4
Average	7.3	8.5	9.4	11.7	12.7	15.7
Stdev	0.9	0.8	0.9	1.0	1.0	1.1
%CV	11.8	9.2	9.2	8.2	7.9	7.0

Table B.13.3

Phase angle, δ (degrees), test results for 116-3 at 25ºC

	25Hz	10Hz	5Hz	1Hz	0.5Hz	0.1Hz
Sample-1	20.4	22.8	24.4	28.3	29.3	31.8
Sample-2	19.3	21.4	23.0	26.7	27.7	30.4
Sample-3	19.0	20.8	21.9	25.2	26.2	29.0
Average	19.5	21.7	23.1	26.7	27.7	30.4
Stdev	0.8	1.0	1.3	1.5	1.5	1.4
%CV	3.9	4.7	5.4	5.8	5.6	4.6

Table B.13.4

Phase angle, δ (degrees), test results for 116-3 at 37.8ºC

	25Hz	10Hz	5Hz	1Hz	0.5Hz	0.1Hz
Sample-1	29.1	30.9	31.6	33.3	33.3	33.1
Sample-2	27.4	29.3	30.3	32.4	32.5	32.7
Sample-3	27.0	28.9	29.8	32.2	32.6	34.0
Average	27.8	29.7	30.6	32.6	32.8	33.3
Stdev	1.1	1.1	0.9	0.6	0.4	0.6
%CV	3.9	3.6	3.1	1.8	1.3	1.9

Table B.13.5

Phase angle, δ (degrees), test results for 116-3 at 54.4ºC

	25Hz	10Hz	5Hz	1Hz	0.5Hz	0.1Hz
Sample-1	35.3	37.1	36.3	33.6	31.8	27.4
Sample-2	34.4	36.6	36.1	34.0	32.5	28.6
Sample-3	34.4	36.2	35.6	34.7	33.5	30.8
Average	34.7	36.6	36.0	34.1	32.6	28.9
Stdev	0.5	0.5	0.4	0.6	0.9	1.7
%CV	1.5	1.3	1.0	1.6	2.6	6.0

Table B.14.1

Phase angle, δ (degrees), test results for 116-4 at -10ºC

	25Hz	10Hz	5Hz	1Hz	0.5Hz	0.1Hz
Sample-1	0.5	1.9	2.2	3.2	3.7	4.8
Sample-2	0.3	2.4	3.0	4.2	4.8	6.3
Sample-3	0.6	1.5	2.0	2.9	3.3	4.3
Average	0.5	1.9	2.4	3.5	3.9	5.1
Stdev	0.2	0.5	0.5	0.7	0.8	1.0
%CV	32.8	23.6	22.4	19.8	20.0	20.1

Table B.14.2

Phase angle, δ (degrees), test results for 116-4 at 4.4ºC

	25Hz	10Hz	5Hz	1Hz	0.5Hz	0.1Hz
Sample-1	7.2	8.5	9.8	12.2	13.4	16.5
Sample-2	7.3	8.5	9.4	11.7	12.8	15.8
Sample-3	7.5	8.9	9.9	12.5	13.7	17.1
Average	7.3	8.6	9.7	12.1	13.3	16.5
Stdev	0.2	0.2	0.3	0.4	0.5	0.6
%CV	2.4	2.5	2.9	3.1	3.5	3.8

Table B.14.3

Phase angle, δ (degrees), test results for 116-4 at 25ºC

	25Hz	10Hz	5Hz	1Hz	0.5Hz	0.1Hz
Sample-1	20.3	22.6	24.1	28.0	29.1	32.0
Sample-2	19.9	21.9	23.3	26.9	28.0	30.6
Sample-3	20.1	22.3	23.7	27.3	28.2	30.4
Average	20.1	22.2	23.7	27.4	28.4	31.0
Stdev	0.2	0.3	0.4	0.5	0.6	0.9
%CV	1.0	1.5	1.7	2.0	2.2	2.9

Table B.14.4

Phase angle, δ (degrees), test results for 116-4 at 37.8ºC

	25Hz	10Hz	5Hz	1Hz	0.5Hz	0.1Hz
Sample-1	30.0	32.0	33.1	35.2	35.1	35.2
Sample-2	29.1	30.9	31.8	33.5	33.2	32.8
Sample-3	28.6	30.6	31.4	33.0	32.8	32.3
Average	29.2	31.2	32.1	33.9	33.7	33.4
Stdev	0.7	0.8	0.9	1.1	1.2	1.5
%CV	2.3	2.5	2.8	3.3	3.6	4.6

Table B.14.5

Phase angle, δ (degrees), test results for 116-4 at 54.4ºC

	25Hz	10Hz	5Hz	1Hz	0.5Hz	0.1Hz
Sample-1	36.0	38.3	37.4	34.8	32.9	29.0
Sample-2	35.5	37.0	36.2	34.2	32.5	29.0
Sample-3	35.1	36.4	35.3	33.2	31.6	28.1
Average	35.5	37.2	36.3	34.0	32.3	28.7
Stdev	0.4	0.9	1.1	0.8	0.6	0.5
%CV	1.2	2.5	2.9	2.4	2.0	1.7

Table B.15.1

Phase angle, δ (degrees), test results for 190-1 at -10ºC

	25Hz	10Hz	5Hz	1Hz	0.5Hz	0.1Hz
Sample-22	1.5	2.5	3.5	4.9	5.4	6.8
Sample-28	1.4	2.6	3.6	5.0	5.4	6.8
Sample-33	1.7	2.8	3.7	5.0	5.4	6.9
Average	1.5	2.6	3.6	5.0	5.4	6.8
Stdev	0.1	0.2	0.1	0.1	0.0	0.1
%CV	8.0	7.1	2.4	1.0	0.2	0.9

Table B.15.2

Phase angle, δ (degrees), test results for 190-1 at 4.4ºC

	25Hz	10Hz	5Hz	1Hz	0.5Hz	0.1Hz
Sample-22	3.5	6.4	7.8	10.6	11.8	15.0
Sample-28	3.4	6.0	7.2	9.7	10.7	13.6
Sample-33	2.6	6.0	7.3	9.8	10.9	13.7
Average	3.2	6.1	7.4	10.0	11.1	14.1
Stdev	0.5	0.2	0.3	0.5	0.6	0.8
%CV	16.2	3.6	4.4	4.9	5.1	5.7

Table B.15.3

Phase angle, δ (degrees), test results for 190-1 at 25ºC

	25Hz	10Hz	5Hz	1Hz	0.5Hz	0.1Hz
Sample-22	15.0	18.5	20.9	26.8	29.2	30.4
Sample-28	13.6	17.0	19.2	24.0	25.9	28.2
Sample-33	13.9	17.8	20.1	25.1	27.0	28.9
Average	14.2	17.8	20.1	25.3	27.4	29.2
Stdev	0.7	0.8	0.9	1.4	1.7	1.1
%CV	5.2	4.4	4.4	5.6	6.2	3.9

Table B.15.4

Phase angle, δ (degrees), test results for 190-1 at 37.8ºC

	25Hz	10Hz	5Hz	1Hz	0.5Hz	0.1Hz
Sample-22	27.4	30.0	31.8	33.4	30.9	25.8
Sample-28	25.2	27.9	29.0	31.8	30.0	25.8
Sample-33	25.4	28.2	29.1	31.6	29.3	25.6
Average	26.0	28.7	30.0	32.2	30.0	25.8
Stdev	1.2	1.2	1.6	1.0	0.8	0.1
%CV	4.5	4.1	5.3	3.1	2.6	0.4

Table B.15.5

Phase angle, δ (degrees), test results for 190-1 at 54.4ºC

	25Hz	10Hz	5Hz	1Hz	0.5Hz	0.1Hz
Sample-22	30.6	28.2	26.3	22.6	20.5	15.6
Sample-28	28.7	27.6	26.3	22.3	20.7	15.4
Sample-33	31.2	31.0	29.9	24.3	22.7	18.4
Average	30.2	28.9	27.5	23.0	21.3	16.4
Stdev	1.3	1.8	2.1	1.1	1.2	1.7
%CV	4.3	6.2	7.7	4.9	5.7	10.3

Table B.16.1

Phase angle, δ (degrees), test results for 190-2 at -10ºC

	25Hz	10Hz	5Hz	1Hz	0.5Hz	0.1Hz
Sample-2	2.0	3.1	4.0	5.4	6.0	7.4
Sample-4	1.5	2.3	3.1	4.2	4.6	5.5
Sample-11	1.9	2.9	3.8	5.2	5.6	6.8
Average	1.8	2.8	3.6	4.9	5.4	6.6
Stdev	0.2	0.4	0.5	0.6	0.7	1.0
%CV	13.7	15.1	13.3	12.7	13.8	15.1

Table B.16.2

Phase angle, δ (degrees), test results for 190-2 at 4.4ºC

	25Hz	10Hz	5Hz	1Hz	0.5Hz	0.1Hz
Sample-2	4.2	6.7	8.0	10.6	11.7	14.8
Sample-4	2.8	5.3	6.3	8.1	8.8	10.8
Sample-11	2.3	6.3	7.4	9.8	10.8	13.7
Average	3.1	6.1	7.2	9.5	10.4	13.1
Stdev	1.0	0.7	0.9	1.3	1.5	2.0
%CV	31.2	12.2	12.4	13.8	14.3	15.6

Table B.16.3

Phase angle, δ (degrees), test results for 190-2 at 25ºC

	25Hz	10Hz	5Hz	1Hz	0.5Hz	0.1Hz
Sample-2	14.2	17.7	19.8	25.1	27.0	29.4
Sample-4	10.7	13.8	15.5	19.9	21.6	24.3
Sample-11	12.8	16.7	18.9	24.1	25.9	28.5
Average	12.5	16.1	18.1	23.1	24.9	27.4
Stdev	1.8	2.0	2.2	2.8	2.9	2.7
%CV	14.2	12.6	12.5	11.9	11.6	9.8

Table B.16.4

Phase angle, δ (degrees), test results for 190-2 at 37.8ºC

	25Hz	10Hz	5Hz	1Hz	0.5Hz	0.1Hz
Sample-2	25.9	29.1	30.2	30.6	30.0	24.9
Sample-4	19.7	22.8	24.2	27.7	28.4	28.2
Sample-11	23.9	27.1	28.6	31.1	30.9	27.4
Average	23.2	26.3	27.7	29.8	29.8	26.8
Stdev	3.2	3.2	3.1	1.8	1.3	1.7
%CV	13.8	12.2	11.3	6.2	4.2	6.4

Table B.16.5

Phase angle, δ (degrees), test results for 190-2 at 54.4ºC

	25Hz	10Hz	5Hz	1Hz	0.5Hz	0.1Hz
Sample-2	30.5	30.2	28.7	24.0	21.7	16.0
Sample-4	26.6	27.9	28.2	28.0	27.4	23.3
Sample-11	29.1	29.6	28.7	24.9	23.3	17.9
Average	28.7	29.2	28.5	25.7	24.2	19.1
Stdev	2.0	1.2	0.3	2.1	2.9	3.8
%CV	6.8	4.1	1.0	8.1	12.1	19.8

Table B.17.1

Phase angle, δ (degrees), test results for 190-3 at -10ºC

	25Hz	10Hz	5Hz	1Hz	0.5Hz	0.1Hz
Sample-28	1.5	2.4	3.3	4.6	5.0	6.1
Sample-29	1.9	3.0	3.8	5.1	5.5	6.8
Sample-30	1.6	2.5	3.4	4.7	5.2	6.3
Average	1.7	2.6	3.5	4.8	5.2	6.4
Stdev	0.2	0.3	0.2	0.3	0.3	0.3
%CV	12.4	11.3	6.6	5.6	5.0	5.3

Table B.17.2

Phase angle, δ (degrees), test results for 190-3 at 4.4ºC

	25Hz	10Hz	5Hz	1Hz	0.5Hz	0.1Hz
Sample-28	3.5	5.9	7.0	9.1	10.0	12.4
Sample-29	2.8	5.7	6.8	8.8	9.7	12.0
Sample-30	3.5	6.1	7.2	9.4	10.4	13.0
Average	3.3	5.9	7.0	9.1	10.0	12.5
Stdev	0.4	0.2	0.2	0.3	0.4	0.5
%CV	12.7	3.2	2.7	3.5	3.5	4.0

Table B.17.3

Phase angle, δ (degrees), test results for 190-3 at 25ºC

	25Hz	10Hz	5Hz	1Hz	0.5Hz	0.1Hz
Sample-28	6.9	14.7	17.0	21.3	23.4	26.3
Sample-29	12.3	15.1	17.2	21.6	23.4	25.6
Sample-30	13.2	16.6	18.6	23.3	25.3	27.7
Average	10.8	15.5	17.6	22.1	24.0	26.5
Stdev	3.4	1.0	0.8	1.1	1.1	1.0
%CV	31.5	6.5	4.8	4.9	4.7	3.9

Table B.17.4

Phase angle, δ (degrees), test results for 190-3 at 37.8ºC

	25Hz	10Hz	5Hz	1Hz	0.5Hz	0.1Hz
Sample-28	21.5	24.6	26.2	28.5	29.4	26.7
Sample-29	21.9	24.8	26.3	28.9	28.4	25.4
Sample-30	23.8	27.0	28.5	30.2	30.2	25.9
Average	22.4	25.4	27.0	29.2	29.4	26.0
Stdev	1.2	1.3	1.3	0.9	0.9	0.7
%CV	5.5	5.2	4.8	3.0	3.1	2.6

Table B.17.5

Phase angle, δ (degrees), test results for 190-3 at 54.4ºC

	25Hz	10Hz	5Hz	1Hz	0.5Hz	0.1Hz
Sample-28	27.6	28.0	27.9	26.1	24.5	19.7
Sample-29	27.8	28.4	28.1	25.4	23.0	18.4
Sample-30	29.9	28.6	27.7	23.3	21.3	16.4
Average	28.4	28.4	27.9	24.9	22.9	18.2
Stdev	1.2	0.3	0.2	1.5	1.6	1.7
%CV	4.4	1.0	0.6	6.0	6.9	9.2

Table B.18.1

Phase angle, δ (degrees), test results for 190-4 at -10ºC

	25Hz	10Hz	5Hz	1Hz	0.5Hz	0.1Hz
Sample-1	2.3	4.0	4.9	6.5	7.1	8.8
Sample-3	1.9	3.4	4.4	6.0	6.6	8.5
Sample-4	2.1	3.5	4.5	6.3	7.0	9.1
Average	2.1	3.6	4.6	6.2	6.9	8.8
Stdev	0.2	0.3	0.3	0.2	0.3	0.3
%CV	8.7	8.7	6.6	3.8	3.7	3.8

Table B.18.2

Phase angle, δ (degrees), test results for 190-4 at 4.4ºC

	25Hz	10Hz	5Hz	1Hz	0.5Hz	0.1Hz
Sample-1	5.7	9.4	11.5	15.5	17.3	21.4
Sample-3	5.9	9.5	11.2	15.0	16.7	20.6
Sample-4	6.3	9.2	10.8	14.7	16.7	21.0
Average	5.9	9.4	11.2	15.1	16.9	21.0
Stdev	0.3	0.2	0.4	0.4	0.4	0.4
%CV	5.1	1.6	3.1	2.6	2.1	1.9

Table B.18.3

Phase angle, δ (degrees), test results for 190-4 at 25ºC

	25Hz	10Hz	5Hz	1Hz	0.5Hz	0.1Hz
Sample-1	20.7	24.5	27.0	32.8	34.0	32.5
Sample-3	21.4	24.9	27.1	32.5	33.2	31.0
Sample-4	21.8	25.3	28.0	33.3	34.0	31.6
Average	21.3	24.9	27.3	32.9	33.7	31.7
Stdev	0.5	0.4	0.5	0.4	0.5	0.8
%CV	2.6	1.7	2.0	1.3	1.4	2.4

Table B.18.4

Phase angle, δ (degrees), test results for 190-4 at 37.8ºC

	25Hz	10Hz	5Hz	1Hz	0.5Hz	0.1Hz
Sample-1	29.5	31.7	32.1	31.9	30.3	24.3
Sample-3	29.0	30.7	30.5	29.6	28.0	21.9
Sample-4	29.5	31.8	31.7	30.4	28.5	22.7
Average	29.3	31.4	31.4	30.6	29.0	23.0
Stdev	0.3	0.6	0.8	1.2	1.2	1.2
%CV	1.0	1.8	2.6	3.8	4.3	5.2

Table B.18.5

Phase angle, δ (degrees), test results for 190-4 at 54.4ºC

	25Hz	10Hz	5Hz	1Hz	0.5Hz	0.1Hz
Sample-1	29.8	27.8	25.7	21.5	19.5	14.9
Sample-3	28.1	25.9	23.8	19.4	17.2	12.9
Sample-4	29.5	27.7	25.7	21.4	19.1	15.2
Average	29.1	27.1	25.1	20.8	18.6	14.3
Stdev	0.9	1.1	1.1	1.2	1.2	1.3
%CV	3.2	3.9	4.3	5.8	6.6	8.9

Table B.19.1

Phase angle, δ (degrees), test results for ALF-1 at -10ºC

	25Hz	10Hz	5Hz	1Hz	0.5Hz	0.1Hz
Sample-1	1.5	2.7	3.6	4.9	5.4	6.7
Sample-4	1.8	2.9	3.8	5.0	5.5	6.7
Sample-8	1.7	2.9	3.8	5.1	5.6	6.8
Average	1.7	2.8	3.7	5.0	5.5	6.8
Stdev	0.2	0.1	0.1	0.1	0.1	0.0
%CV	9.2	2.8	2.4	1.5	1.8	0.6

Table B.19.2

Phase angle, δ (degrees), test results for ALF-1 at 4.4ºC

	25Hz	10Hz	5Hz	1Hz	0.5Hz	0.1Hz
Sample-1	1.9	6.8	8.1	10.8	12.1	15.5
Sample-4	4.3	6.7	7.9	10.1	11.2	14.0
Sample-8	2.6	6.6	7.8	10.3	11.3	14.3
Average	2.9	6.7	7.9	10.4	11.5	14.6
Stdev	1.2	0.1	0.2	0.3	0.5	0.8
%CV	42.6	1.5	1.9	3.3	4.2	5.5

Table B.19.3

Phase angle, δ (degrees), test results for ALF-1 at 25ºC

	25Hz	10Hz	5Hz	1Hz	0.5Hz	0.1Hz
Sample-1	15.5	20.0	22.5	28.4	30.2	32.0
Sample-4	14.1	17.8	20.2	25.7	27.5	30.2
Sample-8	15.4	18.7	20.9	26.3	27.8	29.8
Average	15.0	18.8	21.2	26.8	28.5	30.6
Stdev	0.8	1.1	1.2	1.4	1.5	1.2
%CV	5.1	5.9	5.6	5.2	5.1	3.8

Table B.19.4

Phase angle, δ (degrees), test results for ALF-1 at 37.8ºC

	25Hz	10Hz	5Hz	1Hz	0.5Hz	0.1Hz
Sample-1	29.4	31.9	34.0	33.3	31.9	26.0
Sample-4	25.5	28.1	29.1	30.1	29.6	26.1
Sample-8	26.6	29.1	29.9	29.9	29.0	24.6
Average	27.1	29.7	31.0	31.1	30.2	25.5
Stdev	2.0	2.0	2.6	1.9	1.5	0.8
%CV	7.4	6.7	8.5	6.3	5.0	3.2

Table B.19.5

Phase angle, δ (degrees), test results for ALF-1 at 54.4ºC

	25Hz	10Hz	5Hz	1Hz	0.5Hz	0.1Hz
Sample-1	31.7	30.3	28.2	22.0	19.6	14.6
Sample-4	29.1	28.6	27.1	22.8	20.7	16.1
Sample-8	29.5	27.9	26.3	21.4	19.5	14.8
Average	30.1	28.9	27.2	22.1	19.9	15.2
Stdev	1.4	1.3	0.9	0.7	0.7	0.8
%CV	4.7	4.4	3.4	3.2	3.4	5.4

Table B.20.1

Phase angle, δ (degrees), test results for LA1-1 at -10ºC

	25Hz	10Hz	5Hz	1Hz	0.5Hz	0.1Hz
Sample-7	1.8	2.9	3.8	5.1	5.9	7.1
Sample-8	2.4	3.6	4.6	6.2	6.6	7.9
Sample-9	1.4	2.6	3.2	4.6	5.1	6.2
Average	1.9	3.0	3.9	5.3	5.9	7.1
Stdev	0.5	0.5	0.7	0.8	0.8	0.9
%CV	27.0	16.9	18.2	15.4	12.8	12.0

Table B.20.2

Phase angle, δ (degrees), test results for LA1-1 at 4.4ºC

	25Hz	10Hz	5Hz	1Hz	0.5Hz	0.1Hz
Sample-7	2.4	8.2	9.5	12.3	13.4	16.4
Sample-8	3.3	6.1	9.2	12.0	12.9	16.1
Sample-9	1.8	6.9	8.4	11.2	12.5	15.4
Average	2.5	7.1	9.0	11.8	12.9	16.0
Stdev	0.8	1.1	0.6	0.5	0.5	0.5
%CV	31.3	15.0	6.4	4.5	3.7	3.3

Table B.20.3

Phase angle, δ (degrees), test results for LA1-1 at 25ºC

	25Hz	10Hz	5Hz	1Hz	0.5Hz	0.1Hz
Sample-7	16.7	19.8	22.0	26.8	28.5	29.6
Sample-8	19.2	22.3	24.9	30.6	32.2	33.4
Sample-9	15.8	18.8	20.9	26.0	27.7	29.3
Average	17.3	20.3	22.6	27.8	29.4	30.8
Stdev	1.8	1.8	2.1	2.4	2.4	2.3
%CV	10.2	9.0	9.1	8.8	8.3	7.3

Table B.20.4

Phase angle, δ (degrees), test results for LA1-1 at 37.8ºC

	25Hz	10Hz	5Hz	1Hz	0.5Hz	0.1Hz
Sample-7	24.5	27.0	28.5	29.6	29.7	25.9
Sample-8	25.5	28.2	29.5	30.3	30.3	25.7
Sample-9	23.9	26.9	28.4	30.5	31.0	26.7
Average	24.6	27.4	28.8	30.1	30.3	26.1
Stdev	0.8	0.7	0.7	0.5	0.7	0.5
%CV	3.3	2.7	2.3	1.6	2.2	2.0

Table B.20.5

Phase angle, δ (degrees), test results for LA1-1 at 54.4ºC

	25Hz	10Hz	5Hz	1Hz	0.5Hz	0.1Hz
Sample-7	29.7	29.0	28.3	25.1	23.1	19.3
Sample-8	28.7	28.6	27.4	23.9	21.9	16.8
Sample-9	30.3	28.8	28.2	24.6	22.6	17.7
Average	29.5	28.8	28.0	24.5	22.5	17.9
Stdev	0.8	0.2	0.5	0.6	0.6	1.3
%CV	2.8	0.7	1.8	2.4	2.6	7.0

Table B.21.1

Phase angle, δ (degrees), test results for LA1-2 at -10ºC

	25Hz	10Hz	5Hz	1Hz	0.5Hz	0.1Hz
Sample-8	1.5	2.1	3.3	4.4	5.0	6.4
Sample-9	2.2	3.9	4.6	6.4	6.8	7.9
Sample-12	1.9	2.9	3.9	5.1	5.6	6.9
Average	1.9	3.0	3.9	5.3	5.8	7.1
Stdev	0.4	0.9	0.7	1.0	0.9	0.8
%CV	18.8	30.4	16.5	19.1	15.8	10.8

Table B.21.2

Phase angle, δ (degrees), test results for LA1-2 at 4.4ºC

	25Hz	10Hz	5Hz	1Hz	0.5Hz	0.1Hz
Sample-8	1.1	9.0	10.3	12.9	14.0	16.6
Sample-9	3.3	7.2	8.3	10.4	11.3	13.6
Sample-12	1.9	8.7	10.0	12.7	13.9	16.5
Average	2.1	8.3	9.5	12.0	13.0	15.6
Stdev	1.1	1.0	1.0	1.4	1.5	1.7
%CV	53.9	11.6	10.9	11.5	11.6	11.0

Table B.21.3

Phase angle, δ (degrees), test results for LA1-2 at 25ºC

	25Hz	10Hz	5Hz	1Hz	0.5Hz	0.1Hz
Sample-8	16.5	19.2	21.2	25.3	26.8	28.1
Sample-9	16.2	19.9	22.0	26.8	28.4	29.7
Sample-12	14.3	19.8	21.9	26.6	28.1	28.9
Average	15.6	19.6	21.7	26.2	27.7	28.9
Stdev	1.2	0.4	0.5	0.8	0.9	0.8
%CV	7.7	2.1	2.2	3.1	3.1	2.9

Table B.21.4

Phase angle, δ (degrees), test results for LA1-2 at 37.8ºC

	25Hz	10Hz	5Hz	1Hz	0.5Hz	0.1Hz
Sample-8	23.7	26.1	27.5	29.7	29.8	27.1
Sample-9	22.8	25.2	26.5	28.4	29.2	26.8
Sample-12	24.5	27.1	28.0	28.4	28.2	24.2
Average	23.6	26.1	27.3	28.9	29.1	26.0
Stdev	0.8	1.0	0.8	0.7	0.8	1.6
%CV	3.5	3.8	2.8	2.6	2.8	6.0

Table B.21.5

Phase angle, δ (degrees), test results for LA1-2 at 54.4ºC

	25Hz	10Hz	5Hz	1Hz	0.5Hz	0.1Hz
Sample-8	26.8	26.4	25.7	23.3	21.9	17.8
Sample-9	25.8	25.2	24.2	22.3	20.8	17.4
Sample-12	26.0	25.3	24.1	21.0	19.3	15.3
Average	26.2	25.6	24.7	22.2	20.7	16.8
Stdev	0.6	0.7	0.9	1.2	1.3	1.4
%CV	2.2	2.6	3.7	5.3	6.2	8.2

Table B.22.1

Phase angle, δ (degrees), test results for I10-1 at -10ºC

	25Hz	10Hz	5Hz	1Hz	0.5Hz	0.1Hz
Sample-4	6.0	6.4	6.3	6.7	6.8	7.9
Sample-6	2.7	4.5	5.2	7.0	7.9	9.9
Sample-12	2.2	3.6	4.5	6.0	6.6	8.1
Average	3.6	4.8	5.3	6.6	7.1	8.7
Stdev	2.1	1.5	0.9	0.6	0.7	1.1
%CV	58.2	30.4	16.9	8.5	10.5	12.8

Table B.22.2

Phase angle, δ (degrees), test results for I10-1 at 4.4ºC

	25Hz	10Hz	5Hz	1Hz	0.5Hz	0.1Hz
Sample-4	5.8	8.3	9.5	12.0	13.4	17.4
Sample-6	6.4	9.6	11.3	14.5	16.0	19.2
Sample-12	5.6	7.9	9.1	12.7	13.6	17.4
Average	5.9	8.6	10.0	13.0	14.3	18.0
Stdev	0.4	0.9	1.1	1.3	1.5	1.0
%CV	7.3	10.4	11.4	9.8	10.2	5.7

Table B.22.3

Phase angle, δ (degrees), test results for I10-1 at 25ºC

	25Hz	10Hz	5Hz	1Hz	0.5Hz	0.1Hz
Sample-4	19.3	22.8	24.8	30.7	31.5	31.8
Sample-6	19.1	22.9	24.8	30.2	30.4	30.1
Sample-12	18.8	22.5	24.4	30.1	31.7	31.4
Average	19.1	22.7	24.7	30.3	31.2	31.1
Stdev	0.3	0.2	0.2	0.3	0.7	0.9
%CV	1.5	1.0	0.9	1.1	2.1	2.8

Table B.22.4

Phase angle, δ (degrees), test results for I10-1 at 37.8ºC

	25Hz	10Hz	5Hz	1Hz	0.5Hz	0.1Hz
Sample-4	28.7	31.4	32.2	31.6	30.1	25.2
Sample-6	26.7	29.0	29.3	29.1	28.1	23.6
Sample-12	27.9	29.9	29.8	29.1	27.6	23.0
Average	27.8	30.1	30.4	29.9	28.6	23.9
Stdev	1.0	1.2	1.6	1.5	1.3	1.2
%CV	3.5	4.1	5.2	4.9	4.7	4.9

Table B.22.5

Phase angle, δ (degrees), test results for I10-1 at 54.4ºC

	25Hz	10Hz	5Hz	1Hz	0.5Hz	0.1Hz
Sample-4	28.4	26.6	25.1	22.6	20.5	16.7
Sample-6	30.5	28.5	26.3	22.0	19.4	15.1
Sample-12	28.3	26.7	25.5	21.1	19.1	13.7
Average	29.0	27.3	25.6	21.9	19.7	15.2
Stdev	1.2	1.1	0.6	0.7	0.8	1.5
%CV	4.2	3.9	2.3	3.3	3.9	9.7

Table B.23.1

Phase angle, δ (degrees), test results for I10-2 at -10ºC

	25Hz	10Hz	5Hz	1Hz	0.5Hz	0.1Hz
Sample-2	3.6	5.6	7.1	8.4	9.0	10.6
Sample-7	4.7	7.2	7.6	8.8	9.1	11.1
Sample-8	3.8	5.7	6.6	7.7	8.3	9.6
Average	4.1	6.2	7.1	8.3	8.8	10.4
Stdev	0.6	0.9	0.5	0.6	0.4	0.8
%CV	14.4	14.2	7.5	6.7	4.9	7.4

Table B.23.2

Phase angle, δ (degrees), test results for I10-2 at 4.4ºC

	25Hz	10Hz	5Hz	1Hz	0.5Hz	0.1Hz
Sample-2	6.2	8.8	10.3	13.3	15.3	17.7
Sample-7	6.8	9.1	10.7	13.5	14.6	17.6
Sample-8	6.1	8.9	10.2	13.1	14.2	16.9
Average	6.4	9.0	10.4	13.3	14.7	17.4
Stdev	0.4	0.1	0.2	0.2	0.6	0.4
%CV	5.6	1.7	2.4	1.2	3.8	2.4

Table B.23.3

Phase angle, δ (degrees), test results for I10-2 at 25ºC

	25Hz	10Hz	5Hz	1Hz	0.5Hz	0.1Hz
Sample-2	18.9	23.1	24.4	29.5	32.9	35.4
Sample-7	18.4	22.1	23.5	29.1	30.7	31.8
Sample-8	17.9	21.5	23.1	29.1	30.0	32.0
Average	18.4	22.2	23.7	29.2	31.2	33.1
Stdev	0.5	0.8	0.7	0.2	1.5	2.0
%CV	2.6	3.6	2.8	0.7	4.7	6.1

Table B.23.4

Phase angle, δ (degrees), test results for I10-2 at 37.8ºC

	25Hz	10Hz	5Hz	1Hz	0.5Hz	0.1Hz
Sample-2	27.2	31.3	30.9	33.7	35.2	36.7
Sample-7	25.9	28.1	28.6	31.4	32.8	29.3
Sample-8	25.6	28.0	29.3	30.9	31.3	21.1
Average	26.2	29.1	29.6	32.0	33.1	29.0
Stdev	0.9	1.9	1.2	1.5	2.0	7.8
%CV	3.3	6.5	4.0	4.7	6.0	26.9

Table B.23.5

Phase angle, δ (degrees), test results for I10-2 at 54.4ºC

	25Hz	10Hz	5Hz	1Hz	0.5Hz	0.1Hz
Sample-2	33.9	32.9	31.3	28.7	27.6	24.0
Sample-7	31.2	30.3	29.9	28.4	28.5	25.5
Sample-8	30.0	28.8	27.8	26.7	25.7	22.3
Average	31.7	30.6	29.7	27.9	27.2	24.0
Stdev	2.0	2.1	1.7	1.1	1.4	1.6
%CV	6.3	6.7	5.8	3.9	5.1	6.6

Table B.24.1

Phase angle, δ (degrees), test results for I55-1 at -10ºC

	25Hz	10Hz	5Hz	1Hz	0.5Hz	0.1Hz
Sample-5	0.6	2.8	3.7	5.1	5.7	7.0
Sample-8	1.0	3.3	4.3	5.8	6.5	7.7
Sample-4	1.8	4.3	5.2	6.7	7.3	8.5
Average	1.1	3.5	4.4	5.9	6.5	7.7
Stdev	53.2	22.1	17.1	13.3	11.9	9.6
%CV	0.6	2.8	3.7	5.1	5.7	7.0

Table B.24.2

Phase angle, δ (degrees), test results for I55-1 at 4.4ºC

	25Hz	10Hz	5Hz	1Hz	0.5Hz	0.1Hz
Sample-5	7.1	8.2	8.9	10.8	11.7	13.9
Sample-8	7.3	8.4	9.1	11.0	11.9	14.4
Sample-4	7.0	7.8	8.3	10.0	10.9	13.3
Average	7.2	8.1	8.8	10.6	11.5	13.9
Stdev	2.2	4.0	4.8	5.0	4.5	4.2
%CV	7.1	8.2	8.9	10.8	11.7	13.9

Table B.24.3

Phase angle, δ (degrees), test results for I55-1 at 25ºC

	25Hz	10Hz	5Hz	1Hz	0.5Hz	0.1Hz
Sample-5	16.8	18.4	19.6	22.4	23.4	25.9
Sample-8	19.9	21.7	22.8	25.6	26.2	28.2
Sample-4	17.0	18.9	20.2	23.6	24.5	27.3
Average	17.9	19.7	20.8	23.9	24.7	27.1
Stdev	10.0	9.1	8.1	6.8	5.8	4.3
%CV	16.8	18.4	19.6	22.4	23.4	25.9

Table B.24.4

Phase angle, δ (degrees), test results for I55-1 at 37.8ºC

	25Hz	10Hz	5Hz	1Hz	0.5Hz	0.1Hz
Sample-5	25.0	26.7	27.6	29.5	29.5	29.9
Sample-8	25.5	27.3	28.1	30.0	30.0	30.4
Sample-4	24.0	25.9	26.9	29.0	29.4	30.4
Average	24.8	26.6	27.5	29.5	29.6	30.2
Stdev	3.1	2.6	2.2	1.6	1.0	1.0
%CV	25.0	26.7	27.6	29.5	29.5	29.9

Table B.24.5

Phase angle, δ (degrees), test results for I55-1 at 54.4ºC

	25Hz	10Hz	5Hz	1Hz	0.5Hz	0.1Hz
Sample-5	31.9	33.4	32.7	31.6	30.7	29.2
Sample-8	31.6	33.2	32.7	31.7	30.8	28.7
Sample-4	32.6	34.1	33.6	32.6	31.4	29.0
Average	32.0	33.6	33.0	32.0	31.0	29.0
Stdev	1.7	1.5	1.7	1.6	1.2	0.7
%CV	31.9	33.4	32.7	31.6	30.7	29.2

Table B.25.1

Phase angle, δ (degrees), test results for I55-2 at -10ºC

	25Hz	10Hz	5Hz	1Hz	0.5Hz	0.1Hz
Sample-1	1.2	3.0	4.0	5.3	5.8	7.1
Sample-2	1.5	3.5	4.5	5.9	6.4	7.7
Sample-3	1.3	3.2	4.2	5.6	6.1	7.5
Average	1.3	3.3	4.2	5.6	6.1	7.4
Stdev	9.1	7.7	5.6	5.4	4.8	4.5
%CV	1.2	3.0	4.0	5.3	5.8	7.1

Table B.25.2

Phase angle, δ (degrees), test results for I55-2 at 4.4ºC

	25Hz	10Hz	5Hz	1Hz	0.5Hz	0.1Hz
Sample-1	7.1	8.1	9.1	11.4	12.5	15.5
Sample-2	7.7	8.9	9.6	11.8	12.8	15.5
Sample-3	7.5	8.5	9.3	11.3	12.2	14.8
Average	7.4	8.5	9.3	11.5	12.5	15.3
Stdev	3.9	4.6	2.6	2.4	2.4	2.6
%CV	7.1	8.1	9.1	11.4	12.5	15.5

Table B.25.3

Phase angle, δ (degrees), test results for I55-2 at 25ºC

	25Hz	10Hz	5Hz	1Hz	0.5Hz	0.1Hz
Sample-1	18.0	20.2	21.7	25.6	26.7	29.9
Sample-2	16.7	18.7	20.0	23.5	24.7	27.9
Sample-3	16.2	18.4	19.9	23.6	24.8	28.0
Average	17.0	19.1	20.5	24.2	25.4	28.6
Stdev	5.4	5.1	5.0	4.8	4.5	4.0
%CV	18.0	20.2	21.7	25.6	26.7	29.9

Table B.25.4

Phase angle, δ (degrees), test results for I55-2 at 37.8ºC

	25Hz	10Hz	5Hz	1Hz	0.5Hz	0.1Hz
Sample-1	28.5	30.5	31.6	34.1	34.1	34.7
Sample-2	28.0	30.1	31.1	33.6	33.5	34.2
Sample-3	27.1	28.9	29.7	31.6	31.5	31.7
Average	27.9	29.9	30.8	33.1	33.0	33.5
Stdev	2.5	2.8	3.1	3.9	4.0	4.8
%CV	28.5	30.5	31.6	34.1	34.1	34.7

Table B.25.5

Phase angle, δ (degrees), test results for I55-2 at 54.4ºC

	25Hz	10Hz	5Hz	1Hz	0.5Hz	0.1Hz
Sample-1	27.9	28.2	27.3	23.1	20.8	16.2
Sample-2	27.3	27.8	27.3	24.1	22.0	17.2
Sample-3	26.7	26.9	25.6	21.6	19.3	14.9
Average	27.3	27.6	26.7	22.9	20.7	16.1
Stdev	2.2	2.5	3.7	5.4	6.6	7.3
%CV	27.9	28.2	27.3	23.1	20.8	16.2

Table B.26.1

Phase angle, δ (degrees), test results for I10-3 at -10ºC

	25Hz	10Hz	5Hz	1Hz	0.5Hz	0.1Hz
Sample-4	2.9	4.6	5.7	6.8	7.7	8.8
Sample-5	4.0	5.1	5.9	7.4	8.0	9.6
Sample-6	2.4	4.2	5.2	6.6	7.3	8.6
Average	3.1	4.6	5.6	6.9	7.7	9.0
Stdev	0.8	0.4	0.4	0.4	0.3	0.5
%CV	25.7	9.4	6.8	5.9	4.5	5.9

Table B.26.2

Phase angle, δ (degrees), test results for I10-3 at 4.4ºC

	25Hz	10Hz	5Hz	1Hz	0.5Hz	0.1Hz
Sample-4	7.6	9.2	11.0	13.9	14.9	17.8
Sample-5	8.1	10.5	11.9	15.3	16.6	19.9
Sample-6	6.5	9.1	10.5	13.2	14.6	17.1
Average	7.4	9.6	11.1	14.1	15.4	18.3
Stdev	0.8	0.7	0.7	1.1	1.1	1.4
%CV	10.7	7.6	6.1	7.8	7.3	7.8

Table B.26.3

Phase angle, δ (degrees), test results for I10-3 at 25ºC

	25Hz	10Hz	5Hz	1Hz	0.5Hz	0.1Hz
Sample-4	18.9	22.5	24.5	27.1	28.2	29.4
Sample-5	19.5	22.8	25.2	29.7	30.9	30.6
Sample-6	17.8	20.7	23.0	27.2	28.0	28.9
Average	18.7	22.0	24.2	28.0	29.0	29.6
Stdev	0.9	1.1	1.1	1.5	1.6	0.9
%CV	4.8	5.2	4.7	5.2	5.6	3.0

Table B.26.4

Phase angle, δ (degrees), test results for I10-3 at 37.8ºC

	25Hz	10Hz	5Hz	1Hz	0.5Hz	0.1Hz
Sample-4	25.2	27.5	28.3	29.3	27.8	24.8
Sample-5	26.7	28.8	29.0	28.0	26.1	22.4
Sample-6	25.0	27.2	27.9	28.8	27.9	25.3
Average	25.6	27.8	28.4	28.7	27.2	24.2
Stdev	0.9	0.9	0.6	0.6	1.0	1.6
%CV	3.7	3.2	2.1	2.2	3.7	6.5

Table B.26.5

Phase angle, δ (degrees), test results for I10-3 at 54.4ºC

	25Hz	10Hz	5Hz	1Hz	0.5Hz	0.1Hz
Sample-4	30.3	27.3	25.3	23.6	21.5	17.8
Sample-5	28.8	23.0	21.6	17.8	16.5	12.6
Sample-6	28.1	26.7	25.8	24.0	21.1	17.6
Average	29.0	25.7	24.2	21.8	19.7	16.0
Stdev	1.1	2.3	2.3	3.5	2.8	3.0
%CV	3.9	9.1	9.5	15.8	14.3	18.6

Table B.27.1

Phase angle, δ (degrees), test results for 964-1 at -10ºC

	25Hz	10Hz	5Hz	1Hz	0.5Hz	0.1Hz
Sample-3	1.9	3.5	4.5	6.1	6.8	8.4
Sample-4	1.7	3.0	3.9	5.3	5.9	7.3
Sample-6	1.8	3.1	4.2	5.5	5.9	7.3
Average	1.8	3.2	4.2	5.6	6.2	7.7
Stdev	0.1	0.3	0.3	0.4	0.5	0.7
%CV	7.1	8.0	7.4	7.8	8.2	8.6

Table B.27.2

Phase angle, δ (degrees), test results for 964-1 at 4.4ºC

	25Hz	10Hz	5Hz	1Hz	0.5Hz	0.1Hz
Sample-3	4.5	7.4	8.8	11.6	12.8	16.1
Sample-4	4.9	7.6	9.0	11.9	13.1	16.5
Sample-6	4.3	7.0	8.2	10.8	11.8	14.8
Average	4.5	7.3	8.7	11.4	12.6	15.8
Stdev	0.3	0.3	0.4	0.6	0.7	0.9
%CV	7.3	4.3	4.8	5.1	5.2	5.4

Table B.27.3

Phase angle, δ (degrees), test results for 964-1 at 25ºC

	25Hz	10Hz	5Hz	1Hz	0.5Hz	0.1Hz
Sample-3	17.2	20.7	23.1	28.5	30.0	31.0
Sample-4	17.2	20.4	22.8	29.1	30.7	31.8
Sample-6	16.1	19.6	21.8	27.0	28.9	30.1
Average	16.8	20.2	22.6	28.2	29.8	31.0
Stdev	0.7	0.6	0.7	1.1	0.9	0.8
%CV	3.9	2.7	3.1	3.8	3.1	2.6

Table B.27.4

Phase angle, δ (degrees), test results for 964-1 at 37.8ºC

	25Hz	10Hz	5Hz	1Hz	0.5Hz	0.1Hz
Sample-3	27.8	30.5	31.8	32.6	31.0	25.4
Sample-4	26.4	29.0	29.9	30.6	29.5	24.7
Sample-6	25.1	27.6	28.5	29.2	27.7	23.9
Average	26.4	29.0	30.1	30.8	29.4	24.7
Stdev	1.4	1.4	1.6	1.7	1.7	0.7
%CV	5.1	4.9	5.5	5.5	5.6	3.0

Table B.27.5

Phase angle, δ (degrees), test results for 964-1 at 54.4ºC

	25Hz	10Hz	5Hz	1Hz	0.5Hz	0.1Hz
Sample-3	29.7	28.0	26.6	21.5	19.0	15.0
Sample-4	31.2	30.1	28.2	23.6	21.4	16.9
Sample-6	28.3	28.2	26.5	22.9	20.1	15.7
Average	29.7	28.8	27.1	22.7	20.1	15.8
Stdev	1.5	1.2	0.9	1.1	1.2	1.0
%CV	5.0	4.0	3.4	4.8	5.9	6.1

Table B.28.1

Phase angle, δ (degrees), test results for 964-2 at -10ºC

	25Hz	10Hz	5Hz	1Hz	0.5Hz	0.1Hz
Sample-25	1.5	2.4	3.2	4.3	4.7	5.7
Sample-26	1.6	2.1	2.9	3.9	4.3	5.1
Sample-27	1.4	2.4	3.2	4.2	4.4	5.2
Average	1.5	2.3	3.1	4.1	4.5	5.3
Stdev	0.1	0.2	0.2	0.2	0.2	0.3
%CV	8.5	7.3	4.9	4.9	4.8	5.8

Table B.28.2

Phase angle, δ (degrees), test results for 964-2 at 4.4ºC

	25Hz	10Hz	5Hz	1Hz	0.5Hz	0.1Hz
Sample-25	2.4	5.2	6.2	8.0	8.8	11.0
Sample-26	1.5	4.6	5.5	7.2	7.9	10.0
Sample-27	1.1	4.0	4.8	6.2	6.7	8.1
Average	1.6	4.6	5.5	7.1	7.8	9.7
Stdev	0.7	0.6	0.7	0.9	1.0	1.5
%CV	42.1	13.2	12.6	13.1	13.2	15.0

Table B.28.3

Phase angle, δ (degrees), test results for 964-2 at 25ºC

	25Hz	10Hz	5Hz	1Hz	0.5Hz	0.1Hz
Sample-25	11.2	14.4	16.4	21.0	22.9	26.1
Sample-26	8.0	13.5	15.5	20.2	21.9	25.0
Sample-27	8.0	10.7	12.3	15.3	16.7	19.3
Average	9.0	12.9	14.7	18.8	20.5	23.5
Stdev	1.8	1.9	2.2	3.1	3.3	3.6
%CV	20.3	14.9	14.8	16.3	16.3	15.5

Table B.28.4

Phase angle, δ (degrees), test results for 964-2 at 37.8ºC

	25Hz	10Hz	5Hz	1Hz	0.5Hz	0.1Hz
Sample-25	22.7	26.0	27.9	31.2	32.5	30.0
Sample-26	20.8	24.2	26.0	29.9	30.9	29.7
Sample-27	16.0	19.0	20.7	24.0	25.4	25.2
Average	19.8	23.1	24.9	28.4	29.6	28.3
Stdev	3.5	3.6	3.7	3.9	3.7	2.7
%CV	17.4	15.8	14.9	13.6	12.5	9.6

Table B.28.5

Phase angle, δ (degrees), test results for 964-2 at 54.4ºC

	25Hz	10Hz	5Hz	1Hz	0.5Hz	0.1Hz
Sample-25	29.1	30.0	29.8	27.1	25.2	20.4
Sample-26	28.2	29.2	29.4	27.4	26.0	21.6
Sample-27	22.9	24.2	24.9	25.7	25.4	22.9
Average	26.7	27.8	28.0	26.7	25.5	21.6
Stdev	3.4	3.1	2.7	0.9	0.4	1.3
%CV	12.6	11.2	9.8	3.4	1.6	5.8

APPENDIX C

Flow Time, Flow Number, and Loaded Wheel Tracking Test Result

Table C.1
Flow time test results

Traffic Category	Mixtures	Flow Time (F_T), Seconds				Stdev	CV%
		Sample-1	Sample-2	Sample-3	Average		
Level 1	LA9-1	20	23	15	19	4.1	20.9
	US90-1	1053	836	980	956	110.4	11.5
	LPC-1	398	243	305	315	78.0	24.7
Level 2	ALF-1	320	200	178	233	76.4	32.8
	190-1	926	1652	875	1151	434.6	37.8
	190-2	3504	955	1483	1981	1345.4	67.9
	190-3	631	1279	1091	1000	333.4	33.3
	190-4	100	45	84	76	28.3	37.1
Level 3	I10-1	1453	990	1266	1236	232.9	18.8
	I10-2	10000	10000	10000	10000	NA	NA
	I10-3	10000	10000	10000	10000	NA	NA
	964-1	2280	778	257	1105	1050.4	95.1
	964-2	245	296	415	319	87.2	27.4

Table C.2

Flow number test results

Traffic Category	Mixtures	Flow Number (F_N), Cycles				StDev	CV%
		Sample-1	Sample-2	Sample-3	Average		
Level 1	LA9-1	264	170	151	195	61	31.0
	US90-1	3296	3320	4032	3549	418	11.8
	LPC-1	3304	3248	1640	2731	945	34.6
	3121-1	1728	1400	1312	1480	219	14.8
	3121-2	256	1544	185	662	765	115.6
	3121-3	1112	1392	1072	1192	174	14.6
	171-1	274	261	304	280	22	7.9
	171-2	221	188	376	262	100	38.4
	171-3	288	536	732	519	223	42.9
	171-4	258	278	3680*	268	14	5.3
	116-1	3758	4154	10000*	3956	280	7.1
	116-2	1056	1000	1369	1142	199	17.4
	116-3	10000*	2466	3296	2881	587	20.4
	116-4	1360	1422	1229	1337	99	7.4
Level 2	ALF-1	1876	724	2176	1592	767	48.1
	190-1	2816	3344	3440	3200	336	10.5
	190-2	10000	10000	10000	10000	0	0.0
	190-3	10000*	4288	4352	4320	45	1.0
	190-4	892	305	262	486	352	72.4
Level 3	I10-1	6224	5168	4560	5317	842	15.8
	I10-2	10000	10000	10000	10000	0	0.0
	I10-3	10000	10000	10000	10000	0	0.0
	964-1	10000*	4160	4128	4144	23	0.5
	964-2	3560	4304	10000*	3932	526	13.4

* Numbers were excluded as outliers.

Table C.3

Loaded wheel tracking test results

Traffic Category	Mixtures	Rut Depth (mm)			Stdev	CV%
		Sample-1	Sample-2	Average		
Level 1	LA9-1	3.16	3.55	3.4	0.27	8.2
	US90-1	1.63	3.32	2.5	1.19	48.1
	LPC-1	2.16	2.94	2.5	0.56	21.8
	3121-1	5.19	4.53	4.9	0.47	9.6
	3121-2	5.80	5.45	5.6	0.25	4.4
	3121-3	4.63	6.79	5.7	1.53	26.7
	171-1	7.19	5.47	6.3	1.22	19.2
	171-2	7.80	9.02	8.4	0.86	10.3
	171-3	6.53	5.59	6.1	0.66	11.0
	171-4	5.88	6.70	6.3	0.58	9.2
	116-1	2.84	4.56	3.7	1.22	32.9
	116-2	2.94	5.77	4.4	2.00	45.9
	116-3	4.12	2.79	3.5	0.94	27.2
	116-4	3.41	3.87	3.6	0.33	8.9
Level 2	ALF-1	5.70	5.10	5.4	0.42	7.9
	190-1	13.90	15.60	14.8	1.20	8.1
	190-2	2.30	1.80	2.1	0.35	17.2
	190-3	18.40	24.30	21.4	4.17	19.5
	190-4	4.13	8.78	6.5	3.29	51.0
Level 3	I10-1	3.30	4.30	3.8	0.71	18.6
	I10-2	3.40	4.10	3.8	0.49	13.2
	I10-3	2.30	2.30	2.3	0.00	0.0
	964-1	4.70	3.70	4.2	0.71	16.8
	964-2	5.90	4.20	5.1	1.20	23.8

APPENDIX D

Specimen Preparation and Test Procedures

Specimen Preparation

The specimens for the dynamic modulus test, flow number and flow time test were prepared in the same manner since these tests have the same requirements of 150-mm in height and 100-mm in diameter. The procedure for preparation of the specimens is explained in the next section. The specimens tested for dynamic modulus in the indirect tensile mode have different dimensions, and they were prepared through a different procedure as explained in the following section.

Specimen Preparation for AMPTs

All the asphalt mixtures were aged at 135ºC (short term oven aging) for four hours before compaction. Required dimensions for the AMPT specimens were 100-mm in diameter and 150-mm in height, for a height to diameter ratio of 1.5 *[2]*. Initially the mixtures were compacted into gyratory plugs of 150-mm in diameter and 178-mm in height using a Superpave gyratory compactor (SGC). These specimens were prepared to reach target air voids of 8.5.

Then test specimens, 100-mm in diameter, were cored from the center of plugs using a portable core drilling machine, as shown in Figure D.1. The cored specimen from the gyratory compacted specimen and an outer ring are also shown in the figure. After the specimen was cored, a grinding machine was used to grind approximately 14-mm from each end of the cored sample, as shown in Figure D. 2. It was ensured that the final specimen of 150-mm in height and 100-mm in diameter had a parallel surface and met the specification requirements *[2]*.

(a) (b)

Figure D. 1 a) Portable core drilling machine b) the cored sample

(a) (b)

(c)

Figure D. 2 a) Grinding machine and sample b) cut core and its ends c) diameter of a core

(a) (b)

Figure D. 3 Instrumentation: a) installation of LVDT mount b) mounted LVDT

It was also ensured that the final specimens reached target air voids of 7±0.5. During the process of specimen preparation, if the required air voids was not met, or segregation was observed, then the specimen was discarded and additional specimens were made. At least three specimens were made per each mixture for replicate testing. After the specimens were made to the required dimensions, studs were fixed on the specimen using glue, and a pressure machine was used to apply pressure on the studs until the studs were firmly fixed on the specimen for instrumentation, as shown in Figure D.3. The pressure was applied for approximately 45 minutes, and then the sample was removed from the machine, and clamps were mounted to accommodate the deformation measuring equipment, which has the gauge length of 70-mm.

Specimen Preparation for Dynamic Modulus in Indirect Tension Mode

The asphalt mixtures were aged at 135ºC (short term oven aging) for four hours before compaction. The required dimensions for the specimens were 150-mm in diameter and 38-mm in height. Initially the mixtures were compacted into gyratory plugs of 150-mm in diameter and 60-mm in height using a Superpave gyratory compactor (SGC). The grinding machine was used to grind approximately 11-mm from both ends of the specimen. It was ensured that the specimen reached 7±0.5, or the specimen was discarded.

After the sample was made to required dimensions, four studs were stuck on both faces of the specimen using a plastic setup, which had magnetic spots to hold the studs, as shown in Figure D. 4. Super glue was applied to the studs after they were placed in the magnetic spots, and a plastic template was placed over the sample. After 45 minutes, the plastic template was removed and the specimen was mounted with extensometers for both vertical and horizontal displacement measurements, as shown in Figure D. 4.

(a) (b)

Figure D. 4 Instrumentation: a) installation of gage point b) mounted extensometer

Laboratory Test Methods

Different laboratory test methods used in this study were (1) Dynamic modulus (|E*|) in axial mode, (2) Flow Time (F_T), (3) Flow Number (F_N), (4) Dynamic modulus (|E*|) in IDT mode and (5) Loaded Wheel Tracking (LWT) Device test. The procedures for conducting these tests are explained briefly in the following sections.

Dynamic Modulus Test (Axial)

The dynamic modulus test is a compression test, which was standardized in 1979 as ASTM D3497, "Standard Test Method for Dynamic Modulus of Asphalt Concrete Mixtures" *[37]*. This test was conducted in accordance with AASHTO Provisional Standard TP62-03**,** and the NCHRP project 9-19 *[38, 39]*. This test consists of applying a uniaxial sinusoidal (i.e., haversine) compressive stress to an unconfined or confined HMA cylindrical test specimen, as shown in Figure 1. The stress to strain relationship under a continuous sinusoidal loading for linear viscoelastic materials is defined by a complex number called the "complex modulus" (E*). The absolute value of the complex modulus (E*) is defined as the dynamic modulus. The dynamic modulus is mathematically defined as the maximum (i.e., peak)

dynamic stress (σ_0) amplitude, divided by the peak recoverable strain (ε_0) amplitude, represented by equation (17).

$$|E^*| = \frac{\sigma_0}{\varepsilon_0} \quad (17)$$

This test was conducted at -10, 4.4, 25, 37.8 and 54.4C at loading frequencies of 0.1, 0.5, 1.0, 5, 10, 25 Hz at each temperature *[39]*. The samples were tested in an increasing order of temperature, and for each temperature the samples were tested in decreasing order of frequency. This temperature-frequency sequence was carried out to cause minimum damage to the specimen before the next sequential test. The dynamic modulus test was conducted in a Universal Testing Machine (UTM), which includes the loading device, specimen deformation setup, environmental chamber and control and data acquisition system, as shown in Figure D.5. The UTM load cell had a capacity of 25KN. For measuring the axial deformations, three linear variable differential transducers were used. The LVDTs had a range of 1-mm and were placed on the sample at 120º degrees. During the testing, the data was collected for the last six cycles and the required parameters were calculated by the UTM software and reported. At the end of test at each frequency, the permanent deformation of the sample should not exceed 1000 microstrain *[39]*. If a sample exceeded this limit, then the sample was discarded, and the testing was repeated on a new sample for all temperatures and frequencies. The dynamic modulus (|E*|), which is a measure of the material stiffness, and the phase angle δ, which is a measure of the viscoelastic properties of the material, were determined from this test.

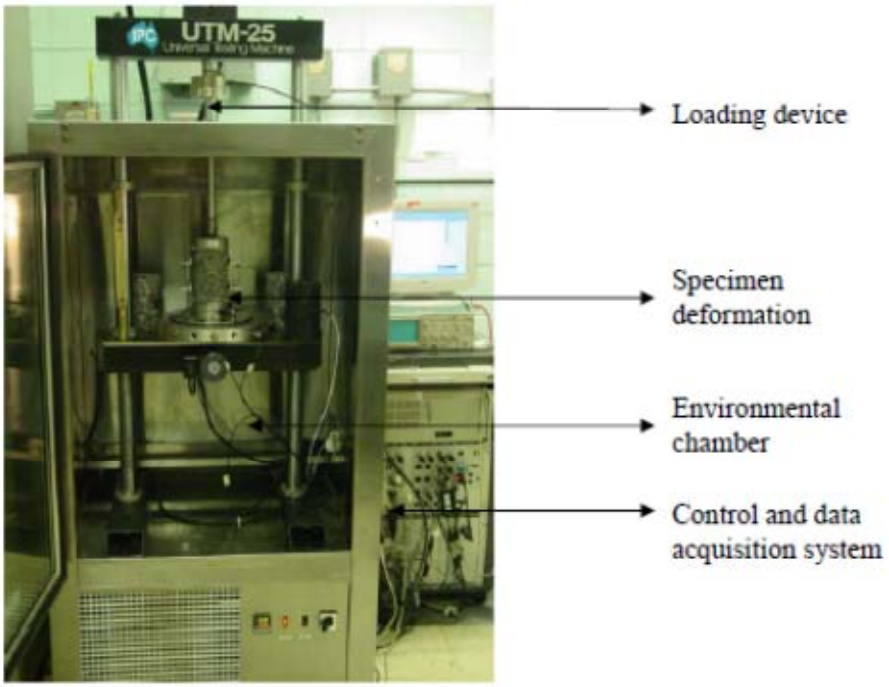

Figure D. 5 Universal Testing Machine (UTM)-25

Flow Time/Static Creep Test

A selected number of mixtures included in the study were tested for the flow time determination. In the flow time test, a total strain-time relationship for a mixture is obtained experimentally *[40]*. The flow time test is a variation of the simple compressive creep test that has been used in the past to measure the rutting potential of asphalt concrete mixtures *[41]*. The starting point of tertiary deformation, or flow time, obtained from the creep test was evaluated in 1991 by Witczak *[25]*. In this test, a static load was applied to the specimen and the resulting strains were recorded as functions of time. The flow time is defined as the time corresponding to the minimum rate of change in axial strain during the creep test. It is determined by the differentiation of the strain versus time curve.

Figure D.6 represents the loading pattern, creep response, three stage curve of accumulated permanent strain and computation of flow time *[25]*. The three stages are: 1) primary stage, 2) secondary stage, and 3) tertiary stage, as mentioned previously in the literature review section.

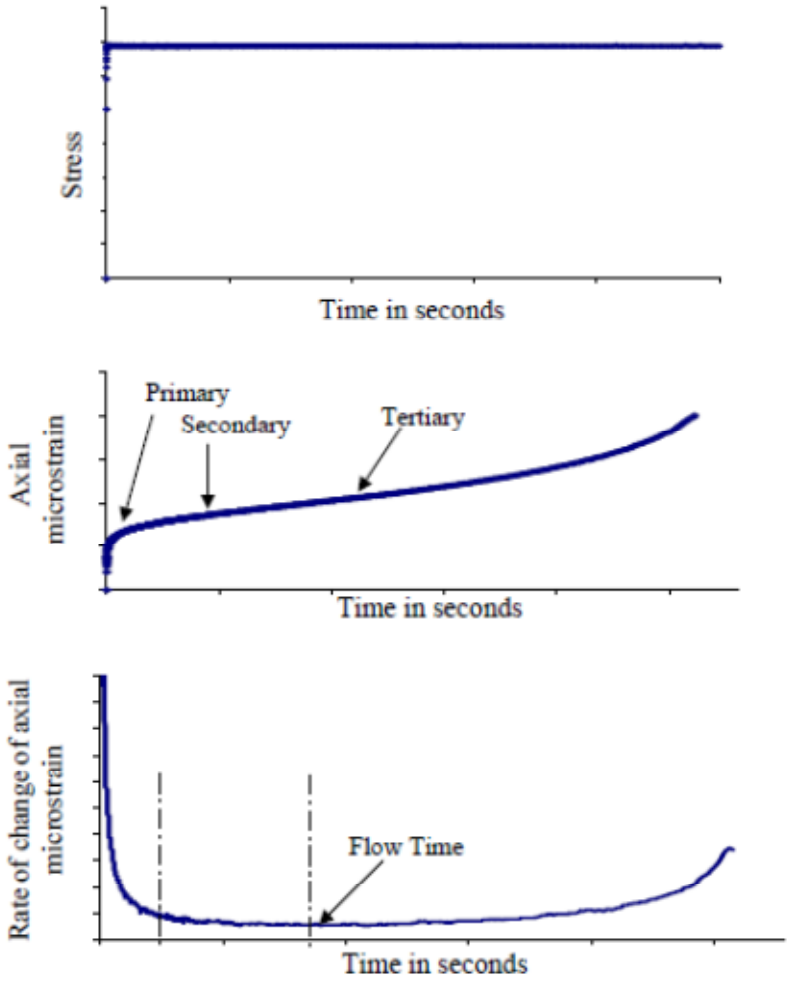

Figure D.6 Typical creep test response, three stage curve of axial microstrain and computation of flow time

This test was conducted in accordance with the test method described in Annex B of the NCHRP Report 513 *[39]*. In this test, a cylindrical sample was subjected to a static axial load, and the resulting axial strain response of the specimen was measured and used to calculate the flow time. The test was conducted at a single effective temperature, T_{eff}, and design stress level. This test is generally conducted on specimens having 100-mm in diameter and 150-mm in height for mixtures with nominal maximum size aggregates less than or equal to 37.5-mm (1.5 in). The parameters that are calculated from the flow time testing are: 1) flow time in seconds, 2) slope of flow curve, and 3) intercept parameter of flow curve.

The flow time slope and intercept were calculated from compliance D(t) vs. time in a log-log scale, as shown in Figure D.6. The stress level and effective temperature are two important aspects of this test. The stress level should not be very high, as this might cause rapid failure of the sample and hinder in comparing the results for different mixtures. The stress level

should be reasonable enough so as to attain the tertiary flow in reasonable time. Generally, the effective temperature used is based on historical temperature data of the place, where the hot mix asphalt mixtures are used. Since the high pavement temperature of T_{eff} (PD) for permanent deformation in Louisiana was found to be 48°C, the tests need to be conducted at a temperature equal to or higher than this temperature in order to characterize the permanent deformation characteristic of HMA mixtures selected *[42]*. So, 54.4°C was selected as an effective temperature for conducting the flow time test. The testing was done in a UTM machine.

Flow Number/ Repeated Loading Test

Most of the mixtures included in the study were tested for the flow number determinations. The flow number test is used to determine the permanent deformation characteristic of hot mix asphalt mixtures by applying a repeated haversine load for several thousand cycles on a cylindrical asphalt sample and recording the cumulative permanent deformation as a function of the number of cycles. This approach was first used by Monismith in the mid-1970s using uniaxial compression tests *[43]*. Similar to the creep test, the cumulative permanent strain curve can be divided into three stages: 1) primary stage, 2) secondary stage, and 3) tertiary stage.

The starting point, or cycle number, at which tertiary flow occurs, is referred to as the flow number, as described in Section 2.6. This test was conducted in accordance with the test method described in Annex B of the NCHRP Report 513 *[40]*. The load was applied for 0.1 second with a rest period of 0.9 second in one cycle, as shown in Figure D.7. This test was conducted for 10,000 cycles. This test is generally conducted on specimens having 100 mm in diameter and 150-mm in height for mixtures with nominal maximum size aggregates less than or equal to 37.5 mm (1.5 in). The flow number was determined by differentiating the permanent strain versus the number of load cycles curve. Figure D. 7 represents an example of a typical permanent axial strain response and computation of flow number. The parameters that can be determined from this test are: 1) flow number in cycles, 2) slope of flow curve, and 3) intercept parameter of flow curve.

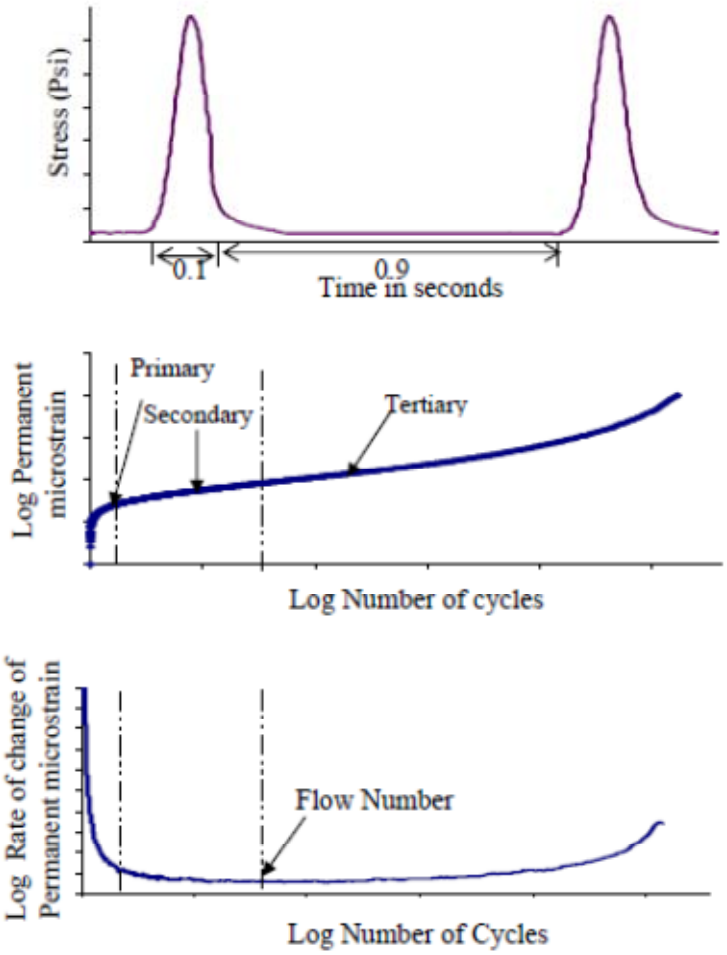

Figure D.7 Three-stage curve of permanent axial microstrain and computation of flow number

The flow number slope and intercept were calculated from permanent microstrain vs. number of load cycles from the flow curve shown in Figure D. 7. The stress level and effective temperature were two important aspects of this test. The test was conducted at a stress level of 30psi (0.207 MPa). A higher stress level might cause rapid failure of the sample and hinder comparing the results for different mixtures. The 30psi (0.207 MPa) stress level was selected to ensure that no rapid failure would occur. The stress level should be reasonable enough so as to attain the tertiary flow in reasonable time. The test was conducted at an effective temperature of 54.4ºC, since it was higher than the historical temperature data of the Louisiana, which is 48ºC. The testing was conducted in the UTM machine.

Dynamic Modulus |E* | in Indirect Tension Mode (IDT)

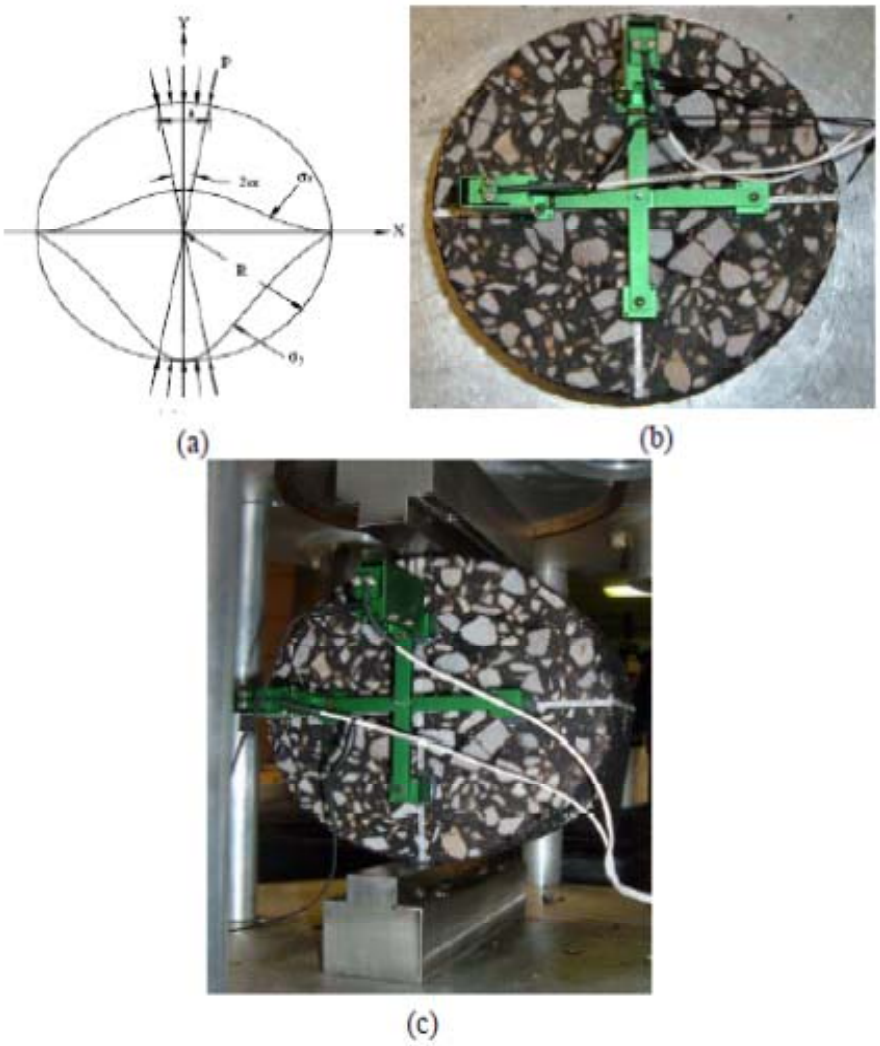

Figure D.8 a) Schematic of the IDT specimen subjected to a strip load; b) Surface-mounted LVDTs; c) IDT test setup

Few selected mixtures included in the study were tested for the dynamic modulus determination under indirect tension (IDT) mode of loading. The dynamic modulus test in the indirect tension mode is a variation of the dynamic modulus test in the axial mode. The dynamic modulus test protocol in the axial mode calls for the axial compression testing of 100-mm diameter and 150-mm tall asphalt concrete specimens. When the cores are obtained from the pavements in the field, they usually do not meet the height requirements as required for testing to determine the dynamic modulus in the axial direction. In that circumstance, the

indirect mode of testing can be a viable alternative to measuring the dynamic modulus in uniaxial compression *[34]*.

In the IDT test, 150-mm diameter gyratory specimens were compacted to a 60-mm height. The ends were cut so that the final height was 38-mm. The LVDTs were mounted on each of the specimen faces using 76.2-mm gauge length, as shown in Figure D.8 b). The IDT specimen subjected to a strip load, and the test set up is shown in Figure D.8 c). The IDT testing was done at 4.4, 25, and 37.8ºC at 10, 5, 1, 0.5, 0.1 and 0.01 Hz. The testing was conducted in a closed-loop servo-hydraulic machine, manufactured by MTS, using a 10kip load cell. A temperature chamber was used to control the test temperature. Dummy specimens with thermocouples embedded in the middle of the specimen were also used to monitor the temperature of the testing specimens.

In this study, an attempt was made to compare values of the dynamic modulus obtained from the axial and IDT mode. The procedure used to calculate the dynamic modulus in the IDT mode is different when compared to axial dynamic modulus. The dynamic modulus was calculated in the procedure developed by Kim *[34]*. In this comparative study, the author concluded that the dynamic moduli, obtained from the indirect tension mode and axial mode, were statistically indifferent.

Loaded Wheel Tracking (LWT) Device Test

The loaded wheel tracking device (also known as Hamburg wheel tracking device) test is a torture test. The test produces damage on samples by rolling a steel wheel across the surface of asphalt concrete slabs that are submerged under water at 50ºC (122ºF) for 20,000 passes. The slabs have a length of 320-mm (12.6 in.), a width of 260-mm (10.2 in.), and a thickness of 80-mm (3.2 in.).

These slabs are secured in reusable steel containers using plaster of paris, and are then placed into the wheel tracking device. The device tests two slabs simultaneously using two reciprocating solid steel wheels. The wheels have a width of 47-mm (1.85 in.) and a diameter of 203.5-mm. The applied load is 710N (160 lb), and it moves at a speed of 1.1km/h (0.68 mph). Each wheel rolls 230-mm (9.1 in.) before reversing direction. The device operates at 53 ± 2 passes/min. The rut depth obtained from this test was used for the data analysis and comparison with other tests. Two slabs were tested for each mixture. After duplicate specimens were placed in the device and pre-conditioned under water at 50°C, the wheels were set in motion to reciprocate over tested slabs to produce rutting**.** The test was conducted at 50°C for 20,000 cycles, or until 20-mm of deformation measured, whichever is reached

first. Figure D. 9 shows the loaded wheel tracking device used in this study. The average rut depths were recorded continuously during the test.

Figure D. 9 Loaded Wheel Tracking device

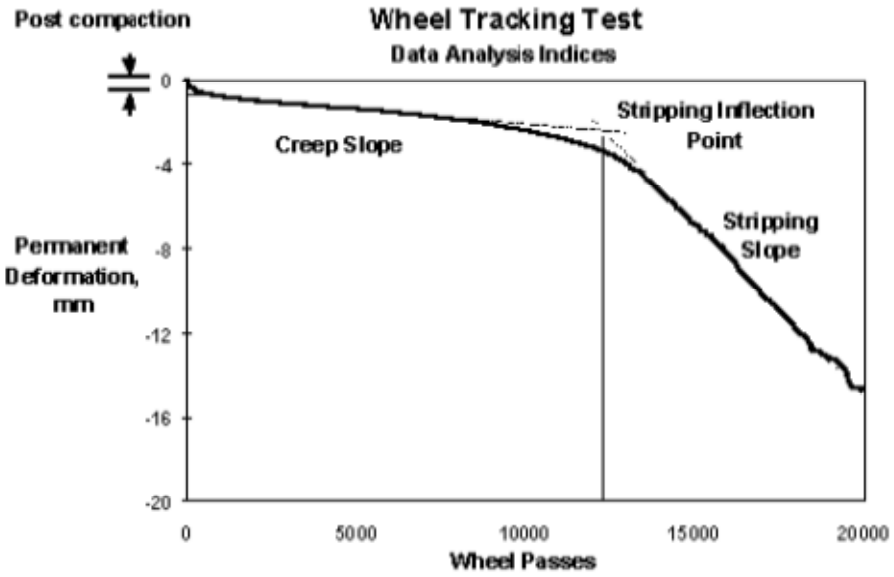

Figure D.10 Typical curve of Loaded Wheel Tracking Test Result

Four indices, shown in Figure D. 10, were used to quantify the test results:

- Post-Compaction Consolidation: It is the amount of deformation, which rapidly occurs during the first few minutes of the test, due to the compacting effort of the steel wheel on the specimen. A low post-compaction consolidation value is desirable, since it would indicate that the compaction during laboratory fabrication was near optimum levels.
- Creep Slope: It is the inverse of the rate of deformation in the linear region of the deformation curve. This linear region starts after the post-compaction effects have ended and before the beginning of stripping. It is reported in passes per mm. The higher the inverse creep slope, the more resistant the mixture is to permanent deformation.
- Stripping Slope: It is the inverse of the rate of deformation in the linear region of the deformation curve, after the beginning of the stripping until the end of test. It is reported as passes/mm. The lower the inverse stripping slopes are, the more severe moisture damages occur.
- Stripping Inflection Point: It is the number of passes at the intersection of the creep slope and the stripping slope. The stripping inflection point is related to the mechanical energy required to produce stripping; therefore a higher stripping inflection point indicates that a mixtures is less likely to strip.

APPENDIX E

Asphalt Layer Input Instructions to the Pavement ME Design Software

Figure E.1 presents the asphalt layer parameters required for Level 1 design with the Pavement ME software for Louisiana conditions. The mixture and binder moduli data are presented in Tables E.1-E.8 and Tables E.9-E.12 respectively and can also be imported directly into the design software using the included data files. The *.dwn and *.bif files contain the mixture and binder data respectively.

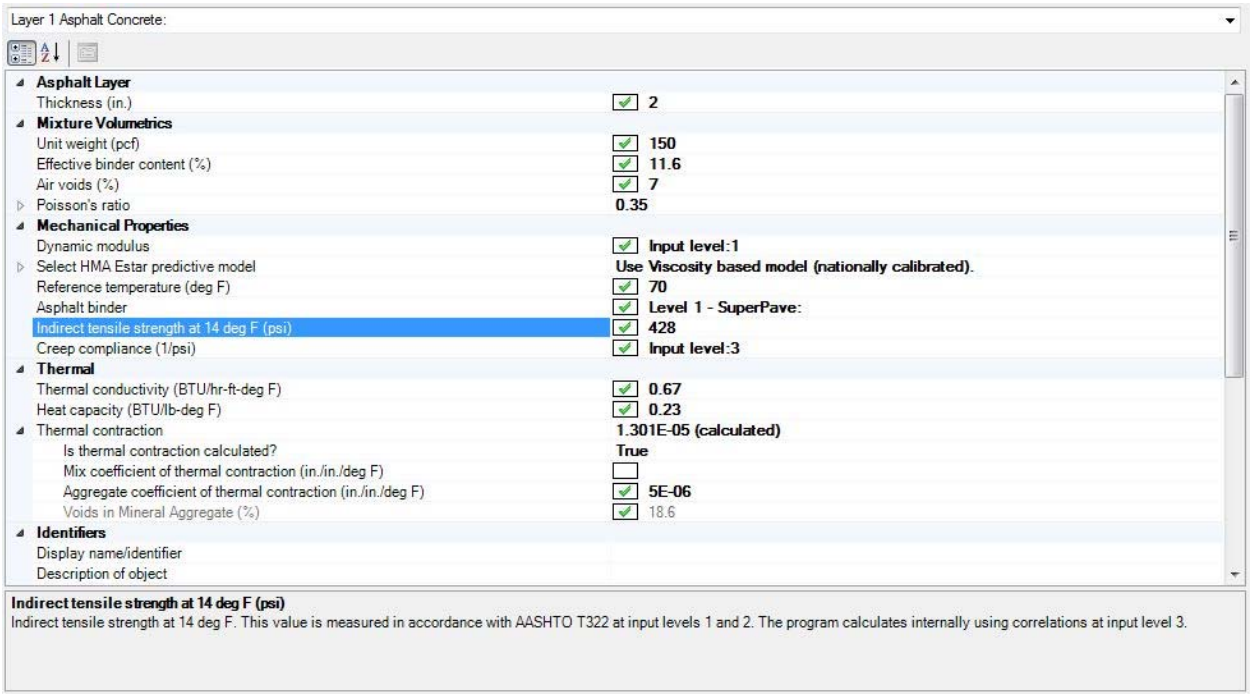

Figure E.1
Asphalt layer inputs

An explanation of each of the items is given below:

1. Asphalt layer
    a. Thickness: Project specific
2. Mixture volumetrics
    a. Unit weight: Calculate from JMF (62.4 * G_{mb})
    b. Effective binder content by volume (V_{be}): Calculate from JMF

$$V_{be} = G_{mb}\left[\frac{P_b}{G_b} - (100 - P_b)\frac{(G_{se} - G_{sb})}{G_{se} * G_{sb}}\right]$$

    c. Air voids: Enter in-place voids
    d. Poisson's ratio: Use 0.35

3. Mechanical Properties
    a. Dynamic modulus: Use data from files provided or copy data from Tables 1-8, corresponding to the Nominal Maximum Aggregate Size (NMAS) of the mixture. The files are organized as follows:

Superpave Traffic Level	**NMAS (mm)**	**Filename**
1	12.5	L1-12.5mm.dwn
	19	L1-19mm.dwn
	25	L1-25mm.dwn
Average (level 1)		L1-avg.dwn
2	12.5	L2-12.5mm.dwn
	19	L2-19mm.dwn
	25	L2-25mm.dwn
Average (level 2)		L2-avg.dwn

    b. E* predictive model: Use the nationally calibrated model
    c. Reference temperature: Use default (70°F)
    d. Asphalt binder: Use data from files provided or copy data from Tables 9-12, corresponding to the Performance Grade (PG) of the binder. The files are organized as follows:

PG	**Filename**
64-22	64-22Average.bif
70-22	70-22Average.bif
76-22	76-22Average.bif

    e. Indirect tensile strength: Use 428 psi
    f. Creep compliance: Use level 3
4. Thermal
    a. Thermal conductivity: Use default (0.67)
    b. Heat capacity: Use default (0.23)
    c. Thermal contraction
        i. Is contraction calculated: Choose True
        ii. Mix coefficient: Use default (1.3E-5 in./in./°F)
        iii. Aggregate coefficient: Use default (5.0E-6 in./in./°F)

Table E.1
Mixture dynamic modulus values (psi) for Level 1, 12.5 mm NMAS

Hz / °F	0.1	0.5	1	5	10	25
14	2378808	2656157	2762236	2995589	3086439	3186107
40	1176658	1539473	1703130	2084151	2247802	2452306
77	173887	302477	381840	632224	766006	954252
100	51963	85959	111158	209659	272500	384323
130	22070	29892	34534	55251	70455	105035

Table E.2
Mixture dynamic modulus values (psi) for Level 1, 19 mm NMAS

Hz / °F	0.1	0.5	1	5	10	25
14	3333551	3612829	3715854	3918650	3991771	4076828
40	1722006	2190718	2399880	2874294	3071074	3316650
77	315554	538549	656513	984298	1141543	1369494
100	74702	150904	200321	378790	482613	646820
130	14284	26895	36603	79921	110608	178227

Table E.3
Mixture dynamic modulus values (psi) for Level 1, 25 mm NMAS

Hz / °F	0.1	0.5	1	5	10	25
14	2708282	2985835	3107307	3362451	3457645	3584019
40	1521427	1903035	2062140	2418120	2567141	2745103
77	261112	437437	542759	856173	1012876	1215908
100	75639	126304	164966	295317	379051	509395
130	33036	44065	53110	87694	111912	159758

Table E.5
Mixture dynamic modulus values (psi) for Level 1 (average)

Hz / °F	0.1	0.5	1	5	10	25
14	2806880	3084940	3195132	3425563	3511952	3615651
40	1473364	1877742	2055050	2458855	2628672	2838020
77	250184	426155	527038	824232	973475	1179885
100	67435	121056	158815	294589	378055	513513
130	23130	33617	41416	74289	97658	147673

Table E.6
Mixture dynamic modulus values (psi) for Level 2, 12.5 mm NMAS

Hz / °F	0.1	0.5	1	5	10	25
14	2651644	2984124	3120374	3412119	3525828	3664185
40	1416116	1777508	1940922	2314394	2477064	2706040
77	281066	451237	544393	817030	950774	1151196
100	84956	146156	185270	322611	396183	521822
130	40569	53368	62879	100395	127346	180752

Table E.7
Mixture dynamic modulus values (psi) for Level 2, 19 mm NMAS

Hz / °F	0.1	0.5	1	5	10	25
14	2792249	3112513	3245188	3532334	3640969	3789966
40	1552022	1932169	2093724	2483294	2633553	2806510
77	288355	475668	587670	936768	1095572	1294295
100	74421	120168	152469	275539	348903	491669
130	38115	48345	54923	82364	103792	147904

Table E.8
Mixture dynamic modulus values (psi) for Level 2, 25 mm NMAS

Hz / °F	0.1	0.5	1	5	10	25
14	2699709	3003521	3125123	3379721	3503157	3641843
40	1549782	1908206	2065159	2429791	2586651	2790682
77	339005	526838	638508	965907	1130791	1321798
100	101546	159397	204388	357801	442876	588681
130	49365	63976	75549	118669	149072	206757

Table E.9
Mixture dynamic modulus values (psi) for Level 2 (average)

Hz / °F	0.1	0.5	1	5	10	25
14	2714534	3033386	3163562	3441391	3556651	3698665
40	1505973	1872628	2033268	2409160	2565756	2767744
77	302809	484581	590190	906569	1059046	1255763
100	86975	141907	180709	318650	395987	534057
130	42683	55229	64450	100476	126736	178471

Table E.10
Binder complex shear modulus and phase angle (PG 64-22)

°F	G* (Pa)	Phase angle (degree)
104.0	62267	76.2
122.0	13583	80.8
147.2	1952	85.7

Table E.11
Binder complex shear modulus and phase angle (PG 70-22)

°F	G* (Pa)	Phase angle (degree)
104.0	77400	71.0
140.0	5377	76.3
158.0	1705	78.4

Table E.12
Binder complex shear modulus and phase angle (PG 76-22)

°F	G* (Pa)	Phase angle (degree)
104.0	92883	66.1
122.0	26267	65.4
140.0	8492	65.5
158.0	3108	67.2
168.8	1773	68.6